

Mathematical Modelling of Macrophage Phenotype Selection and its Role in Inflammation

Suliman Almansour

*A thesis submitted in partial fulfilment of the requirements of
Nottingham Trent University for the degree of Doctor of Philosophy.*

May 2024

Copyright Statement

This work is the intellectual property of the author. You may copy up to 5% of this work for private study, or personal, non-commercial research. Any re-use of the information contained within this document should be fully referenced, quoting the author, title, university, degree level and pagination. Queries or requests for any other use, or if a more substantial copy is required, should be directed in the owner(s) of the Intellectual Property Rights.

Abstract

Macrophages play a wide range of roles in resolving the inflammatory damage that underlies many medical conditions, and have the ability to adopt different phenotypes in response to different environmental stimuli. Categorising macrophage phenotypes exactly is a difficult task, and there is disparity in the literature around the optimal nomenclature to describe these phenotypes; however, what is clear is that macrophages can exhibit both pro- and anti-inflammatory behaviours dependent upon their phenotype, rendering mathematical models of the inflammatory response potentially sensitive to their description of the macrophage populations that they incorporate. Many previous models of inflammation include a single homogenised macrophage population with both pro- and anti-inflammatory functions. Here, we build upon these existing models to include explicit descriptions of distinct macrophage phenotypes and examine the extent to which this influences the inflammatory dynamics that the models emit.

This research aims to provide useful insights into the essential role of macrophage phenotypes in inflammation. We present a series of corresponding mathematical models of increasing biological complexity and examine the resulting dynamics via numerical simulation and bifurcation analysis. We begin by examining three ordinary differential equation (ODE)-based models that describe: a single homogenised macrophage population; two distinct macrophage populations with opposing pro/anti-inflammatory phenotypes; and a variant of the second model that also includes neutrophil-driven dynamics. We then build on these models to construct a partial differential equation (PDE) model that considers macrophage phenotypes to lie on a continuous spectrum of inflammatory activity.

We analyse our models via numerical simulation in Matlab and dynamical systems analysis in XPPAUT. We investigate the different qualitative behaviours presented by our models via Matlab and discuss them in terms of the inflammatory response and its potential outcomes. We also use bifurcation diagrams provided by XPPAUT to investigate how variation in the system's key parameters influences the switch be-

tween chronic and healthy outcomes. We show that models that account for distinct macrophage phenotypes separately can offer more realistic steady state solutions than precursor models do (better capturing the anti-inflammatory activity of tissue-resident macrophages), and that variations in macrophage polarisation can underlie a switch between chronic steady state outcomes and oscillations reminiscent of inflammatory conditions with relapsing-remitting characteristics. Finally, we reflect on the conclusions of our analysis in the context of the ongoing hunt for potential new therapies for inflammatory conditions, highlighting manipulation of macrophage polarisation states as a potential therapeutic target.

Acknowledgements

I would like to express my sincere gratitude to my supervisors, Martin Nelson, Jonathan Crofts, and Joanne Dunster, for their invaluable advice, ongoing support, and patience during my PhD studies. Their profound knowledge and wealth of experience have encouraged me throughout my academic research and daily life. I will forever appreciate their mentorship and kindness.

I extend my heartfelt thanks to Nadia Chuzhanova, Matt Tranter, and all members of the Mathematics Department at NTU for their invaluable support.

I am grateful to my beloved mother, family, and friends for their constant encouragement and unwavering support during my academic pursuits. Their belief in me has been my pillar of strength.

I owe an immeasurable debt of gratitude to my wife, Banan, and my children, Hamam, Abdulrahman, and Tasneem. Their unwavering support and understanding have made my life and studies in the UK a truly fulfilling experience. Completing this journey without their love and encouragement would have been impossible. This thesis is dedicated to them.

Declarations

I declare that the thesis has been composed by myself and that the work has not been submitted for any other degree or professional qualification. I confirm that the work submitted is my own, except where work which has formed part of jointly-authored publications has been included.

Parts of this thesis have been prepared for publication:

1. S. Almansour, J.L. Dunster, J.J. Crofts, M.R. Nelson. A systematic evaluation of the influence of macrophage phenotype descriptions on inflammatory dynamics. *Mathematical Medicine and Biology: A Journal of the IMA*, 2024, dqae004. DOI: 10.1093/imammb/dqae004.
2. S. Almansour, J.L. Dunster, J.J. Crofts, M.R. Nelson. Modelling the continuum of macrophage phenotypes and their role in inflammation. (Submitted to *Mathematical Biosciences* special issue entitled “Dynamical Systems in the Life Sciences”, April 2024; under review.)

Publication 1 encompasses the work of Chapters 2–4. Publication 2 encompasses the work of Chapter 5.

Contents

1	Introduction	1
1.1	Inflammation and its roles in health and disease	3
1.2	The biology of the inflammatory response	7
1.2.1	Inflammatory response mechanisms	8
1.2.2	Acute inflammation	10
1.2.3	Chronic inflammation	11
1.3	Key cells involved in inflammation	14
1.3.1	Macrophages and their functions in the body	16
1.3.2	Pro-inflammatory macrophage polarisation and related mediators	19
1.3.3	Anti-inflammatory macrophage polarisation and related mediators	21
1.4	Previous mathematical models of inflammation	23
1.4.1	Models containing a single homogenised macrophage population	24
1.4.2	Models containing multiple macrophage populations	26
1.5	Thesis overview	28
2	A Simple Baseline Model With One Homogenised Macrophage Population	30
2.1	Model derivation	31
2.1.1	Parameters	32
2.1.2	Non-dimensionalisation	35
2.2	Identification and classification of steady state solutions	36
2.3	Results	40
2.3.1	Numerical results	40
2.3.2	Bifurcation analysis	43

2.4	Discussion	49
3	Modelling The Roles of Distinct Macrophage Phenotypes	51
3.1	Model derivation	52
3.1.1	Parameters and non-dimensionalisation	55
3.2	Identification and classification of steady state solutions	56
3.3	Numerical simulations	59
3.4	Bifurcation analysis	61
3.5	Discussion	69
4	Incorporating The Role of Neutrophils	71
4.1	Model derivation	72
4.1.1	Parameters and non-dimensionalisation	74
4.2	Identification and classification of steady state solutions	76
4.3	Numerical Simulations	79
4.4	Bifurcation analysis	82
4.5	Discussion	88
5	Modelling The Continuum of Macrophage Phenotypes	90
5.1	Model derivation	91
5.1.1	Nondimensionalisation	93
5.1.2	Parameters	94
5.2	Numerical scheme	96
5.3	Results	98
5.3.1	Stability of the zero state	99
5.3.2	Analysis for $R(p) = 1$	100
5.3.3	The effect of variations in $R(p)$	107
5.4	Discussion	112
6	Conclusions	117
6.1	Thesis summary	117
6.2	Targets for future work	122

CONTENTS

6.2.1	Context-specific models	123
6.2.2	Addressing the lack of corresponding experimental data	124
6.2.3	Alternative modelling approaches	125
A	List of bifurcations	127
	References	128

Introduction

Inflammation plays a critical role in the development of many diseases and health conditions. Therefore, a comprehensive understanding of the inflammatory process and its resolution is essential for the development of new treatments and therapies. Inflammation is a natural response of the immune system to infection, injury or harmful stimuli, and it involves a multiplicity of cellular and molecular events. Inflammation serves as the body's first line of defence against harmful agents, and plays a pivotal role in the healing process. The primary function of inflammation is to protect living tissue by eliminating injurious stimuli and restoring tissue homeostasis. Inflammation can be either acute or chronic. Acute inflammation is the immune system's initial response to injury and is generally beneficial to the body. In contrast, chronic inflammation is a harmful type that can lead to significant organ dysfunction. It is associated with a wide range of chronic diseases and is one of the leading causes of death worldwide (Pahwa *et al.*, 2018). Therefore, it is crucial to pay attention to chronic inflammatory diseases and seek to provide more effective treatment methods to promote healing in chronic conditions or reduce harm to damaged tissues.

Inflammation is the biological reaction of the innate immune system, which can enhance the body's immune system against infections and other diseases. However, it can be potentially detrimental to the body and lead to further tissue damage, contributing to the development of various inflammation-related diseases. Therefore, the inflammatory response is a strictly regulated process that seeks to maintain tissue homeostasis and prevent excessive tissue damage that could lead to prolonged inflammation.

Macrophages are crucial components of the immune system and play an essential role in the initiation and resolution of inflammation. They are also considered a potential therapeutic target for maintaining tissue integrity and homeostasis. Macrophages are multifunctional immune cells that play pivotal roles in resolving the inflammatory

damage that underlies many medical conditions. Their functions include recognising and eliminating diseased cells and foreign materials, removing debris and dead cells, releasing of pro-inflammatory and anti-inflammatory cytokines, and repairing tissue (Eming *et al.*, 2007; Hirayama *et al.*, 2018). These activities are vital for maintaining overall health and tissue integrity. Macrophages are heterogeneous and highly plastic cells, and thus, they have the ability to switch between different phenotypes with different functional properties in response to diverse micro-environmental stimuli.

Strictly classifying macrophage phenotypes is a challenging task due to the high plasticity and heterogeneity of macrophages, and there is a contrast in the literature on the ideal nomenclature to describe these phenotypes. However, it is evident that macrophages can exhibit both pro- and anti-inflammatory behaviours depending on their phenotype. Moreover, they can display a spectrum of intermediate behaviours among these contrasting phenotypes, with the ability to switch into different phenotypes in response to gradual changes in their microenvironment (Palma *et al.*, 2018). Therefore, mathematical models of the inflammatory response are sensitive to the description of the macrophage populations they incorporate.

Many previous theoretical models of inflammation have focused largely on its temporal dynamics, and how the inflammation outcomes fluctuate between a healthy resolution and chronic inflammation. These models typically neglect macrophage phenotypes and include a single population of macrophages with both pro- and anti-inflammatory functions. In this research, we build upon these existing models by incorporating detailed descriptions of distinct macrophage phenotypes and exploring how much this impacts the inflammatory dynamics generated by these models. The aim of this work is to construct and analyse four related models of inflammatory dynamics that include increasing levels of complexity regarding descriptions of macrophage phenotypes and other aspects of the inflammatory response.

In this chapter, we present an overview of the main topics covered in this work. Firstly, Section 1.1 begins with an introduction to inflammation and a brief overview of the medical conditions associated with it. Section 1.2 provides a biological description of the mechanisms underlying the inflammatory response and the types of inflammation. In Section 1.3, we review the immune cells involved in the inflammation process with a focus on describing macrophage phenotypes and their role in the inflammatory response. Section 1.4 reviews relevant literature in the mathematical modelling of inflammation. Finally, we provide an overview of the major topics discussed in the whole thesis by outlining each chapter's content in Section 1.5.

1.1 Inflammation and its roles in health and disease

Inflammation is a complex biological response to injury, infection, or tissue damage, and it involves a wide range of cellular and molecular processes, including recognising and eliminating noxious agents, removing damaged cells and debris, and repairing tissue (Chen *et al.*, 2018; Pahwa *et al.*, 2021). Inflammation plays an essential part in the body's natural defense mechanism, protecting living tissue by destroying and removing injurious stimuli to maintain overall health and restore tissue homeostasis (Gabay, 2006; Chai *et al.*, 2015; Placha & Jampilek, 2021). Here, we briefly review inflammation within organs with a focus on the correlation between inflammation and related diseases, along with biomarkers associated with these diseases.

When tissues are injured, an inflammatory response is activated in order to identify and eliminate the causative agent of the damage to protect the tissues from injury or disease. The causes of inflammation, also known as etiologies, are varied and may be non-infectious or infectious agents (Chen *et al.*, 2018). Non-infectious agents may be physical (such as burns, foreign bodies, tissue injury, or trauma), chemical (such as toxic compounds, fatty acids, or chemical irritants), or biological (such as damaged cells). Infectious agents may be pathogens, such as viruses, bacteria, and other organisms (Chen *et al.*, 2018; Furman *et al.*, 2019; Pahwa *et al.*, 2021). Sometimes, inflammation occurs due to the immune system mistakenly perceiving the body's cells or tissues as harmful agents (foreign intruders). Thus, this immune system's reaction may lead to autoimmune diseases like type 1 diabetes (Noble, 2015; Kakleas *et al.*, 2015).

As a part of the immune system, inflammation plays a key role in protecting the body from disease-causing pathogens and repairing damaged tissues. However, inflammation can evolve into a chronic condition due to constant stimulation of the inflammatory factors, which increases the risk of developing several diseases (Furman *et al.*, 2019; Niu *et al.*, 2021). Recent studies have revealed that inflammation plays a major role in the development of a variety of fatal or chronic diseases and have focused on identifying inflammation-associated biomarkers and investigating associations between prolonged inflammation and disease (Chen *et al.*, 2018; Reddy *et al.*, 2019). Figure 1.1 illustrates some common diseases and conditions that are associated with chronic inflammation. Hence, targeting inflammation and identifying the causes of prolonged inflammation provides an alternative approach to developing effective treatments and improving therapeutic outcomes for associated diseases (Liu *et al.*, 2017; Furman *et al.*, 2019; Niu *et al.*, 2021).

Nowadays, obesity poses a serious threat to public health worldwide due to its associ-

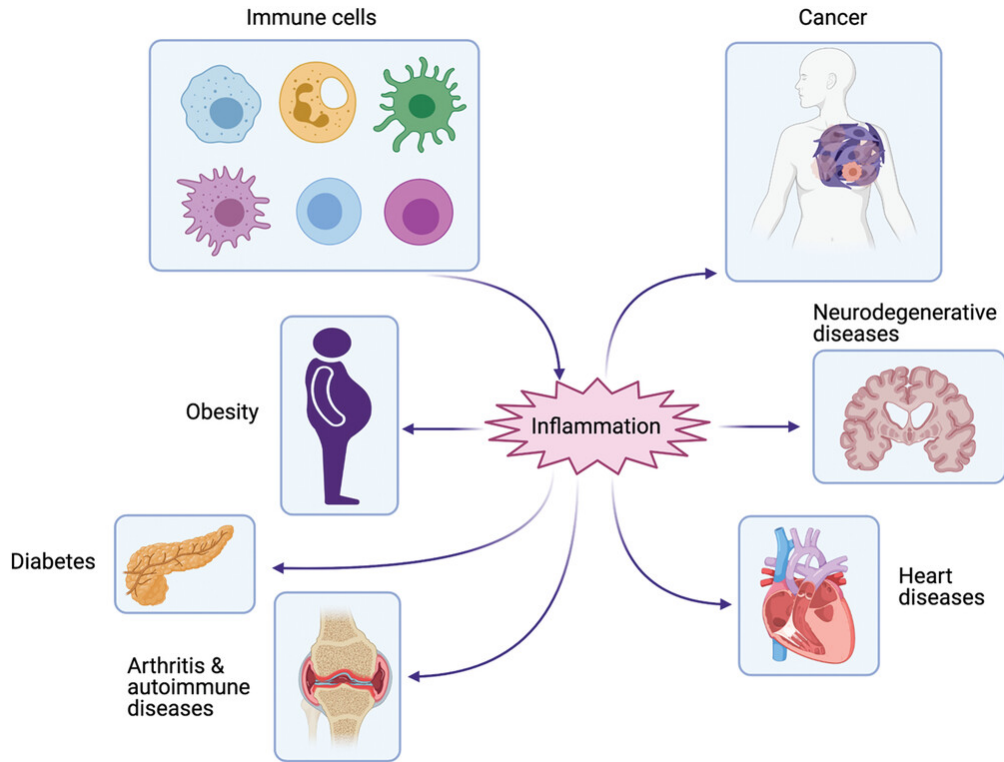


Figure 1.1: Immune cells are involved in the inflammatory response and may contribute to the development of inflammation-related diseases. Source: Niu *et al.* (2021).

ation with potential risks of diseases such as cardiovascular diseases, type 2 diabetes, and fatty liver disease (Piché *et al.*, 2020; Blüher & Müller-Wieland, 2022). Recently, increasing evidence suggests that inflammation plays a central role in the development of obesity and obesity-associated diseases such as type 2 diabetes (Wellen *et al.*, 2005; Zatterale *et al.*, 2020). Increased accumulation of macrophages in adipose tissues leads to an elevated level of reactive oxygen species, resulting in metabolic disorders and insulin resistance (Du Clos, 2000; Wang *et al.*, 2021). In addition, the overproduction of tumour necrosis factors (TNF- α) in adipose tissue is a key feature of obesity and contributes significantly to insulin resistance (Wellen *et al.*, 2005; Engin, 2017). Hence, in order to enhance obesity treatment outcomes, attention should be directed towards developing effective treatment options that target inflammation and the signalling pathways that underlie it (Zatterale *et al.*, 2020; Piché *et al.*, 2020).

Similarly, inflammation is associated with neurodegenerative diseases such as Parkinson's disease, multiple sclerosis, and Alzheimer's disease (Paolini P. *et al.*, 2021). According to World Health Organisation estimates, the number of people affected by neurodegenerative diseases is expected to exceed 70 million by the year 2030 and over 106 million by 2050 (Amor *et al.*, 2014). Recent research suggests that various stimuli

such as ageing, injury, or illness, may induce microglia, thus initiating an inflammatory cascade (Griffin, 2006; Amor *et al.*, 2014). With a thorough understanding of both neurodegenerative disorders and the innate immune system, it is crucial to protect the central nervous system from damage by precisely controlling the immune response (Ransohoff & Brown, 2012; Andreasson *et al.*, 2016; Paolini P. *et al.*, 2021). Therefore, inflammation-targeted therapeutic approaches are necessary to protect the central nervous system from harm, providing alternative treatment possibilities for neurodegenerative diseases.

The prevalence of type 2 diabetes is rising worldwide, and 90% of diabetic patients have insulin resistance (Zimmet *et al.*, 2001; Sjöholm & Nyström, 2006). The precise mechanisms by which inflammation affects pancreatic cells and leads to the development of insulin resistance are still poorly understood (Donath & Shoelson, 2011). Type 2 diabetes is associated with significant public health issues such as obesity and premature cardiovascular morbidity (Dandona *et al.*, 2004; Sjöholm & Nyström, 2006; Wondmkun, 2020). Several studies have described inflammation as a key pathogenetic factor in type 2 diabetes and the development of insulin resistance (Bloomgarden, 2003; Taylor, 2012; Cruz *et al.*, 2013; Wen & Duffy, 2017). Hallmarks of inflammation linked with type 2 diabetes include tumour necrosis factor (TNF- α), interleukin-6 (IL-6), and some antidiabetic agents such as glitazones that reduce insulin resistance and insulin itself (Krentz & Bailey, 2005; Mirza *et al.*, 2012; Liu *et al.*, 2016; Chaudhury *et al.*, 2017). Recent research has shown that anti-inflammatory drugs may counteract inflammation, improve glucose tolerance, and reduce the risk of type 2 diabetes (Deans & Sattar, 2006; Esser *et al.*, 2015; Kuryłowicz & Koźniewski, 2020) although traditional treatments still focus on reducing hyperglycemia (Inzucchi *et al.*, 2012). In order to improve the prediction of early disturbances in insulin sensitivity, it is essential to identify the inflammatory signalling pathways and biomarkers associated with type 2 diabetes in greater detail. This may lead to new perspectives on the diagnosis and treatment of insulin resistance.

There is a growing need to understand the inflammatory mechanisms underlying the pathogenesis of heart disease. Metabolic syndrome, which comprises type 2 diabetes and obesity, is among the significant factors that drive the development of heart disease (Han & Lean, 2016). Many studies have established that inflammatory cells and pathways can contribute to the development of heart diseases (Anker & von Haehling, 2004; Ferrucci & Fabbri, 2018). Due to the impact of these diseases (type 2 diabetes and obesity) and their close associations with heart disease, researchers have been motivated to investigate further the common inflammatory biomarkers between these often over-

lapping medical conditions (Han & Lean, 2016; Ferrucci & Fabbri, 2018). Following this pattern, Anker & von Haehling (2004) and Madjid & Willerson (2011) demonstrate that the progression of chronic heart failure is associated with pro-inflammatory cytokines such as interleukin (IL)-1, IL-6, and tumour necrosis factor (TNF- α), which are also prevalent indicators of type 2 diabetes and obesity. As illustrated by Koenig (2001) and Ferrucci & Fabbri (2018), high levels of inflammatory markers, such as C-reactive protein, are linked to an increased risk of cardiovascular disease events. With an improved understanding of inflammation-related heart disease, new insights are opening up into potential markers of underlying cardiovascular and atherosclerosis risk.

In recent decades, the robust association between tumour malignancies and inflammation has been gradually recognised. In some types of cancer, inflammatory conditions precede the development of malignancy, and thus tumour cells often tend to develop in areas of infection due to the body's natural response (Colotta *et al.*, 2009; Gkretsi *et al.*, 2017). Inflammation increases the risk of developing certain cancers because an inflammatory component is often present in the microenvironment of most neoplastic tissues (Mantovani *et al.*, 2008; Colotta *et al.*, 2009). Therefore, the triggers of chronic inflammation may increase the risk of various types of cancer, such as mucosal lymphoma, liver carcinoma, gastric cancer, cervical, colon cancer, and prostate cancer (Mantovani *et al.*, 2008; Candido & Hagemann, 2013). It is estimated that 15–20% of cancer deaths worldwide are associated with inflammatory responses and underlying infections (Mantovani *et al.*, 2008). One of the critical hallmarks of cancer-related inflammation is the infiltration of immune cells into tumour tissues, especially tumour-associated macrophages, to counteract infection by producing nitrogen and reactive oxygen species (Kuper *et al.*, 2001). In addition, the presence of inflammatory cytokines and inflammatory mediators in tumour tissues, such as tumour necrosis factor (TNF- α), interleukin-1 (IL-1), IL-23, and IL-6, promotes a pro-inflammatory microenvironment metastasis and cancer progression (Voronov *et al.*, 2003; Karin, 2006; Langowski *et al.*, 2006). In the tumour microenvironment, cancer-related inflammation affects many aspects of malignancy, including angiogenesis, malignant cell proliferation and survival, and subverts adaptive immune responses (Mantovani *et al.*, 2008; Colotta *et al.*, 2009; Candido & Hagemann, 2013). Increased vascular permeability is a common characteristic of inflammation and is also frequently observed in solid tumours with leaky arteries (Küppers *et al.*, 2013). Thus, recent studies have revealed molecular pathways that connect inflammation and cancer, leading to the identification of new target molecules. These molecules and pathways involved in cancer-related inflammation may help improve the diagnosis and therapies that target the inflammatory components of the microenvironment (Mantovani *et al.*, 2008; Colotta *et al.*, 2009).

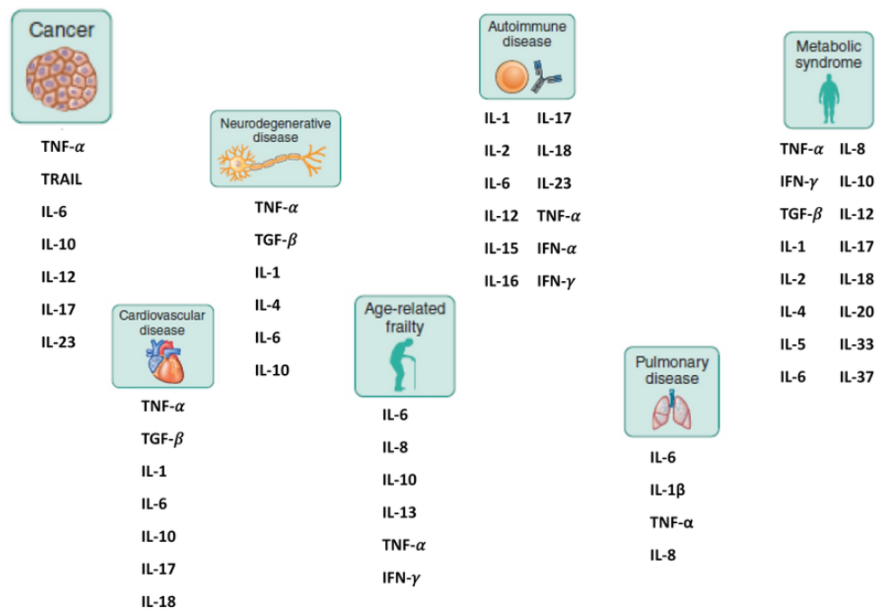


Figure 1.2: Cytokines as biomarkers for various inflammatory diseases. Image based on material taken from Liu *et al.* (2021).

Inflammation is a major driving force underlying many fatal or serious diseases and their progression. As a result, biomarkers of inflammation are certainly of attain growing significance in clinical research (Brenner *et al.*, 2014; Reddy *et al.*, 2019). Studies conducted by Reddy *et al.* (2019) and Liu *et al.* (2021) reveal that when the body experiences inflammation due to an injury or disease, it often exhibits a higher level of certain substances known as inflammatory markers or biomarkers, such as cytokines (*e.g.* tumour necrosis factor (TNF- α) and interleukin-1 (IL-1)), acute-phase proteins (*e.g.* C-reactive protein), and inflammation-related growth factors. These biomarkers play a key role in identifying and monitoring the level of inflammation in the body. Figure 1.2 illustrates cytokines that act as biomarkers of inflammation in associated diseases. Controlling inflammation by targeting biomarkers of inflammation may reduce associated risks and lead to the development of more effective strategies for treating patients.

1.2 The biology of the inflammatory response

Inflammation is a natural response of the immune system to a variety of factors, including both infectious and non-infectious agents (Chen *et al.*, 2018). These factors trigger an inflammatory response, in which inflammatory cells migrate from blood vessels into damaged tissues to eliminate the aetiologies of inflammation that can potentially cause tissue injury or disease (Chen *et al.*, 2018). This response can be defined as a

protective mechanism that stimulates the body's defences against harmful agents and maintains the body's normal function (Ortega-Gómez *et al.*, 2013). Inflammation has been recognised as a major force underlying many serious diseases, such as type 2 diabetes (Zatterale *et al.*, 2020), cardiovascular disease (Piché *et al.*, 2020), rheumatoid arthritis (Libby, 2008), and inflammatory bowel disease (Ansar *et al.*, 2016). Here, we briefly review the basic mechanisms of the inflammatory response and the types of inflammations: acute and chronic.

1.2.1 Inflammatory response mechanisms

The immune system is activated when the body suffers an injury or detects harmful agents that may cause infection or disease. In response to injury or disease, the body releases a cascade of inflammatory mediators that vary in nature, function and timespan of effectiveness to regulate, stimulate, and eventually resolve inflammation (Chen *et al.*, 2018; Liu *et al.*, 2021). Inflammatory mediators oversee and regulate the inflammatory response through a complex network composed of a wide range of molecules and chemical signals, including chemokines, cytokines, leukotrienes, prostaglandins, and other signalling molecules (Abdulkhaleq *et al.*, 2018; Liu *et al.*, 2021). They can have both pro- and anti-inflammatory effects and are used as biomarkers for many diseases (Abdulkhaleq *et al.*, 2018; Liu *et al.*, 2021; Małkowska & Sawczuk, 2023). During the inflammatory process, the immune system triggers several reactions to initially move proteins, fluid, and immune cells from the bloodstream to the injury site (Soehnlein & Lindbom, 2010; Ortega-Gómez *et al.*, 2013). This can be achieved through the following mechanisms that occur within microcirculation as reported in Medzhitov (2008) and Granger & Senchenkova (2010): (i) vasodilation (expansion of small blood vessels); (ii) increased blood flow and fluid exudation to the site of inflammation; (iii) increased vascular permeability; (iv) infiltration of cells (increased leukocyte recruitment and accumulation at the site of injury), controlled by cytokines and chemotactic factors; (v) the release of plasma proteins and inflammatory mediators; and (vi) activation of the immune system.

Upon tissue injury, immune cells, such as dendritic cells and tissue-resident macrophages, release a wide array of chemokines and pro-inflammatory cytokines such as interleukins IL-1, IL-4, IL-6, and tumour necrosis factor-alpha (TNF- α), that induce the chemotaxis of leukocytes from the general circulation into the injury sites (Davies *et al.*, 2013; Liu *et al.*, 2021). Tissue-resident macrophages play a crucial role in eliminating harmful stimuli by phagocytosis (Davies *et al.*, 2013). Once leukocytes reach the injury sites, they are activated by various cytokines and chemokines released

by the tissue-resident macrophages. When activated, leukocytes secrete more pro- and anti-inflammatory cytokines that facilitate and inhibit inflammation and mediators of inflammation to regulate the inflammatory response (Muller, 2013). Neutrophils are the initial and most prevalent inflammatory cells in the early stages of inflammation (Soehnlein & Lindbom, 2010; Ortega-Gómez *et al.*, 2013). Neutrophils can eliminate the detrimental stimuli by phagocytosis or release reactive oxygen species and cytokines (such as IL-1, IL-6, and TNF- α) and reactive oxygen species (Mantovani *et al.*, 2011). Macrophages and neutrophils provide an early response to harmful agents in an effort to contain and eliminate them (Sherwood & Toliver-Kinsky, 2004). Phagocytic cells play a critical role in the body's immune defense, but their action is amplified by lymphocytes such as T-lymphocytes and B-lymphocytes (Sherwood & Toliver-Kinsky, 2004). Lymphocytes play a critical role in mediating inflammation through many complex mechanisms, including the stimulation of lymphocytes, release of cytokines, and antibody production (Ansar *et al.*, 2016). Platelets can also play a primary role in inflammation via platelet aggregation and thrombus formation (Deppermann & Kubes, 2018).

Although the processes underlying the inflammatory response may vary depending on the site of injury and the initial triggers, they all share a common mechanism (Frangogiannis, 2014). According to Chen *et al.* (2018), this common mechanism involves: i) recognition of harmful stimuli by cell surface pattern receptors; ii) activation of inflammatory pathways, which contribute to the production of inflammatory mediators; iii) release of inflammatory markers, including cytokines, proteins, and enzymes, to activate inflammatory cells; iv) recruitment of inflammatory cells to the injury sites.

The resolution of inflammation occurs when the pro-inflammatory response is suppressed to prevent further tissue damage (Ortega-Gómez *et al.*, 2013; Chen *et al.*, 2018). This involves halting the recruitment and infiltration of circulating leukocytes to sites of injury by ceasing pro-inflammatory signalling, resulting in a return of tissue mononuclear cell numbers (such as macrophages) to their normal levels in healthy tissues (Ortega-Gómez *et al.*, 2013).

Therefore, inflammation is a complex process in which both pro- and anti-inflammatory components cooperate to restore a tissue's healthy structure. However, disruption of this process can cause chronic conditions (Ortega-Gómez *et al.*, 2013; Chen *et al.*, 2018). Based on pathological features, inflammation can be classified into two main categories: acute and chronic, each varying in duration and intensity (Pahwa *et al.*, 2021). We explore these types further in the following section.

1.2.2 Acute inflammation

Acute inflammation is the immune system's early (almost immediate) biological response to a variety of factors such as harmful stimuli, microbial invasion, toxic compounds, or trauma, involving a complex series of reactions at both cellular and molecular levels (Medzhitov, 2008; Chen *et al.*, 2018; Pahwa *et al.*, 2021). The acute inflammatory response begins rapidly and escalates over a short time (Chandrasoma & Taylor, 1998; Pahwa *et al.*, 2021).

Symptoms of an acute inflammatory response may persist for a few hours or days, such as cellulitis or acute pneumonia (Chandrasoma & Taylor, 1998; Pahwa *et al.*, 2021). Acute inflammation is characterised by five cardinal signs that can be felt or seen: pain around the area of injury due to the release of chemicals that stimulate sensory (pain-sensitive) nerve endings at the affected area; swelling (tumour) due to accumulation of fluid; warmth (increased heat); visible redness of the inflamed skin due to increased blood flow to the capillaries in the area of the injury; loss of tissue function due to vascular changes (Chandrasoma & Taylor, 1998; Takeuchi & Akira, 2010; Chen *et al.*, 2018; Placha & Jampilek, 2021). These signs are most noticeable when acute inflammation occurs on the body's surface, but not all of them will be apparent when acute inflammation occurs in the internal organs (Chandrasoma & Taylor, 1998). Therefore, symptoms of acute inflammation are not always present because they vary depending on the cause of the injury or the site of injury (Chandrasoma & Taylor, 1998; Chen *et al.*, 2018). However, general symptoms associated with acute inflammation include pain, fatigue, and fever (Chandrasoma & Taylor, 1998).

The acute inflammatory reaction initiates with the release of several pro-inflammatory mediators, including interleukins IL-1, IL-6, IL-8, IL-11, and TNF- α (Abdulhaleq *et al.*, 2018; Liu *et al.*, 2021). The process of acute inflammation involves changes in the microcirculation system, including the dilation of capillaries and arterioles, changes in vascular permeability contributing to increased blood flow and fluid exudation, the release of inflammatory mediators, and the recruitment and accumulation of white blood cells (Chandrasoma & Taylor, 1998; Chertov *et al.*, 2000; Ferrero-Miliani *et al.*, 2007; Chen *et al.*, 2018; Placha & Jampilek, 2021). During an acute inflammatory response, various types of leukocytes are recruited at different times to perform diverse functions. These leukocytes migrate from the vasculature to the site of tissue damage (Soehnlein & Lindbom, 2010; Muller, 2013). Neutrophils are typically the first inflammatory cells to reach at the site of tissue damage, moving rapidly compared to other inflammatory cells at a rate of up to 20 m/min in the interstitial tissue, dominating the early phase of inflammatory response (Ferrero-Miliani *et al.*, 2007; Mantovani *et al.*, 2011). There-

fore, infiltration of neutrophil cells into the inflammation site is one of the hallmarks of acute inflammation (Gabay, 2006; Mantovani *et al.*, 2011). Neutrophils are produced in the bone marrow and released into the bloodstream in an already active form. They are the most abundant type of white blood cells in humans (Kolaczkowska & Kubes, 2013). Following this phase, macrophages and immunologically active cells, such as plasma cells and lymphocytes, arrive at the site of inflammation and predominate the area. These inflammatory cells play a crucial role in the resolution of inflammation (Chandrasoma & Taylor, 1998; Gabay, 2006; Ferrero-Miliani *et al.*, 2007).

Acute inflammation can be thought of as a protective reaction against infections and injury, primarily aimed at eliminating and removing the injurious agent (the agent causing the damage) (Chandrasoma & Taylor, 1998; Ortega-Gómez *et al.*, 2013). However, there are several possible outcomes of the acute inflammatory response: resolution of inflammation where injured tissues return to normal, in which mononuclear leukocytes, such as neutrophils and macrophages, remove the noxious agent and debris; repair, when tissue necrosis occurs before debris and damaged cells have been removed, repair begins with either replacing dead cells with regeneration or repairing them by scar formation; chronic inflammation, when the harmful agent is not eliminated during the acute inflammatory response, the inflammation progresses into chronic inflammation (Chandrasoma & Taylor, 1998; Zhou *et al.*, 2016).

The acute inflammatory response is a process that involves a series of localised cellular changes, which typically resolve within hours to days (Serhan & Savill, 2005). This response is considered healthy when the factors causing the damage are removed, including the return of the number of inflammatory cells to normal and the production of pro-inflammatory mediators is halted while anti-inflammatory mediators are released to promote tissue repair and restoration of function. Otherwise, inflammation can progress to a chronic condition (an unhealthy response) (Serhan & Savill, 2005; Ortega-Gómez *et al.*, 2013; Chen *et al.*, 2018).

1.2.3 Chronic inflammation

Although the process of inflammation is complex and involves a wide range of cellular and molecular interactions, dysfunctions of these reactions may affect the normal physiological course of inflammation and cause chronic inflammation (Serhan & Savill, 2005; Pahwa *et al.*, 2021). Chronic inflammation can result from a wide range of factors contributing to its development and proliferation, leading to further damage to tissues. Therefore, chronic inflammation is the sum of body tissue responses against a persistent offending agent, such as viruses, bacteria, toxic chemicals and other noxious

stimuli that can inevitably cause tissue injury or disease (Chandrasoma & Taylor, 1998; Lawrence & Gilroy, 2007). The chronic inflammatory response is slow and persists for an extended time, ranging from months to years or even a lifetime in some chronic inflammatory diseases due to a sustained inflammatory response, such as autoimmune diseases and atherosclerosis (Chandrasoma & Taylor, 1998; Pahwa *et al.*, 2021).

Most manifestations of acute inflammation persist when the inflammation progresses into a chronic state, including increased blood flow in capillaries and arterioles, vasodilatation, vascular permeability, fluid extravasation, and the influx of inflammatory cells into the affected tissue (Ferrero-Miliani *et al.*, 2007; Pahwa *et al.*, 2021). Although the symptoms of chronic inflammation can be silent, common signs may include chronic fatigue, arthralgia, body pain, anxiety, mood disorders, or frequent infections (Chandrasoma & Taylor, 1998; Pahwa *et al.*, 2021). In general, the extent and impact of chronic inflammation vary with the immune system's ability to overcome the cause of the injury and repair damaged tissue (Pahwa *et al.*, 2021; Placha & Jampilek, 2021). At the cellular level, chronic inflammation is characterized by the continuous recruitment of mononuclear cells, such as lymphocytes, macrophages, plasma cells, and fibroblasts (Ferrero-Miliani *et al.*, 2007; Yousuf *et al.*, 2019; Placha & Jampilek, 2021; Pahwa *et al.*, 2021). Thus, a hallmark of chronic inflammation is the presence of mononuclear cells (monocytes), such as macrophages and lymphocytes, at the site of inflammation. Monocytes migrate into the injured tissue through the capillary wall to replace short-lived neutrophils (Gabay, 2006; Ferrero-Miliani *et al.*, 2007). Monocyte-derived macrophages produce a range of pro-inflammatory cytokines, chemokines, and growth factors. Overproduction of these mediators negatively affects tissues, leading to dysfunction of organs and plasma cells and further developing tissue damage (Milenkovic *et al.*, 2019). According to the preceding, the inflammatory response involves a series of biochemical events that may lead to either resolution (a healthy response) or chronic inflammation (an unhealthy response). Figure 1.3 demonstrates the possible outcomes of inflammation.

Chronic inflammation is associated with a wide range of chronic diseases including, but not limited to, heart disease, numerous autoimmune diseases, type 2 diabetes, cancer, arthritis, kidney and liver diseases, and bowel diseases (Chandrasoma & Taylor, 1998; Zhou *et al.*, 2016). The prevalence of chronic diseases is expected to increase throughout the world over the next three decades (Pahwa *et al.*, 2021; Placha & Jampilek, 2021). Thus, chronic inflammatory diseases are considered to be some of the world's most common causes of death (Deepak *et al.*, 2019; Placha & Jampilek, 2021). Chronic inflammation is accompanied by a persistent release of pro-inflammatory me-

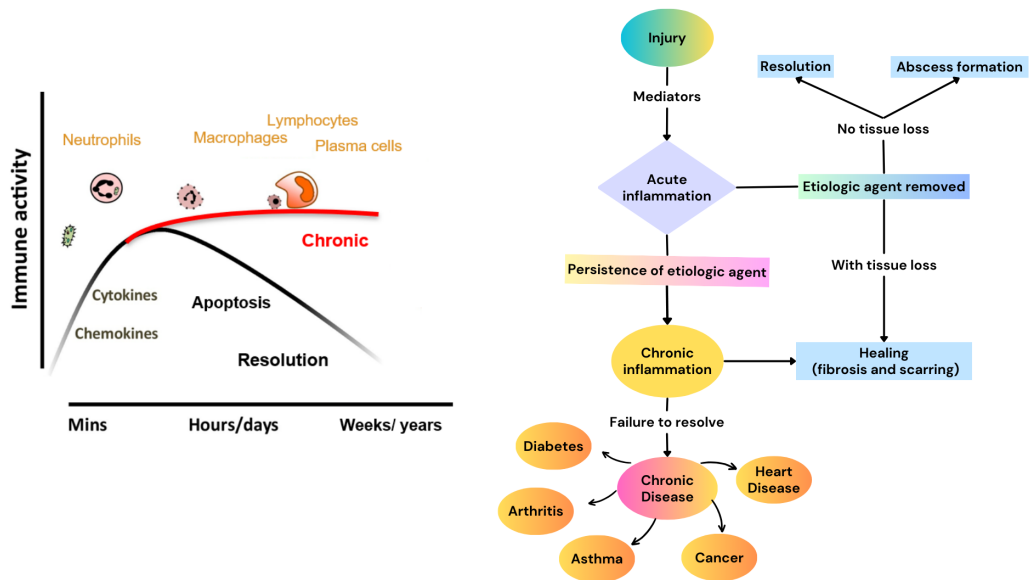


Figure 1.3: The possible outcomes of inflammation are varied. Resolution occurs when damaged tissue returns to its normal morphology, function, and homeostasis. However, tissue necrosis may precede the removal of debris and damaged cells, resulting in healing through the replacement of connective tissue (dead and damaged cells) with regeneration via fibrosis formation or repair through scar formation. Acute inflammation progresses into chronic inflammation when harmful agents remain uneliminated, leading to the sustained release of inflammatory mediators and persistent recruitment of leukocytes to the inflammation site.

diators and the accumulation of inflammatory cells at the inflammation site due to the inability of the immune system to eliminate pathogens and their penetration into affected tissues (Medzhitov, 2008; Placha & Jampilek, 2021; Pahwa *et al.*, 2021). Unfortunately, chronic inflammation can eventually lead to loss of tissue function due to abnormalities in tissue structure after regeneration and replacement by fibrous tissue (Ferrero-Miliani *et al.*, 2007).

Finally, we can think of acute inflammation as the immune system's natural response to injury that is generally beneficial to the body, particularly during infectious challenges. In contrast, chronic inflammation is the persistent harmful type because it is associated with many chronic inflammatory diseases that can subsequently lead to significant organ dysfunction. Table 1.1 summarizes some of the major differences between acute and chronic inflammation.

Feature	Acute	Chronic
Onset	immediate	delayed
Duration	short (hours to days)	long (weeks to years)
Cause	tissue injury or harmful pathogens that the immune system can eliminate	foreign bodies and pathogens that remain in the body and the immune system can not remove them
Inflammatory cells	mainly neutrophils, followed by macrophages	macrophages, lymphocytes, and plasma cells.
Vascular changes (Outcomes)	resolution of inflammation, abscess formation, chronic inflammation	tissue destruction, scar tissue, fibrosis

Table 1.1: Differences between acute and chronic inflammation.

1.3 Key cells involved in inflammation

White blood cells, also known as leukocytes, are the primary cellular components of human blood that contain a nucleus, distinguishing them from other blood cells (Khamael *et al.*, 2020; Kannan *et al.*, 2023). They are produced by hematopoietic stem cells found in the bone marrow and are present throughout the body, including the lymphatic system, connective tissues, and the bloodstream (Yao *et al.*, 2021). White blood cells play a vital role in the immune system by protecting the body from infections and diseases.

White blood cells can be categorized into two main groups: granulocytes (including neutrophils, basophils, and eosinophils) and agranulocytes. The agranulocytes are further divided into monocytes, which differentiate into either macrophages or dendritic cells, and lymphocytes (including B-cells and T-cells) (Yao *et al.*, 2021; Baghel *et al.*, 2022). Each type of white blood cell has different morphological features such as size, nucleus, shape, texture, and shape of the cytoplasm (Khamael *et al.*, 2020). They also have the unique function of defending the body against foreign particles. Figure 1.4 illustrates the different types of white blood cells in the body.

Granulocytes have large nuclei and visible granules in the cytoplasm, and their lifespan within the tissue ranges from hours to days. The diameter of the largest cell is about 12–20 μm (Al-Dulaimi *et al.*, 2018). Neutrophils are the most abundant type of white blood cells, representing 50–70% of the total white blood cells, with a diameter of approximately 10–18 μm (Al-Dulaimi *et al.*, 2018; Yao *et al.*, 2021). Monocytes are

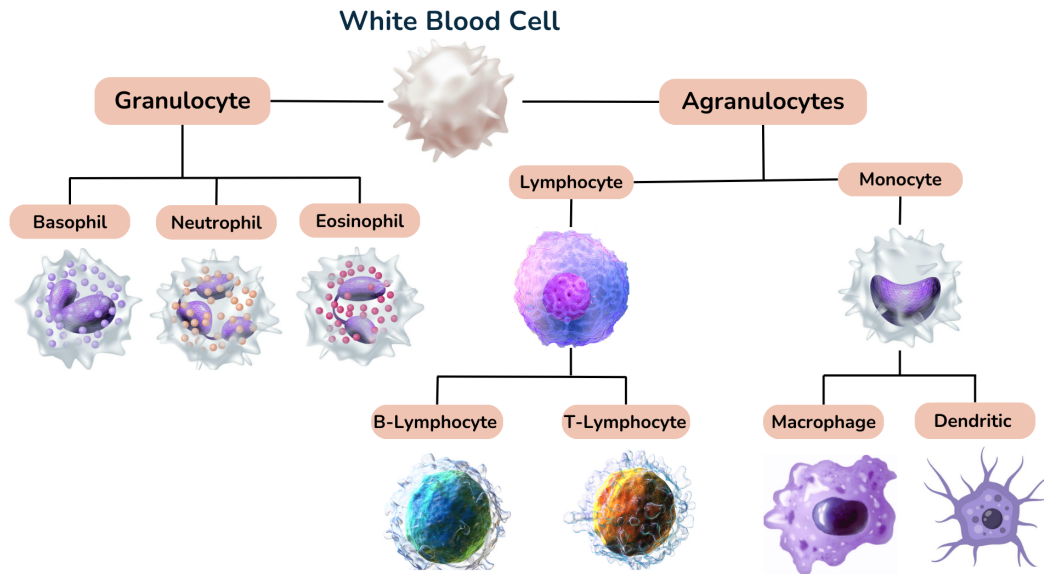


Figure 1.4: Different types of white blood cells.

longer-lived cells and the largest type of white blood cells with a diameter of approximately 10–30 μm , containing only a single nucleus (Abbas & Rydh, 2012). Neutrophils and monocytes both function as phagocytic cells. The sizes and lifespans of white blood cells can be influenced by various factors, including the cell's activation state, the type of infection, and their specific tissue environment (Al-Dulaimi *et al.*, 2018).

White blood cells account for only 1% of the total human blood volume (Jiang *et al.*, 2022). In a healthy body, the count of white blood cells ranges from 4,500 to 11,000 per microliter (Riley & Rupert, 2015; Gajbhiye & Aate, 2023). These cells play a significant role in monitoring an individual's health condition and diagnosing various blood-related diseases. A low count of white blood cell can be due to several reasons, such as certain medications or due to something more serious, like a weakened immune system (HIV/AIDS) or blood cancer (leukaemia) (Suryani *et al.*, 2015; Gajbhiye & Aate, 2023). Therefore, a human body that suffers from a low number of white blood cells is more susceptible to infections and chronic diseases due to the body's lack of immune cells to counter foreign particles such as invading bacteria and viruses. On the other hand, when the number of white blood cells in the body is higher than normal (also known as leukocytosis), it often indicates that the body is fighting infection, injury, or inflammation (Riley & Rupert, 2015), but in rare cases, it indicates something more serious, such as myelodysplastic syndrome (Ghoti *et al.*, 2007). The following section briefly reviews macrophages and their function in the body.

1.3.1 Macrophages and their functions in the body

Circulating macrophages are a type of white blood cell originating from circulating monocytes produced by hematopoietic stem cells in the bone marrow (Wynn *et al.*, 2013; Chen & Zhang, 2017; T'Jonck *et al.*, 2018). Tissue-resident macrophages have diverse origins, such as fetal liver monocytes and yolk sac macrophages (Davies *et al.*, 2013; Ginhoux & Guilliams, 2016; Chen & Zhang, 2017). Macrophages are the largest type of white blood cell, with a diameter ranging from 10 to 30 μm , and have a lifespan that varies from months to years (Krombach *et al.*, 1997; Prinyakupt & Pluempitiwiriyawej, 2015).

Macrophages are mononuclear phagocytic cells capable of motility and spread in all tissues and organs of the body (Laskin *et al.*, 2011). They are responsible for engulfing and digesting foreign particles, diseased cells, pathogens, and harmful substances in the body (Wynn *et al.*, 2013). Macrophages are also referred to as “cell-eating machines” or “big eaters of immune cells” (Kain & Halade, 2015; Weigert *et al.*, 2019). In general, macrophages are versatile cells that fulfil various essential activities as part of the innate immune system, including the clearance of cellular debris, tissue maintenance, and regulation of the immune response (Eming *et al.*, 2007; Chen & Zhang, 2017). In response to inflammatory signals, they are rapidly recruited to the site of inflammation or infection to fulfil their role in defence against pathogens (Grabher *et al.*, 2007).

Macrophages and neutrophils are the first white blood cells to respond to infection, acting as the body's first line of defence against pathogens (Wynn *et al.*, 2013; Jackson, 2016). Macrophages recognise foreign invaders, such as bacteria and other harmful organisms, through a special receptor system on their surface called Toll-like receptors (TLRs) (*e.g.* Dectin-1 and the mannose receptor (CD206)). For instance, the mannose receptor (CD206) recognises mannosylated ligands on fungi, viruses, and bacteria (Mills, 2012; Jackson, 2016). Macrophages are attracted to the site of an injury or infection by receiving chemical signals sent by bacteria. Macrophage receptors interact with the surface of the pathogen. They then phagocytose bacteria or unwanted particles, producing reactive oxygen species that kill the phagocytosed cell through a process called phagocytosis, as shown in Figure 1.5. Macrophage receptors can distinguish healthy body cells from foreign particles, such as bacteria, by recognizing the specific structure of proteins on the surface of healthy body cells and pathogen-specific carbohydrate or lipid structures (Taylor *et al.*, 2005; Plüddemann *et al.*, 2006; Gordon, 2016). Therefore, macrophages play a central role in detecting, eliminating and destroying pathogens, apoptotic cells and other harmful organisms by engulfing them (Rogler, 2017).

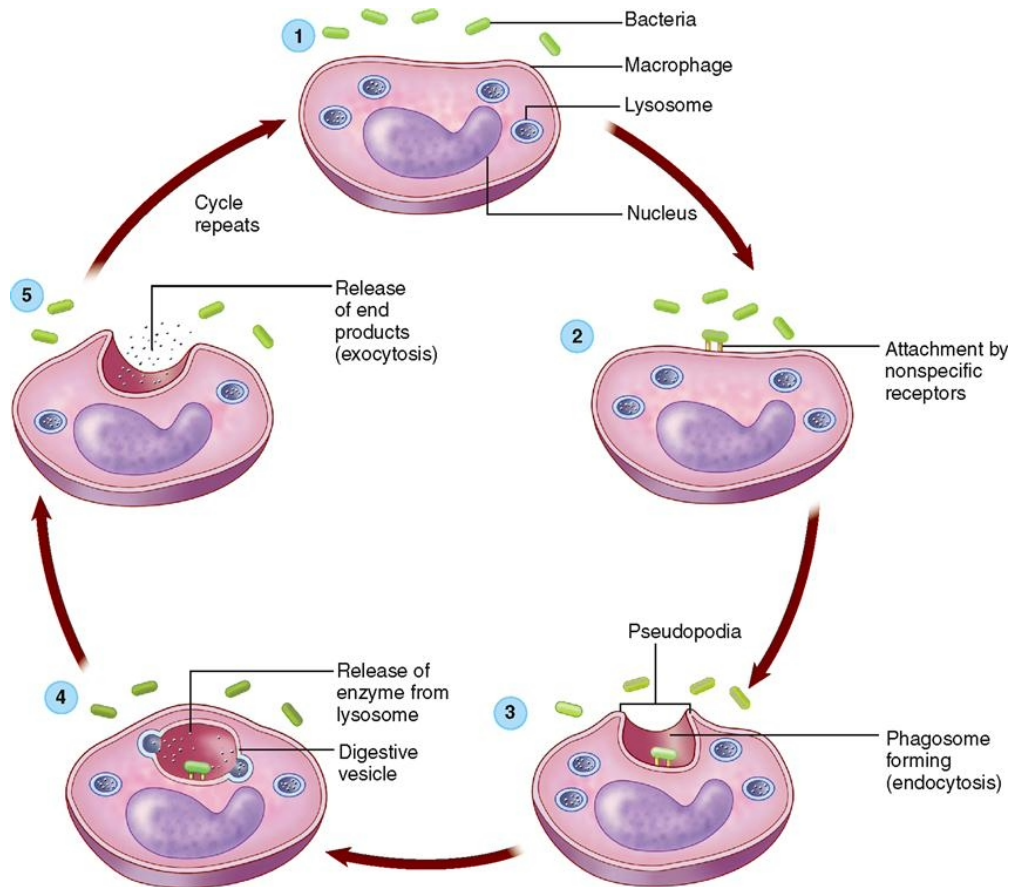


Figure 1.5: Phagocytosis of bacteria by macrophages. Source of image: <https://basicmedicalkey.com/immune-system/>. (Jan. 2023)

Macrophages play a critical role in initiating the inflammatory response by releasing a wide array of cytokines, chemokines, and growth factors that attract other immune cells to the site of inflammation (Hirayama *et al.*, 2018). Moreover, macrophages activate the action of other immune system cells such as lymphocytes. They work to destroy potential pathogens, such as viruses, by presenting antigens (usually protein molecules) to T-lymphocytes to regulate the immune response, and to B-lymphocytes for antibody production (Jackson, 2016). In addition to the prominent role of macrophages in alerting the immune system in case of tissue damage and infection, macrophages also function in physiological healing, repair and remodelling of tissues, and maintaining tissue homeostasis (Laskin *et al.*, 2011; Chen & Zhang, 2017; T'Jonck *et al.*, 2018).

Tissue-resident macrophages have several main common functions, such as phagocytosis, antigen presentation, and initiation of immune responses. Besides these common functions, each macrophage population has a unique function and identity that depends on the tissues in which they reside (Tamoutounour *et al.*, 2013). For exam-

ple, lung alveolar macrophages are involved in the clearance of inhaled pathogens and xenobiotics (Trapnell *et al.*, 2003; Laskin *et al.*, 2011). Microglia macrophages in the brain are essential for brain development and homeostasis, and they are also involved in brain monitoring by constantly probing the cellular environment (Paolicelli *et al.*, 2011). Cardiac macrophages facilitate electrical conduction in the heart through connexin 43-containing gap junctions with cardiomyocytes (Hulsmans *et al.*, 2017). Resident macrophages in the liver (also known as Kupfer cells) are involved in removing endotoxin and other foreign materials from the portal circulation (Laskin *et al.*, 2011).

The function of macrophages varies depending on their response to various signals that they receive from inflammatory mediators. For instance, upon exposure to pro-inflammatory mediators such as tumour necrosis factor (TNF- α) and interleukins IL-8 and IL-12, macrophages are stimulated to recognise and eliminate harmful stimuli, including apoptotic neutrophils (Mantovani *et al.*, 2002; Mosser & Edwards, 2008; Mills, 2012; Hirayama *et al.*, 2018). On the other hand, when exposed to anti-inflammatory mediators such as transforming growth factor- β and interleukins IL-4, IL-10, and IL-13, macrophages are prompted to regulate the inflammatory response and tissue remodelling and repair (Mills, 2012; Dunster, 2016; Ponzoni *et al.*, 2018). Pro- and anti-inflammatory mediators play contrasting roles in the inflammatory response, and macrophages' functions are closely associated with the type of signals they receive from these mediators.

Despite the crucial role that macrophages play in fighting diseases as part of the normal immune response to acute inflammation, they may also have a negative impact on inflammation in the case of aberrations in their activities (Laskin *et al.*, 2011). Several studies have revealed that pathogens directly affect tissue injury, while macrophages indirectly impact the affected tissues, exacerbating tissue injury and its progression into a chronic disease (Laskin *et al.*, 2011; Chen & Zhang, 2017; T'Jonck *et al.*, 2018). This concept regarding the contribution of macrophages to the pathogenesis of many chronic diseases has become popular and well-established, with ample evidence to support it in various organs such as skin (Aitchison *et al.*, 2021), lung (Gwyer Findlay & Hussell, 2012; Aggarwal *et al.*, 2014), liver (Sica *et al.*, 2014), brain (Hu *et al.*, 2015), and kidney (Cao *et al.*, 2015).

Macrophages exhibit remarkable plasticity and heterogeneity in response to various stimuli, allowing them to change into distinct phenotypes with different functional properties during the inflammatory response (Biswas & Mantovani, 2010; Saqib *et al.*, 2018). The functional phenotype of macrophages changes gradually in response to the alterations in their environmental signals and molecular mediators, a process known as

polarisation (Mantovani *et al.*, 2005; Mosser & Edwards, 2008). The process of macrophage polarisation is tightly regulated by a range of chemical signals produced by both pro- and anti-inflammatory mediators, which aim to resolve inflammation and maintain tissue homeostasis (Murray *et al.*, 2014; Saqib *et al.*, 2018).

The classification of macrophages is still considered a controversial topic. However, macrophages can be classified into two main subtypes based on their function: pro-inflammatory macrophages (referred to as M1 or classically-activated) and anti-inflammatory macrophages (also known as M2 or alternatively-activated) (Mosser & Edwards, 2008; Wynn *et al.*, 2013; Martinez & Gordon, 2014; Rigamonti *et al.*, 2014). Alternatively, some scientists claim that a continuum of intermediate phenotypes exists lying between the two extremes above, with phenotypic changes occurring in response to gradual changes in their microenvironment (Palma *et al.*, 2018). These subtypes differ in morphology, cell surface markers, biological functions, type of identifiable pathogens, and secreted cytokines (Torres *et al.*, 2019). However, it should be noted that the binary classification oversimplifies the complex functional activity of these cells and cannot represent most types of macrophages' *in vivo* environments (Wynn *et al.*, 2013; Porcheray *et al.*, 2005).

Dysfunctions in macrophage phenotypes have been associated with several chronic diseases (Funes *et al.*, 2018). For instance, increased infiltration or prolonged activation of pro-inflammatory macrophages can cause an increase in their oxidation products, such as reactive oxygen species, resulting in malfunction, cancer, or autoimmune diseases (Smith *et al.*, 2009). On the other hand, an increased influx of anti-inflammatory macrophages has been associated with a poor prognosis, while a reduced population of anti-inflammatory macrophages could be implicated in the development of injurious inflammation and autoimmunity (Funes *et al.*, 2018). Therefore, understanding the precise roles of macrophage phenotypes may help to reveal potential therapeutic targets in inflammatory diseases. In the following section, we delve into the main features of pro- and anti-inflammatory phenotypes.

1.3.2 Pro-inflammatory macrophage polarisation and related mediators

In the context of inflammation, a cascade of inflammatory mediators, including cytokines and chemokines, is released that direct the inflammatory response and attract immune cells to damaged tissue. Monocytes are recruited from the bloodstream and change into macrophages upon entering infected tissue. These macrophages have the ability to switch towards pro-inflammatory activity in response to environmental cues present at the inflammation site, during which they identify and eliminate

harmful stimuli (Mosser & Edwards, 2008; Sica *et al.*, 2012; Saqib *et al.*, 2018). However, macrophages can also switch to anti-inflammatory activity, suppressing the pro-inflammatory response, removing unwanted substances, and promoting tissue repair. Macrophage influx is expected to become more pro-inflammatory in proportion to the concentration of pro-inflammatory mediators. Conversely, it tends to be anti-inflammatory in proportion to the concentration of more anti-inflammatory mediators (Mosser & Edwards, 2008), as illustrated in Figure 1.6.

Macrophages produce both pro- and anti-inflammatory mediators during the inflammatory response. As a result, these cells have the ability to perform various functions in response to stimuli, including cytokine production, phagocytosis, and tissue repair and remodelling. These macrophages acquire a pro-inflammatory phenotype upon exposure to pro-inflammatory mediators, including interleukins (IL-1 β , IL-8 and IL-12), tumour necrosis factor- α (TNF- α), interferon- γ (IFN- γ), and lipopolysaccharides (LPS) (Mosser & Edwards, 2008; Classen *et al.*, 2009; Sica *et al.*, 2012; Dunster, 2016; Saqib *et al.*, 2018). In addition, several pathways drive macrophages to pro-inflammatory macrophage polarisation, including the LPS/TLR4, IRF/STAT, and NF-KB/PI-3 kinase pathways (Huang *et al.*, 2018).

Macrophages with pro-inflammatory properties eliminate pathogens, present their antigens to the adaptive immune system, and remove debris and dead cells (including apoptotic neutrophils). Moreover, they are involved in producing pro-inflammatory cytokines that promote pro-inflammatory response, such as interleukins (IL-1 β , IL-6, IL-12, and IL-23), TNF- α , reactive oxygen species, reactive nitrogen species, and inducible nitric oxide synthase (Biswas & Mantovani, 2010; Laskin *et al.*, 2011; Saqib *et al.*, 2018; Atri *et al.*, 2018). Therefore, the function of pro-inflammatory macrophages is associated with the high production of pro-inflammatory cytokines. Moreover, phenotypes of pro-inflammatory macrophages are associated with high levels of Th1 cell-attracting chemokines and the major histocompatibility complex class II (MHC II), and the cluster of differentiation like CD68, CD80, and CD86 (Biswas & Mantovani, 2010). Therefore, pro-inflammatory macrophages exhibit potent microbicidal and tumoricidal activity and release several mediators that promote strong pro-inflammatory immune responses (Laskin *et al.*, 2011).

Pro-inflammatory mediators play a crucial role in polarizing the pro-inflammatory macrophage phenotype. However, prolonged activation of pro-inflammatory macrophages can cause exacerbating tissue injury, leading to chronic diseases (Sieweke & Allen, 2013; Italiani & Boraschi, 2014). Macrophages can switch from pro-inflammatory to anti-inflammatory macrophages in response to microenvironmental

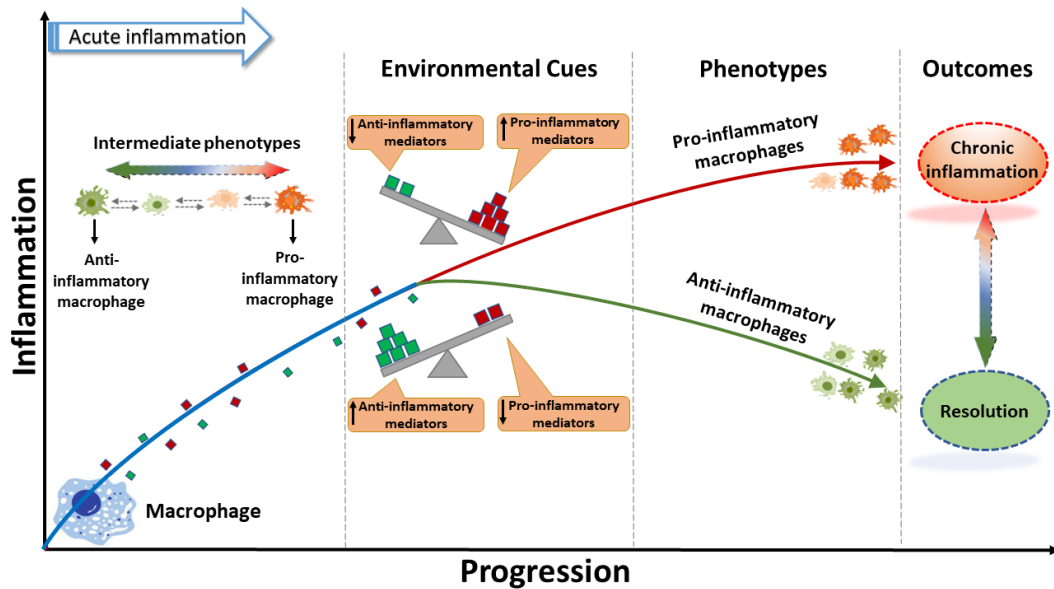


Figure 1.6: Phenotypic switching in macrophages is a dynamic process regulated by the microenvironment, wherein macrophages adopt distinct functions with molecular properties that differentiate phenotypes. Macrophages can change their phenotype in response to environmental cues, with inflammatory mediators playing a crucial role in the polarisation of macrophage phenotype.

cues and vice versa. Pro- and anti-inflammatory macrophages differ in phenotype, stimuli, cytokine release, and functions (Mosser & Edwards, 2008; Martinez *et al.*, 2009; Hirayama *et al.*, 2018). In the following section, we will briefly review anti-inflammatory macrophages.

1.3.3 Anti-inflammatory macrophage polarisation and related mediators

The activity of pro-inflammatory macrophages is balanced by the role of anti-inflammatory macrophages, which endeavour to suppress inflammation (Laskin *et al.*, 2011). The phenotype of anti-inflammatory macrophage can be activated by various stimuli, including interleukins IL-4, IL-10 and IL-13, apoptotic cells, and transforming growth factor- β (TGF- β) (Mosser, 2003; Gordon & Martinez, 2010; Biswas & Mantovani, 2010; Atri *et al.*, 2018). Anti-inflammatory macrophages produce anti-inflammatory cytokines such as interleukin IL-10 and transforming growth factor- β (TGF- β) (Mosser & Edwards, 2008; Martinez *et al.*, 2009; Gordon & Martinez, 2010; Hirayama *et al.*, 2018). Anti-inflammatory macrophages promote an anti-inflammatory response, clear apoptotic cells and debris, promote cell growth, and tissue repair and maintain tissue homeostasis (Atri *et al.*, 2018; Shapouri-Moghaddam *et al.*, 2018). Figure 1.7 illustrates the main triggers and the production linked with each distinct macrophage phenotype.

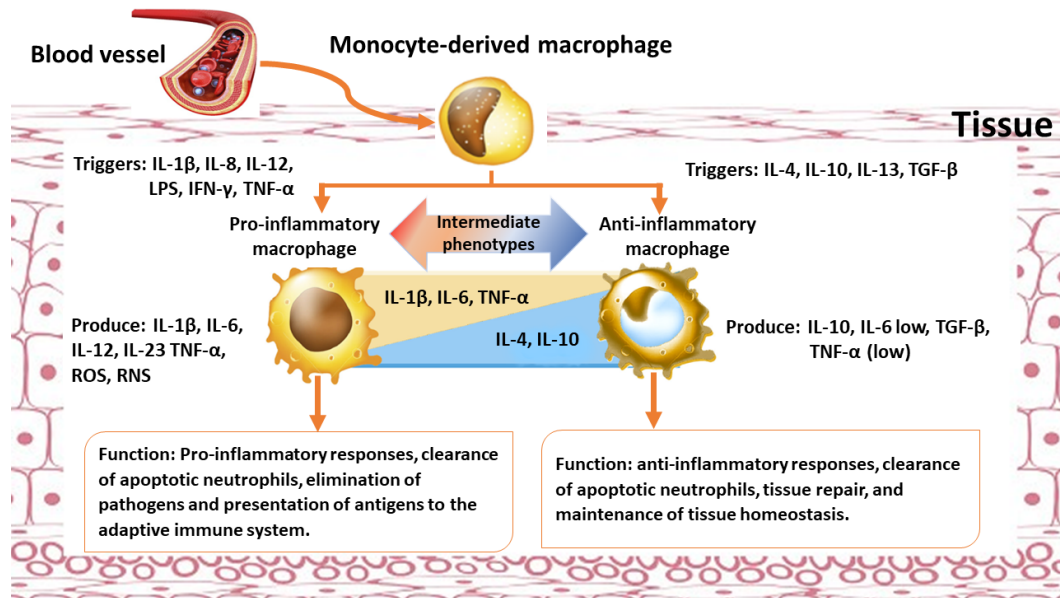


Figure 1.7: Schematic overview of macrophage polarisation: triggers, cytokine release, and functions. Monocytes are recruited from the bloodstream to differentiate into macrophages, acquiring specific phenotypes upon exposure to stimuli. Monocyte-derived macrophages exhibit a continuum of intermediate phenotypes that lie between pro- and anti-inflammatory macrophages, which change in response to gradual changes in their microenvironment. Pro- and anti-inflammatory macrophages differ in phenotype, stimuli, cytokine release, and functions. Pro-inflammatory macrophage polarisation is triggered by interleukins (IL-1 β , IL-8, IL-12), lipopolysaccharide (LPS), tumour necrosis factor- α (TNF- α), and interferon- γ (IFN- γ). In contrast, anti-inflammatory macrophage polarisation is stimulated by interleukins (IL-4, IL-10, IL-13) and transforming growth factor- β (TGF- β). Pro-inflammatory cytokines, such as IL-1 β , IL-6, IL-12, IL-23, TNF- α , reactive oxygen species (ROS), and reactive nitrogen species (RNS), are typically released by pro-inflammatory macrophages. In contrast, anti-inflammatory macrophages produce anti-inflammatory cytokines, such as IL-10 and TGF- β . Both pro- and anti-inflammatory macrophages have different functions. Anti-inflammatory macrophages suppress inflammation by releasing large amounts of IL-4, IL-10 and TGF- β , contributing to the maintenance of tissue homeostasis. Uncontrolled polarisation of macrophages can contribute to chronic disease.

In contrast to pro-inflammatory macrophages, anti-inflammatory macrophages secrete a low level of inflammatory cytokines such as IL-1, IL-6, and TNF- α , but release an elevated level of anti-inflammatory cytokines such as IL-4, IL-10, and IL-13, and transforming growth factor (TGF)- β , to suppress inflammation (Laskin *et al.*, 2011; Chen & Zhang, 2017; Atri *et al.*, 2018). Therefore, maintaining an optimum balance between pro- and anti-inflammatory macrophages is critical in resolving inflammation. Table 1.2 summarises markers used to distinguish between pro- and anti-inflammatory macrophages.

Phenotype	Stimuli	Cytokines, chemokines, and other secreted mediators	Cell expression markers
Pro-inflammatory macrophages	LPS, IFN- γ , TNF- α	TNF- α , IL-1 β , IL-6, IL-12, IL-23, IL-27, NOS, ROS, RNS, CXCL9, CCL8, CCL19, CCL20, CXCL10, CXCL11, CXCL16	IL-12 high, NOS, TLR-2, IL-10 low, TLR-4, MHC-II, CD16, CD32, CD64, CD68, CD80
Anti-inflammatory macrophages	IL-4, IL-13, TGF- β	IL-10, TGF- β , VEGF, TNF- α , IL-1 β , IL-6, CCL17, CCL18, CCL22, CCL24, CXCL13	IL-10 high, MMR/CD206, IL1-ra, TLR-1, VEGF, TNF- α low, IL-12 low, CD86, CD115, CD204, CD163

Table 1.2: Summary of the major biological and physiological markers of pro- and anti-inflammatory macrophage phenotypes observed in living organisms. Abbreviations: LPS= lipopolysaccharide; IFN=interferon; TNF= tumour necrosis factor; IL = interleukin; TGF= transforming growth factor; ROS/RNS= reactive oxygen/nitrogen species; NOS= nitric oxide synthase; CXCL/CCL= chemokine; VEGF= vascular endothelial growth factor; TLR= toll-like receptor; IL1-ra= receptor antagonist; MHC= major histocompatibility complex; MMR= macrophage mannose receptor; CD= cluster of differentiation.

1.4 Previous mathematical models of inflammation

The interest in inflammation has been surging due to its association with a wide range of chronic inflammatory diseases, including cancer, type 2 diabetes, Alzheimer's disease, arthritis, and asthma (Piché *et al.*, 2020; Paolini P. *et al.*, 2021; Wang *et al.*, 2021; Blüher & Müller-Wieland, 2022). The lack of full knowledge of the interactions that regulate the inflammatory process has hindered the development of effective and appropriate therapeutic strategies. Therefore, mathematical modelling of biological processes has captured great interest among the scientific community as it aims to provide reliable simulations that enable us to predict possible outcomes of complex biological issues (Tomlin & Axelrod, 2007; Vasieva *et al.*, 2013). Hence, mathematical models can be used to shed light on some of these aspects to better understand the mechanisms underlying chronic inflammation and identify the inflammatory pathways involved in chronic diseases, which may represent new therapeutic targets.

Various techniques are used in mathematical modelling to capture the interactions underlying the inflammatory process in both a generic context and tailored to particular infections/disease scenarios. These techniques include statistical-technique-based, mathematical analysis-based, and machine learning-based models. (A review of these

is given by Prasad *et al.* (2022).) Furthermore, Vodovotz *et al.* (2013) proposed various approaches that can be used to understand and potentially control the acute inflammatory response, such as *in silico* trials (computational simulations of clinical trials), equation-based models, agent-based models, and hybrid models (combining computational models comprising multiple scales). This section delves into recent studies that model macrophages computationally and mathematically and their role in the inflammatory process.

To date, many mathematical models have been proposed that capture the roles of macrophages and other immune cells in the mechanisms that underlie inflammation. These aspects can be summarized as follows: the influence of motility of inflammatory cells (including neutrophils and macrophages) driven by chemotaxis on the response outcome (Bie *et al.*, 2010; Dunster *et al.*, 2014; Brady *et al.*, 2016; Bayani *et al.*, 2020a; Solis & Azofeifa, 2020); particular roles played by macrophages, such as clearing apoptotic neutrophils (Sherratt & Dallon, 2002; Liang *et al.*, 2007; Raza *et al.*, 2010; Kraakman *et al.*, 2014) and clearing debris or releasing inflammatory mediators; the ability of the inflammatory response to resolve (Reynolds *et al.*, 2006; Delavary *et al.*, 2011; Penner *et al.*, 2012; Shu *et al.*, 2020); and the examination of certain inflammatory diseases that involve macrophage populations (Vodovotz *et al.*, 2004; Marée *et al.*, 2006, 2008; Parameswaran & Patial, 2010; Baker *et al.*, 2013; Dobрева *et al.*, 2021).

1.4.1 Models containing a single homogenised macrophage population

Numerous mathematical models have been proposed to elucidate the roles of macrophages in the resolution of inflammation. However, many of these models take the simplistic approach of assuming a homogenised macrophage population that may encompass a wide range of distinct phenotypes (Kumar *et al.*, 2004; Lelekov-Boissard *et al.*, 2009; Herald, 2010; Penner *et al.*, 2012; Dunster *et al.*, 2014; Bianca *et al.*, 2015; Cooper *et al.*, 2015; Bangsgaard *et al.*, 2017; Bayani *et al.*, 2020a,b; Solis & Azofeifa, 2020). Kumar *et al.* (2004) developed a simple three-dimensional ordinary differential equation model of the inflammatory response to infection, which combines the effects of early-responding immune cells (neutrophils, mediators) and late pro-inflammatory feedback. The model includes interactions between a generic pathogen and two classes of pro-inflammatory responses. After clarifying how model parameters influence response outcomes, the authors provide a diverse therapeutic approach for persistent infectious inflammation (sepsis), focusing on reducing late pro-inflammatory reactions. Reynolds *et al.* (2006) expanded on this work by including a time-dependent anti-inflammatory response and examining how modifying this response might lead

to possible new therapeutic interventions.

Mathematical modelling has been extensively applied to the inflammation process, which involves a single homogenised population of macrophages in response to tissue damage or pathogenic infection, focusing largely on how total numbers/concentrations of cells and mediators evolve temporally in the tissue of interest. Serhan *et al.* (2008) proposed a model of inflammation that studies the dynamics of anti-inflammatory processes. This study presented mechanisms for inflammation resolution involving anti-inflammatory and pro-resolution lipid mediators with neutrophils and macrophages. The authors suggest that the resolution of inflammation derives from anti-inflammatory processes, whereby pro-resolution molecules promote the clearance of apoptotic cells and microbes by macrophages, and anti-inflammatory mediators act to stop and lower neutrophil infiltration to inflamed tissues, enabling return to homeostasis. To overcome the bias of the model toward anti-inflammatory dynamics in the interactions between bacteria and phagocytosing cells, Brady *et al.* (2016) proposed a mathematical model investigating the pro- and anti-inflammatory interactions arising from pathogenic microbial infection. The model was calibrated to experimental data obtained from a sample of 20 healthy young males who received a low-dose intravenous injection of lipopolysaccharide (LPS). This trial measured levels of pro-inflammatory cytokines (chemokine ligand-8 (CXCL8), interleukin-6 (IL-6), and tumour necrosis factor (TNF)) and anti-inflammatory cytokines (interleukin-10 (IL-10)) over 8 hours in a chosen sample. Since relevant cytokines are modelled and taken into account independently, the model lacks the analysis of inflammatory pathways resulting from other mediators that are left out. Brady *et al.* (2018) and Dobрева *et al.* (2021) expanded this work to include the prediction of blood pressure and changes in heart rate variability.

The removal of apoptotic neutrophils by macrophages was considered a significant driver of inflammation resolution in the models developed by Dunster *et al.* (2014). The study used a series of models formulated as systems of ordinary differential equations (ODEs). The minimal model focused on the interactions of a single homogenised population of macrophages, active and apoptotic neutrophil populations, and generic pro-inflammatory mediators. The basic model was expanded to integrate additional positive feedbacks, representing an active neutrophils' ability to release pro-inflammatory mediators and cause damage to healthy tissue. Eventually, anti-inflammatory mediators produced by macrophages were included. The study suggested that the resolution of inflammation is an active anti-inflammatory process, in which macrophages remove the pro-inflammatory activity generated by apoptotic neutrophils that can damage healthy tissue when their toxic content leaks out. The study reported that an effec-

tive approach to resolving inflammation requires targeting both macrophage phagocytosis and neutrophil apoptosis rates. This work was later extended to incorporate spatial descriptions of motile cells and inflammatory mediators via corresponding partial differential equation models (Bayani *et al.*, 2020a) and agent-based models (Bayani *et al.*, 2020b), the latter of which were calibrated against relevant *in vivo* cell trajectory data. Solis & Azofeifa (2020) developed a mathematical model to describe an inflammatory disease that targets macrophages as a potential therapeutic target for resolving inflammation. The ODE model includes a single population of macrophages, active and apoptotic neutrophils and pathogens, and a few pro-inflammatory cytokines. The resolution of inflammation can be improved by stimulating the death rate of neutrophils and the rate at which macrophages engulf dead neutrophils. However, the study did not include all the pro- and anti-inflammatory mediators to investigate the possible outcomes of the inflammatory response.

Many studies have revealed that macrophages produce pro- and anti-inflammatory mediators in response to various environmental cues (Stout *et al.*, 2005; Porcheray *et al.*, 2005; Mosser & Edwards, 2008; Mills, 2012; Martinez & Gordon, 2014; Hirayama *et al.*, 2018). However, it has been observed that many single homogenised macrophage models ignore the inclusion of both generic pro- and anti-inflammatory mediators. For instance, Dunster *et al.* (2014) and Bayani *et al.* (2020a) assumed macrophages only release generic anti-inflammatory mediators to promote their anti-inflammatory role by removing apoptotic neutrophils, overlooking their crucial role in a pro-inflammatory activity involving the release of pro-inflammatory mediators. Many researchers suggest that therapeutic strategies derived from macrophage-centric models, assuming that resolving inflammation solely involves suppressing it, are ineffective because these models ignore the pro-inflammatory role played by macrophages. Instead, they advocate a therapeutic approach that focuses on controlling and reprogramming inflammation as a more effective strategy (Vodovotz *et al.*, 2013; Brady *et al.*, 2016).

1.4.2 Models containing multiple macrophage populations

Some existing models do account for distinct phenotypes separately and have explicitly incorporated two distinct macrophage populations, normally referred to as M1 and M2 (Vaugh & Sherratt, 2006; Wang *et al.*, 2012; Lee *et al.*, 2017; Torres *et al.*, 2019; Shu *et al.*, 2020; Minucci *et al.*, 2021; Dunster *et al.*, 2023; Nelson *et al.*, 2023). Macrophage phenotypes play a crucial role in the development and resolution of inflammation. Dysfunction or disruption between pro- and anti-inflammatory macrophage activities has been implicated in many inflammatory diseases. For instance, the accumulation of M1

macrophages in adipose tissue can lead to atherosclerosis and type 2 diabetes (Mosser & Edwards, 2008; Bie *et al.*, 2010), while overpopulation of M2 macrophages can cause disorders such as allergies and asthma (Delavary *et al.*, 2011). Lee *et al.* (2017) developed a mathematical model of the macrophage response to viral infection to predict the outcomes of the inflammatory response by manipulating the strength and duration of viral infection. The model includes two distinct populations of macrophages (M1 and M2), two cytokines (interferons and IL-4), and two enzymes (nitric oxide synthase and arginase-1). However, the model lacks the analysis of inflammatory pathways resulting from other mediators that have been excluded.

Many researchers have already developed and investigated mathematical models of inflammation that include two distinct populations of macrophages classified into pro- and anti-inflammatory activities with a focus on their dynamics and progression led by infectious sources. To capture the contradictory roles of macrophage phenotypes, Torres *et al.* (2019) developed a cellular-level inflammatory response model focusing on the sequential influx of immune cells in response to a bacterial stimulus. The ODE model includes M1 and M2 macrophages, active and apoptotic neutrophils, pathogens, and an inflammatory stimulus. The model was calibrated to experimental data obtained from a mouse peritonitis model of inflammation, which is frequently used to assess endogenous processes in response to an inflammatory stimulus. The model can predict the outcomes of acute inflammatory responses targeting macrophage phenotypes. The model also reveals that dysfunction of a phenotypic switch of macrophages can disrupt the timely influx and egress of immune cells within the healing process and cause chronic disease. Knowing which subpopulations of macrophages to modulate is essential for development of therapeutic interventions that promote inflammation resolution. The study excluded pro- and anti-inflammatory mediators from the model components since they cannot be measured experimentally; instead, it used feedback loops to describe their effects on the inflammatory response. On the other hand, the authors recommended including pro- and anti-inflammatory mediators to improve a future model since they influence the function of infiltrated immune cells.

To investigate the effects of M1 and M2 macrophages on tumour growth, Shu *et al.* (2020) proposed a simple mathematical model that describes the interactions between the macrophages and tumour cells. The model excluded inflammatory mediators and instead relied on tumour cells to trigger the response. The model consists of three ordinary differential equations, and bifurcation analysis was used to investigate how changes in model parameters affect the outcomes. The study suggests that targeting both the activation rate of M1 and M2 macrophages by tumour cells and the switching

rate between M1 and M2 macrophages could be a dual therapeutic strategy to reduce tumour cells. This study provides evidence of the significant role played by the rate of macrophage phenotype switching (between M1 and M2) as a potential therapeutic target for chronic diseases.

Mathematical modelling has extensively been applied to inflammation in various contexts, including cells, tissues, and organs. Traditional models that take the approach of incorporating all macrophages into a single homogenised population, regardless of their phenotype, provide a useful approach in terms of model tractability. However, they could potentially bias the resulting dynamics if macrophage descriptions are not sufficiently robust. Prior mathematical modelling reveals that the explicit inclusion of distinct populations of opposing macrophage phenotypes can potentially give rise to a more complex range of behaviours than is exhibited by models with a single homogenised population. However, it is currently unclear to what extent this modelling choice affects the range of dynamics and outcomes that the models predict. Furthermore, constructing models that include the full repertoire of macrophage phenotypes in a typical inflammatory environment is challenging, not least given the fast-evolving picture of the complexity of polarisation states, with many intermediate phenotypes lying between the M1 and M2 extremes (Murray *et al.*, 2014). In this work, we seek to further elucidate the potential impact that distinct modelling choices regarding macrophage phenotype descriptions have upon resulting model dynamics, by systematically building the complexity of corresponding models and carefully analysing the resultant changes in our models' predictions. An outline of the structure of this thesis is provided in the following section.

1.5 Thesis overview

In this work, we will present and analyse four models of inflammatory dynamics that incorporate increasing levels of detail regarding the complex roles that macrophages play in resolving inflammatory damage. We begin with three ordinary differential equation (ODE) models and examine the resulting dynamics via numerical simulation in Matlab and bifurcation analysis in XPPAUT. Firstly, in Chapter 2, we present a simple baseline model that neglects a detailed description of the range of macrophage phenotypes involved in a typical inflammatory environment, focusing instead on the interactions of a single homogenised macrophage population with groups of generic pro- and anti-inflammatory mediators. In this chapter, we are primarily interested in how variations in model parameters affect a switch between resolving and chronic out-

comes.

Additional levels of complexity will be added to the ODE model in the following Chapter 3, where the macrophage population is separated into two distinct phenotypes, with pro- and anti-inflammatory roles, the latter being reminiscent of tissue-resident macrophages. Through comparison of the extended model of Chapter 3 with the baseline model of Chapter 2, our aim here is to explore the extent to which the explicit incorporation of distinct macrophage phenotypes influences the models' resulting dynamics.

Macrophages and neutrophils are the main components of the inflammatory response and are the first inflammatory cells to reach the site of inflammation. Neutrophils, which are the most abundant type of white blood cells, play a pivotal role in causing inflammatory damage. Therefore, in Chapter 4, we extend the biological scope of the inflammation model by incorporating additional feedbacks from populations of active and apoptotic neutrophils, and we examine the resulting dynamics. Since the rate of removal of apoptotic neutrophils by macrophages depends strongly on macrophage polarisation, we incorporate corresponding phagocytosis terms into the model of Chapter 4 to further explore these interactions, and elucidate the extent to which phenotype switching affects resulting outcomes in the presence of a potentially damaging neutrophil population.

Crucially, the models of Chapters 3 and 4 incorporate only two distinct macrophage phenotypes with opposing pro- and anti-inflammatory roles; however, as discussed above, there is evidence to suggest that there are a wide range of intermediate macrophage phenotypes that lie between these two extremes. To address this, in Chapter 5, we construct a partial differential equation (PDE) model in which macrophage phenotypes are considered to lie on a continuous spectrum of inflammatory activity. As in previous chapters, we employ numerical simulation in Matlab and bifurcation analysis in XPPAUT to analyse this model. The latter is achieved via semi-discretisation of the PDE model to construct a corresponding ODE approximation that is tractable for bifurcation analysis. Our primary aims here are two-fold. Firstly, we seek to understand the extent to which model observations and conclusions are sensitive to the modelling approach; and, secondly, we seek to expose how intermediate macrophage phenotypes contribute to resulting inflammatory dynamics.

Ultimately, the main conclusions drawn from this work will be presented in Chapter 6, outlining the significant results derived from our investigation into the temporal modelling of inflammation. Potential directions for future work will also be addressed.

A Simple Baseline Model With One Homogenised Macrophage Population

Macrophages are a critical constituent immune cell type that plays an essential role in the inflammatory response, acting as the immune system's first line of defence against infection and tissue damage. These versatile immune cells are involved in various aspects of inflammation, including the recognition and phagocytosis of foreign substances, the clearance of cellular debris, and the release of inflammatory mediators (e.g., cytokines and chemokines). Therefore, macrophages play a crucial role in initiating and resolving inflammation. On the other hand, dysregulation of macrophage functions can lead to chronic inflammation.

In this chapter, we construct a simple model of the inflammatory response focusing on the resolution of inflammation and examine the interactions between a single population of macrophages and groups of generic pro- and anti-inflammatory mediators within a sterile environment. Our aim here is to construct a simple baseline model against which we can compare more advanced models (in later chapters) that take more detailed descriptions of distinct macrophage phenotypes. In our initial inflammatory response model, we are primarily interested in how variations in model parameters affect a switch between resolving and chronic outcomes. We analyse our models through numerical simulation in Matlab and bifurcation analysis in XPPAUT.

2.1 Model derivation

In our simple baseline model, we include a single population of macrophages (of size $m^*(t^*)$), focussing on the interactions between these and generic groups of pro- and anti-inflammatory mediators (of concentrations $c^*(t^*)$ and $g^*(t^*)$ respectively), where t^* denotes time and stars are used to distinguish dimensional variables from their dimensionless counterparts throughout. We assume that there is no direct pathogenic action affecting the physiological behaviour of macrophages, that is the environment is sterile. Thus, the physiological trigger for our inflammation model would be the baseline level of macrophage proliferation occurring in the absence of a mediator, denoted as c_T^* , rather than assuming usual pathways triggered by pathogen detection. We neglect the macrophages' initial activation and differentiation phases. We assume that the macrophage population grows logistically up to a maximum carrying capacity m_{max}^* , but that the rate of proliferation is enhanced in the presence of pro-inflammatory mediators (as is indicated in Jenkins & Allen (2021)). In addition, we assume that macrophages produce both pro- and anti-inflammatory mediators at rates κ_c^* and κ_g^* respectively, and that anti-inflammatory mediators mitigate against inflammatory damage by removing pro-inflammatory mediators at rate δ^* . Our (dimensional) equations for this model are as follows:

$$\frac{dm^*}{dt^*} = k^*(c^* + c_T^*)m^* \left(1 - \frac{m^*}{m_{max}^*}\right) - \gamma_m^* m^*, \quad (2.1a)$$

$$\frac{dc^*}{dt^*} = \kappa_c^* m^* - \delta^* c^* g^* - \gamma_c^* c^*, \quad (2.1b)$$

$$\frac{dg^*}{dt^*} = \kappa_g^* m^* - \gamma_g^* g^*, \quad (2.1c)$$

where $k^* c_T^*$ is the rate of proliferation of macrophages in the absence of pro-inflammatory mediators, and the parameters γ_m^* , γ_c^* and γ_g^* represent natural decay of the corresponding quantities.

The interactions featuring in this baseline model are illustrated in Figure 2.1. We note that the model incorporates both a positive feedback loop via κ_c^* and a negative feedback loop via κ_g^* and δ^* . The positive feedback is based on the ability of macrophages to produce pro-inflammatory mediators via κ_c^* in response to a concentration gradient in the pro-inflammatory mediators, which attract more macrophages to the damaged site. The negative feedback operates through macrophages and anti-inflammatory mediators via κ_g^* and δ^* .

Macrophages produce both pro- and anti-inflammatory mediators, which can either inhibit or promote inflammation. These mediators can influence the behaviour and

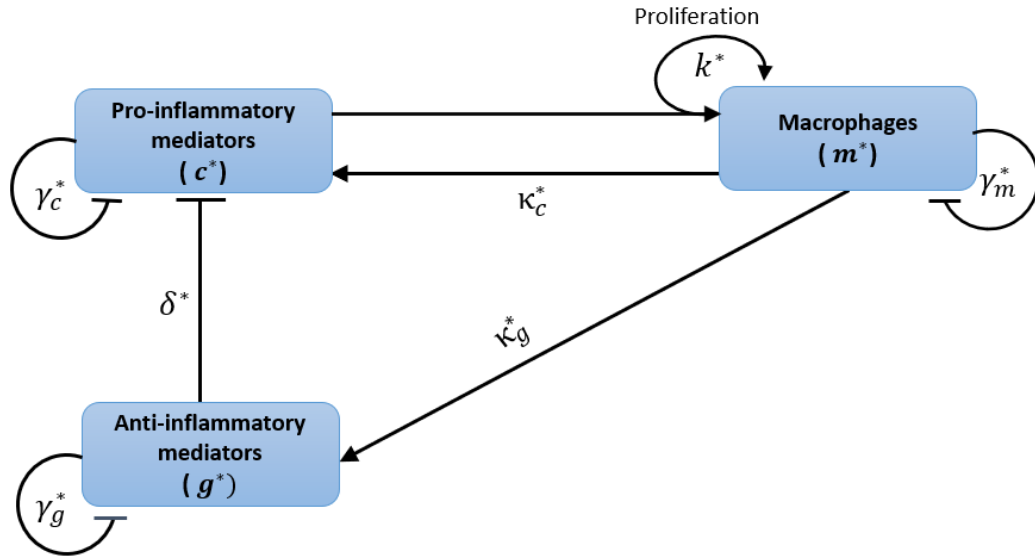


Figure 2.1: Schematic diagram representing (2.1) and illustrating component interactions between a single population of macrophages (m^*) in response to pro- and anti-inflammatory mediators (c^* and g^*), respectively. Arrows indicate positive feedbacks or supply terms; lines terminated with bars indicate negative feedbacks or loss terms.

function of macrophages, thereby affecting the inflammatory response and its regulation and tissue repair. Pro-inflammatory mediators c^* induce macrophages m^* to recognise and eliminate noxious stimuli, while anti-inflammatory mediators g^* stimulate macrophages m^* to tune the inflammatory response, initiate the healing phases during which damaged tissue is replaced (by proliferation) and remodelled, and enhance angiogenesis. Therefore, inflammation is a highly regulated process in which macrophages and pro- and anti-inflammatory components work together to ensure rapid repair and restoration of healthy tissue structure. On the other hand, disruption of this process can contribute to the development of chronic inflammatory diseases.

A summary of the dimensional parameters appearing in (2.1) is presented in Table 2.1. The dimensional parameters are not all known and available in absolute values. Thus, we rely upon empirical data and the current literature to derive proper estimates for the dimensional parameter values. We review these parameter values in detail in Section 2.1.1.

2.1.1 Parameters

Accurately determining many of the dimensional rate parameters that govern a typical inflammatory response is a difficult task, due to a lack of suitable non-invasive experimental protocols (Vaugh & Sherratt, 2007), the fact that relevant mechanisms dif-

Parameter	Definition	Range of values and units	References
γ_c^*	Decay rate of pro-inflammatory mediators	$0.7 - 20 \text{ day}^{-1}$	Waugh & Sherratt (2007) Smith <i>et al.</i> (2011)
γ_g^*	Decay rate of anti-inflammatory mediators	$0.04 - 12.86 \text{ day}^{-1}$	Reynolds <i>et al.</i> (2006) Minucci <i>et al.</i> (2020)
γ_m^*	Decay rate of macrophages	$0.2 - 1.41 \text{ day}^{-1}$	Waugh & Sherratt (2007) Cooper <i>et al.</i> (2015)
κ_g^*	Rate of production of anti-inflammatory mediators	$0.00243 - 1.67 \text{ pg cell}^{-1} \text{ day}^{-1}$	Minucci <i>et al.</i> (2020)
κ_c^*	Rate of production of pro-inflammatory mediators	$0.24 - 41.22 \text{ pg cell}^{-1} \text{ day}^{-1}$	Minucci <i>et al.</i> (2020)
k^*	Rate of macrophages growth	$0.693 \text{ mm}^3 \text{ pg}^{-1} \text{ day}^{-1}$	Waugh & Sherratt (2007)
m_{max}^*	Maximum macrophage population size	$1 \times 10^5 - 11.7 \times 10^5 \text{ cell mm}^{-3}$	Furth (2012)
c_T^*	Rate of macrophage proliferation in the absence of c^*	pg mm^{-3}	
δ^*	Rate at which mediators g^* respond to the signal from mediators c^*	$\text{mm}^3 \text{ pg}^{-1} \text{ day}^{-1}$	

Table 2.1: Summary of the dimensional parameter values of (2.1).

fer greatly depending on the medical condition and the affected tissue (Dunster, 2016; Minucci *et al.*, 2020), markers of acute inflammation are typically short-lived, measuring them *in vivo* is difficult, and the fact that many patients report late as inflammatory conditions worsen (Dunster *et al.*, 2014). Here, we briefly summarise relevant estimates of the dimensional parameters where available, and comment upon how these estimates inform the corresponding choices for our baseline set of dimensionless parameters. The dimensional parameters appearing in (2.1) are summarised in Table 2.1. Mediator decay rates are reasonably well documented in general, but can vary greatly between individual mediators, different tissues and under differing inflammatory conditions. The decay rate of the pro-inflammatory mediators (γ_c^*) is reported to lie in the range $0.7 - 20 \text{ day}^{-1}$ (Waugh & Sherratt, 2007; Smith *et al.*, 2011), while the decay rate of the anti-inflammatory mediators (γ_g^*) is stated to lie in the range $0.04 - 12.86 \text{ day}^{-1}$ (Reynolds *et al.*, 2006; Minucci *et al.*, 2020). Previous works such as Dunster *et al.* (2014) and Bayani *et al.* (2020a) have taken $\gamma_c^* = \gamma_g^* = 3 \text{ day}^{-1}$ as a default value for the decay rate of pro-and anti-inflammatory mediators, respectively. Furthermore, in

a study by Liu *et al.* (2021), it was found that the half-lives of the pro-inflammatory cytokines like IL-1 β , IL-8 and TNF α lie in the range 18.2 – 24 min, and that the anti-inflammatory cytokine IL-1RA decays more slowly with a half-life in the range 4 – 6 h. To further complicate matters, some cytokines (e.g. IL-6) can have both pro- and anti-inflammatory effects (Liu *et al.*, 2021). Here, in the context of our model parameters, we expect that $\gamma_g^* < \gamma_c^*$.

Identifying precise values for parameters controlling macrophage population dynamics is difficult in general, since these depend heavily on the tissue under consideration. However, the rate of macrophage loss (γ_m^*) has been previously documented to lie in the range 0.2 – 1.41 day⁻¹ (Waugh & Sherratt, 2007; Cooper *et al.*, 2015) and the maximum macrophage population size (m_{max}^*) to lie in the range 1×10^5 – 11.7×10^5 cell mm⁻³ (Furth, 2012). Minucci *et al.* (2020) report that the production rate of anti-inflammatory mediators (κ_g^*) to lie in the range 2.43×10^{-3} – 1.67 pg cell⁻¹ day⁻¹, while the production rate of pro-inflammatory mediators (κ_c^*) to be in the range 0.24 – 41.22 pg cell⁻¹ day⁻¹. Macrophages play a crucial role in the production and regulation of cytokines, but have a bias towards pro-inflammatory cytokine production during inflammation. Therefore, it is often observed that the rate of macrophage production of pro-inflammatory cytokines (κ_c^*) is higher than that of anti-inflammatory cytokines (κ_g^*) (*i.e.* damage rate > rate of repair and resolution). In the context of inflammation, it is often expected that $\kappa_c^* \gg \kappa_g^*$ due to the body's natural defence mechanisms against potential threats (Zhu *et al.*, 2014). Waugh & Sherratt (2007) document the macrophage growth rate (k^*) can be determined from the population doubling time, which is around one day, therefore $k^* = \ln 2 = 0.693$ mm³ pg⁻¹ day⁻¹.

Accurately prescribing the rate of proliferation/recruitment of the macrophage populations is hindered by the fact that proliferation rates are known to also depend on the background levels of inflammation (*i.e.* the concentration of pro-inflammatory mediators, c , in our model), as described by Jenkins & Allen (2021). Authors of previous works (Waugh & Sherratt, 2007; Dunster *et al.*, 2014) have tuned macrophage proliferation rate parameters against population doubling time data obtained experimentally, with populations doubling in number roughly every 1 day. Here, we simply assume that proliferation rates should appreciably increase in the presence of pro-inflammatory mediators, so we expect c_T^* to be small in comparison to typical c -values. Similarly, the value of δ^* is known to be influenced by the concentration of pro-inflammatory mediators (c). Therefore, we assume that δ^* is significantly lower than the typical c -values.

2.1.2 Non-dimensionalisation

A non-dimensionalisation technique is usually used to rewrite equations of a dimensional system in dimensionless form. This technique is highly beneficial when working with complex systems with a large number of parameters that may complicate the analysis. The non-dimensionalisation approach simplifies system analysis, enables a more comprehensive understanding of the system's behaviour by identifying and retaining the most influential parameters (*i.e.* reducing the number of system parameters), and provides deeper insights into the underlying dynamics.

We use the asterisk to distinguish dimensional quantities from their dimensionless quantities. Therefore, we nondimensionalise the system of (2.1) by applying the following rescalings:

$$t^* = \frac{1}{\gamma_c^*} t, \quad c^* = \frac{\gamma_c^*}{k^*} c, \quad g^* = \frac{\gamma_c^*}{\delta^* \kappa_g^*} g, \quad m^* = \frac{\gamma_c^{*2}}{\delta^* \kappa_g^*} m, \quad (2.2)$$

to obtain

$$\frac{dm}{dt} = (c + c_T) m \left(1 - \frac{m}{m_{max}}\right) - \gamma_m m, \quad (2.3a)$$

$$\frac{dc}{dt} = \kappa_c m - c g - c, \quad (2.3b)$$

$$\frac{dg}{dt} = m - \gamma_g g, \quad (2.3c)$$

in which we have introduced the following dimensionless parameters:

$$\gamma_g = \frac{\gamma_g^*}{\gamma_c^*}, \quad \gamma_m = \frac{\gamma_m^*}{\gamma_c^*}, \quad c_T = \frac{k^* c_T^*}{\gamma_c^*}, \quad \kappa_c = \frac{k^* \kappa_c^*}{\delta^* \kappa_g^*}, \quad m_{max} = \frac{\delta^* \kappa_g^* m_{max}^*}{\gamma_c^{*2}}. \quad (2.4)$$

The system (2.3) is solved subject to initial conditions representing a baseline presence of macrophages $m(0) = m_0 > 0$ and an initial stimulus of inflammation of the form $c(0) = c_0 > 0$, with $g(0) = 0$.

A review of some relevant parameter estimation can be found in Dunster *et al.* (2014) and Dunster (2016); however, in most cases, it is more practical to estimate the orders of magnitude of corresponding dimensionless parameter groupings based on our knowledge of which mechanisms dominate. Where accurate parameter choices are not known, our approach is to take baseline values that expose the full remit of dynamics and then use bifurcation analysis to explore local sensitivity to these choices. The dimensionless parameters appearing in (2.3) are summarised in Table 2.2, alongside baseline values used in our simulations.

Liu *et al.* (2021) previously state that the decay rate of anti-inflammatory mediators is slightly slower than the decay rate of pro-inflammatory mediators (*i.e.* $\gamma_g^* < \gamma_c^*$). Here,

Parameter	Expression	Meaning	Baseline value
κ_c	$k^* \kappa_c^* / \delta^* \kappa_g^*$	Rate of production of pro-inflammatory mediators	0.35
γ_m	γ_m^* / γ_c^*	Decay rate of macrophages	0.05
γ_g	γ_g^* / γ_c^*	Decay of anti-inflammatory mediators	0.2
c_T	$k^* c_T^* / \gamma_c^*$	Rate of macrophage proliferation in the absence of pro-inflammatory mediators	0.01
m_{max}	$\delta^* \kappa_g^* m_{max}^* / \gamma_c^{*2}$	Maximum macrophage population size	25

Table 2.2: Summary of the dimensionless parameters appearing in (2.3).

we take $\gamma_g = \gamma_g^* / \gamma_c^* = 0.2$ as our default value in Table 2.2, and investigate variations around this value via numerical simulation and bifurcation analysis. According to Waugh & Sherratt (2007) and Cooper *et al.* (2015), the loss of macrophages (γ_m^*) occurs at a slower rate than the decay of pro-inflammatory mediators (γ_c^*); we hence set $\gamma_m = \gamma_m^* / \gamma_c^* < 1$ in Table 2.2.

Macrophage proliferation rates are influenced by the prevailing concentration levels of pro-inflammatory mediators (c) in the affected tissue, as elucidated by Jenkins & Allen (2021). As a result, we reasonably deduce that proliferation rates should increase noticeably in the presence of pro-inflammatory mediators. Hence, we assume that c_T^* is significantly lower than the typical c -values. We therefore set $c_T = 0.01$ in Table 2.2 and investigate the role of this parameter more thoroughly via bifurcation analysis below. Likewise, since the maximal macrophage population size, m_{max}^* , will depend heavily on the size of the tissue of interest, we choose $m_{max} = 25$ as a baseline value. It is known that κ_c^* is affected by both the concentration of pro-inflammatory mediators and the size of the macrophage population, and a critical factor in inducing inflammation. We therefore set $\kappa_c = 0.35$ in Table 2.2 as a baseline value and then study variations of this parameter within our subsequent analysis.

2.2 Identification and classification of steady state solutions

This section aims to find the steady state solutions, also known as equilibrium solutions, of (2.3) and classify them by their stability. The steady state solutions refer to the points at which a dynamic system's behaviour does not change over time. The steady state solutions are particularly important in mathematical models because they provide valuable insights into dynamic systems' behaviour and stability.

To find the steady state solutions of (2.3), we can write it in the following way:

$$\frac{dm}{dt} = (c + c_T) m \left(1 - \frac{m}{m_{max}} \right) - \gamma_m m = f(m, c, g), \quad (2.5a)$$

$$\frac{dc}{dt} = \kappa_c m - c g - c = p(m, c, g), \quad (2.5b)$$

$$\frac{dg}{dt} = m - \gamma_g g = q(m, c, g). \quad (2.5c)$$

Assuming that the system has reached equilibrium, we set the derivatives of equation (2.5) to zero. We therefore solve the following system of simultaneous equations:

$$f(m, c, g) = 0, \implies (c + c_T) m \left(1 - \frac{m}{m_{max}} \right) - \gamma_m m = 0, \quad (2.6a)$$

$$p(m, c, g) = 0, \implies \kappa_c m - c g - c = 0, \quad (2.6b)$$

$$q(m, c, g) = 0, \implies m - \gamma_g g = 0. \quad (2.6c)$$

Solving (2.6b) and (2.6c) in terms of m , we get:

$$g = \frac{m}{\gamma_g}, \quad c = \frac{\kappa_c m}{g + 1} = \frac{\gamma_g \kappa_c m}{\gamma_g + m}, \quad (2.7)$$

Substituting (2.7) in (2.6a) gives:

$$a m^2 + b m + k = 0, \quad (2.8)$$

where,

$$a = -c_T - \kappa_c \gamma_g,$$

$$b = \kappa_c m_{max} \gamma_g - c_T \gamma_g - m_{max} \gamma_m + m_{max} c_T,$$

$$k = m_{max} c_T \gamma_g - m_{max} \gamma_m \gamma_g.$$

It is straightforward to show that the system (2.3) has a steady state at $FP_1 = (m_1, c_1, g_1) = (0, 0, 0)$, which corresponds to a healthy response since all pro-inflammatory components are zero. We also obtain two further steady states, which we denote by $FP_2 = (m_2, c_2, g_2)$ and $FP_3 = (m_3, c_3, g_3)$ by solving (2.8), where

$$m_2 = \frac{-1}{2(c_T + \gamma_g \kappa_c)} \left[c_T \gamma_g + m_{max} (\gamma_m - c_T - \gamma_g \kappa_c) + \left(c_T^2 \gamma_g^2 + m_{max}^2 (c_T^2 + \gamma_m^2 + 2 c_T \gamma_g \kappa_c - 2 c_T \gamma_m + \gamma_g^2 \kappa_c^2 - 2 \gamma_g \gamma_m \kappa_c) + m_{max} (2 c_T^2 \gamma_g + 2 c_T \gamma_g^2 \kappa_c - 2 c_T \gamma_g \gamma_m - 4 \gamma_g^2 \gamma_m \kappa_c) \right)^{1/2} \right], \quad (2.9)$$

$$c_2 = \frac{\kappa_c m_2}{g_2 + 1} = \frac{\gamma_g \kappa_c m_2}{\gamma_g + m_2}, \quad g_2 = \frac{m_2}{\gamma_g}, \quad (2.10)$$

and,

$$\begin{aligned}
 m_3 = \frac{1}{2(c_T + \gamma_g \kappa_c)} & \left[c_T \gamma_g + m_{max} (\gamma_m - c_T - \gamma_g \kappa_c) + \left(c_T^2 \gamma_g^2 \right. \right. \\
 & + m_{max}^2 \left(c_T^2 + \gamma_m^2 + 2 c_T \gamma_g \kappa_c - 2 c_T \gamma_m + \gamma_g^2 \kappa_c^2 - 2 \gamma_g \gamma_m \kappa_c \right) \\
 & \left. \left. + m_{max} \left(2 c_T^2 \gamma_g + 2 c_T \gamma_g^2 \kappa_c - 2 c_T \gamma_g \gamma_m - 4 \gamma_g^2 \gamma_m \kappa_c \right) \right)^{1/2} \right], \quad (2.11)
 \end{aligned}$$

$$c_3 = \frac{\kappa_c m_3}{g_3 + 1} = \frac{\gamma_g \kappa_c m_3}{\gamma_g + m_3}, \quad g_3 = \frac{m_3}{\gamma_g}. \quad (2.12)$$

It is worth pointing out that FP_2 and FP_3 do not exist for all parameter choices listed in Table 2.2, as the steady state value must not be negative. To determine system behaviour close to the steady states, we perform a linear stability analysis; that is, we consider the sign of the real part of the eigenvalues of the Jacobian matrix, which for (2.6) is given by:

$$\mathbf{J} = \begin{pmatrix} \frac{\partial f}{\partial m} & \frac{\partial f}{\partial c} & \frac{\partial f}{\partial g} \\ \frac{\partial p}{\partial m} & \frac{\partial p}{\partial c} & \frac{\partial p}{\partial g} \\ \frac{\partial q}{\partial m} & \frac{\partial q}{\partial c} & \frac{\partial q}{\partial g} \end{pmatrix}. \quad (2.13)$$

The resulting Jacobian matrix \mathbf{J} for (2.6) is given by

$$\mathbf{J} = \begin{pmatrix} \frac{(c + c_T)(m_{max} - 2m)}{m_{max}} - \gamma_m & m \left(1 - \frac{m}{m_{max}} \right) & 0 \\ \kappa_c & -g - 1 & -c \\ 1 & 0 & -\gamma_g \end{pmatrix}. \quad (2.14)$$

For convenience below, we write

$$R = m \left(1 - \frac{m}{m_{max}} \right), \quad S = \frac{(c + c_T)(m_{max} - 2m)}{m_{max}} - \gamma_m. \quad (2.15)$$

Finding the linear stability of the steady state requires finding the eigenvalues, λ . In general, the steady state is stable if all eigenvalues (λ) of the Jacobian matrix \mathbf{J} have a negative real part. For further details about the classification of steady states in a two-dimensional phase space, see Table 2.3.

It is straightforward to show that the eigenvalues are the roots of the following characteristic polynomial

$$|\mathbf{J} - \lambda \mathbf{I}| = \lambda^3 - A_2 \lambda^2 + A_1 \lambda - A_0 = 0 \quad (2.16)$$

Eigenvalues λ_1, λ_2 of A	Case	Stability
Two distinct real eigenvalues	$\lambda_1 < 0, \lambda_2 < 0$	Stable node
	$\lambda_1 > 0, \lambda_2 > 0$	Unstable node
	$\lambda_1 \cdot \lambda_2 < 0$	Unstable (saddle point)
Complex conjugate eigenvalues $\lambda = \alpha \pm \beta i$	$\text{Re}(\lambda) = 0$	Stable centre
	$\text{Re}(\lambda) < 0$	Stable focus point (spiral point)
	$\text{Re}(\lambda) > 0$	Unstable focus point (spiral point)
Repeated real eigenvalue ($\lambda_1 = \lambda_2$) with only one linearly independent eigenvector	$\lambda < 0$	Stable degenerate node (improper)
	$\lambda > 0$	Unstable degenerate node (improper)

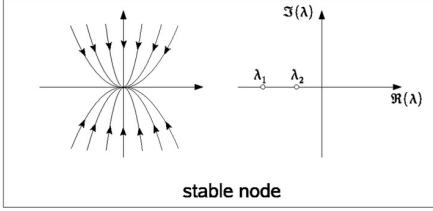
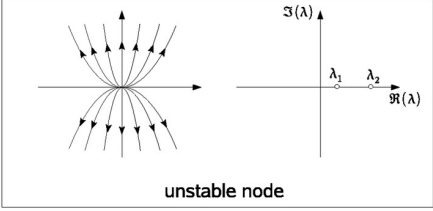
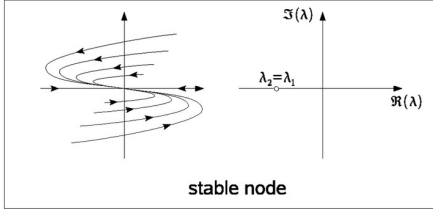
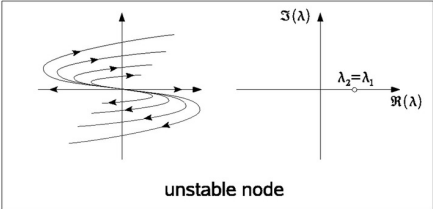
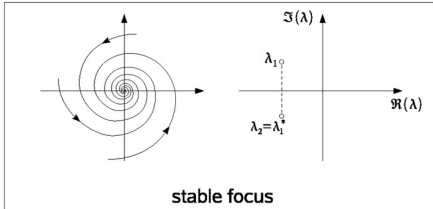
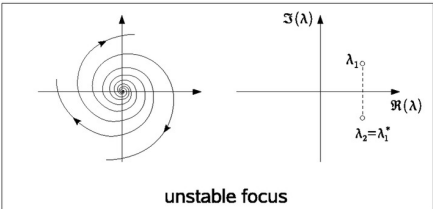
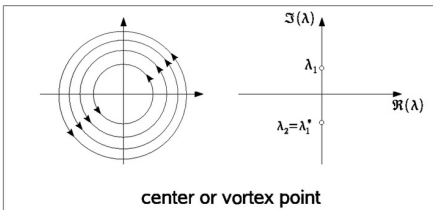
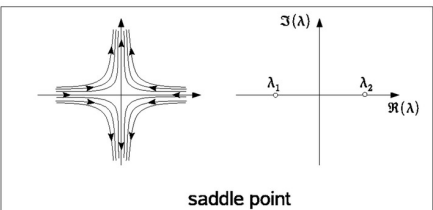
 <p>stable node</p>	 <p>unstable node</p>
 <p>stable node</p>	 <p>unstable node</p>
 <p>stable focus</p>	 <p>unstable focus</p>
 <p>center or vortex point</p>	 <p>saddle point</p>

Table 2.3: Classification of steady states of $x' = Ax$ with $|A - \lambda I| = 0$ and $|A| \neq 0$.

where,

$$A_0 = \det(\mathbf{J}) = \gamma_g S - c R + \gamma_g g S + \gamma_g \kappa_c R, \quad (2.17a)$$

$$\begin{aligned} A_1 &= \frac{1}{2} \left(\text{trace}^2(\mathbf{J}) - \text{trace}(\mathbf{J}^2) \right), \\ &= \frac{1}{2} \left((\gamma_g + g - S + 1)^2 - (g + 1)^2 - 2 \kappa_c R - \gamma_g^2 - S^2 \right), \end{aligned} \quad (2.17b)$$

$$A_2 = \text{trace}(\mathbf{J}) = S - \gamma_g - g - 1. \quad (2.17c)$$

To determine the stability of the zero steady state, $\text{FP}_1 = (g_1, c_1, m_1) = (0, 0, 0)$, we need to compute the eigenvalues, λ , of Jacobian matrix \mathbf{J} in (2.14).

Evaluating (2.14) on FP_1 provides:

$$\mathbf{J}|_{\text{FP}_1} = \begin{pmatrix} -\gamma_g & 0 & 1 \\ 0 & -1 & \kappa_c \\ 0 & 0 & c_T - \gamma_m \end{pmatrix}. \quad (2.18)$$

Thus, to compute the eigenvalues of the matrix \mathbf{J} evaluated at FP_1 , we solve the following equation:

$$\begin{aligned} \det(\mathbf{J} - \lambda \mathbf{I})|_{\text{FP}_1} &= \begin{vmatrix} -\gamma_g - \lambda & 0 & 1 \\ 0 & -1 - \lambda & \kappa_c \\ 0 & 0 & c_T - \gamma_m - \lambda \end{vmatrix} = 0 \\ &= (-\gamma_g - \lambda)(-1 - \lambda)(c_T - \gamma_m - \lambda) = 0. \end{aligned} \quad (2.19)$$

For the zero steady state, $\text{FP}_1 = (g_1, c_1, m_1) = (0, 0, 0)$, all three eigenvalues are real and negative provided that $\gamma_m > c_T$, we find $(\lambda_1, \lambda_2, \lambda_3) = (-\gamma_g, -1, c_T - \gamma_m)$. Therefore, it is straightforward to show that the zero steady state is stable provided that $\gamma_m > c_T$; otherwise, it is unstable. Identifying and classifying the nature of chronic steady states is a more complex task, however; we therefore explore the model's broader dependence on parameter values via bifurcation analysis conducted in XPPAUT.

2.3 Results

In this section, we introduce the outcomes of our investigation into the behaviour of our simple model of inflammation, which simulates the dynamics of the inflammatory response. Our investigation employs two complementary methods: numerical simulation utilising Matlab and bifurcation analysis using XPPAUT. Utilising these approaches, we explore the various qualitative behaviours exhibited by the initial model and examine them in relation to the inflammatory response and its potential outcomes, as well as how alternation in the system's main parameters affects its results.

2.3.1 Numerical results

All numerical simulations of (2.3) were generated using Matlab and, in particular, the ODE solver ode45. Throughout our analysis, we are primarily interested in whether

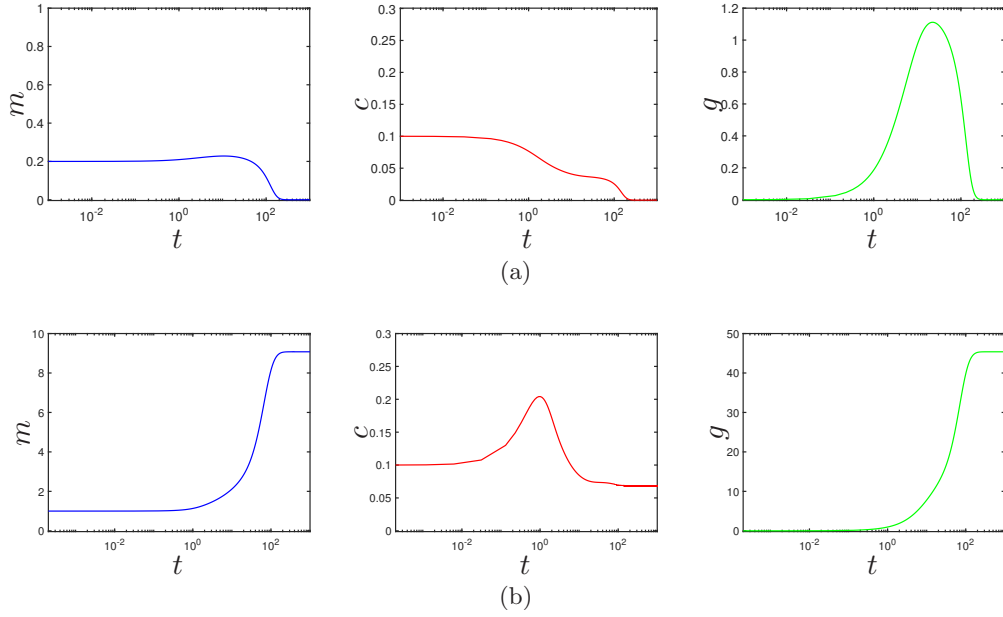


Figure 2.2: Numerical simulations of (2.3) for the parameters of Table 2.2, illustrating that the model is bistable for these parameter values. In (a), we initialise the model with a small stimulus of initial inflammatory damage ($m(0) = 0.2$, $c(0) = 0.1$ and $g(0) = 0$), and this damage eventually subsides with the model attaining a healthy steady state. In (b), we observe that with a larger damage stimulus ($m(0) = 1$, $c(0) = 0.1$ and $g(0) = 0$), the model attains a chronic steady state in which $m, c > 0$.

our model converges to steady states (or periodic structures) that represent either resolution of inflammatory damage (*i.e.* a healthy outcome) or chronic inflammation. The realistic inflammation model typically exhibits bistable behaviour corresponding to a healthy response and an unhealthy response (*i.e.* chronic). We describe a steady state as ‘healthy’ if all the model’s pro-inflammatory components are zero, and ‘chronic’ if pro-inflammatory components attain positive steady state values.

Figure 2.2 illustrates two simulations of (2.3), for the parameter values of Table 2.2 and two differing choices of initial conditions, showing that the model has scope for bistability, with both healthy and chronic steady states stable. In Figure 2.2(a), we initiate the model with a small stimulus of inflammatory damage ($c_0 = 0.1$) and a reasonably small population of macrophages ($m_0 = 0.2$), and observe that the system eventually converges to the healthy steady state, in which the level of macrophages and pro- and anti-inflammatory mediators reaches zero. However, in Figure 2.2(b) we observe that initiating the model with a larger population of macrophages ($m_0 = 1$) results in long-term growth of the macrophage population and an associated increase in pro-inflammatory mediators via the κ_c term in (2.3b), alongside a significantly up-scaled production of anti-inflammatory mediators according to (2.3c). The model attains a steady state with all components positive, which causes sustained damage through κ_c ;

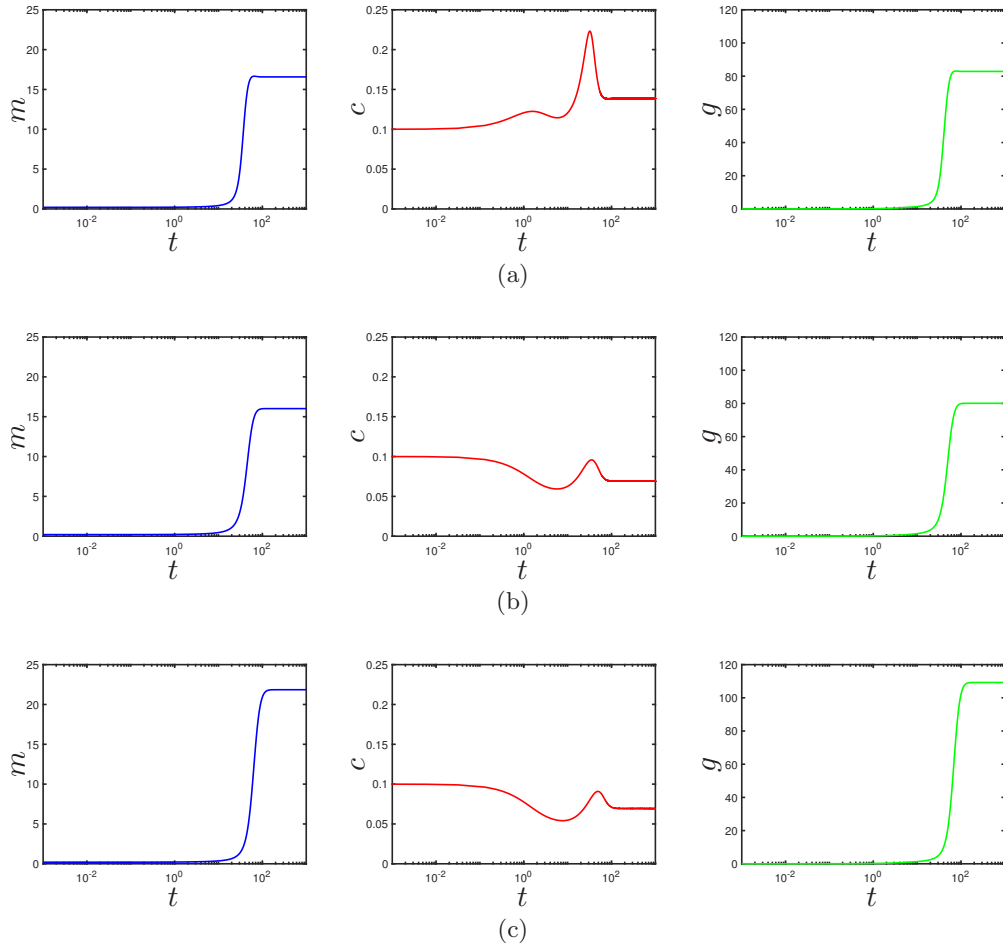


Figure 2.3: Numerical simulations of (2.3) with a small stimulus of initial inflammatory damage ($m(0) = 0.2$, $c(0) = 0.1$ and $g(0) = 0$) showing how the behaviour of the system switches to the chronic condition when we increase the values of pro-inflammatory components. In (a) $\kappa_c = 0.7$, (b) $c_T = 0.07$ and (c) $\gamma_m = 0.01$. All system parameter values (other than those listed above) are held fixed to the values listed in Table 2.2

i.e. a chronic outcome. The key switches between these two outcomes (for parameters fixed) are the magnitude of the inflammatory stimulus (c_0) and the initial size of the macrophage population (m_0); it is pertinent to note that, since the macrophage description of this model attributes both pro- and anti-inflammatory responses to the same macrophage population, larger macrophage populations have the scope to be both detrimental or beneficial as regards the long-term inflammatory outcome.

We find that simulations of (2.3) for the parameters of Table 2.2 with a small stimulus of initial inflammatory damage ($m(0) = 0.2$, $c(0) = 0.1$ and $g(0) = 0$) converges to the healthy steady state, as shown in Figure 2.2(a). However, we observe that the behaviour of the system can switch into a chronic configuration under the same condition ($m(0) = 0.2$, $c(0) = 0.1$ and $g(0) = 0$) through increasing the values of the pro-

inflammatory components (*e.g.* κ_c , c_T , γ_m). In Figure 2.3(a), increased production of pro-inflammatory mediators via κ_c leads to an excessive and persistent release of pro-inflammatory mediators that attract and recruit more macrophages and other immune cells to the site of inflammation. As the concentration of these mediators increases, they may trigger a cascade of events leading to persistent disruption of the immune response and the immune system is unable to resolve the inflammation effectively, which is often associated with chronic inflammation. Similarly, the behaviour of the system exhibits an unhealthy response when the recruitment of macrophages in the absence of pro-inflammatory mediators, through the parameter c_T , is increased, and the size of the macrophage population settled at the damage site becomes excessively large (indicated by a small value of γ_m), as illustrated in Figure 2.3(b) and (c) respectively. The excessive influx of macrophages into the damaged site can lead to an imbalance in the immune response or an overactive immune response, causing exacerbation of inflammation, tissue damage, and progression of the inflammatory condition into a chronic state.

2.3.2 Bifurcation analysis

In this section, we aim to explore how the existence and stability of the steady state solutions change as parameters are varied. We also examine how the change in parameter values will affect the positions of bifurcation points. To achieve this, we employ a numerical bifurcation analysis to investigate how the variation in system parameters affects the system's behaviour. Through this analysis, we gain insights into how changes in the system's parameter values affect its dynamics and stability, enabling a deeper understanding of the inflammatory response to different conditions. Furthermore, bifurcation analysis also aids in identifying unique points known as bifurcation points, at which a dynamical system undergoes a qualitative shift in its behaviour.

Bifurcation analysis is widely used in studying non-linear system dynamics. Bifurcation diagrams can be plotted using software packages such as Matlab and XPPAUT. For more information and references about 'XPPAUT', refer to Ermentrout (2002) and Gandy & Nelson (2022). Figure 2.4 illustrates the basic concepts used in the bifurcation diagram (*e.g.* bistable and monostable regions) where the x -axis represents the bifurcation parameter, and the y -axis shows the set of steady state values for the system's dependent variable. In addition, it shows three steady states; one is zero, located on the x -axis, and two are non-zero steady states. The steady state is called stable if each of its eigenvalues has a negative real part. Here, we use a solid line to indicate a stable steady state while a dashed line for an unstable steady state. The stable non-zero

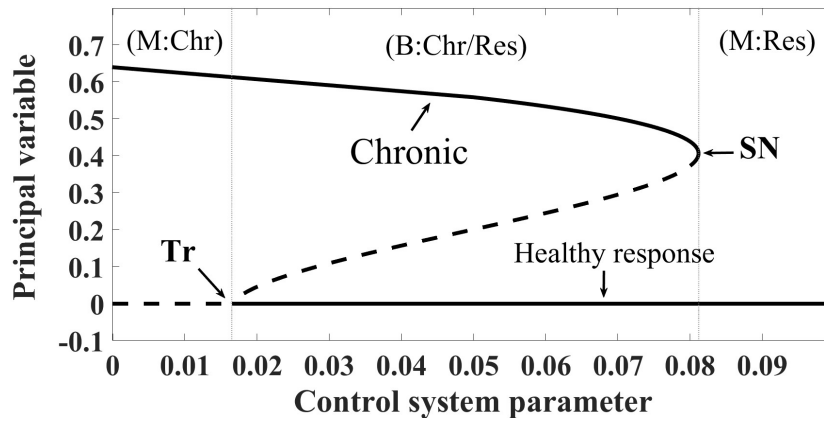


Figure 2.4: An example of a bifurcation diagram illustrating a bistability range of zero and non-zero steady states, bounded by SN and Tr. Solid and dashed lines represent stable and unstable steady states respectively; SN = saddle-node bifurcation; Tr = transcritical bifurcation; “B” = bistable with both healthy and chronic outcomes permissible; “M:Res” = monostable with inflammation resolving; “M:Chr” = monostable with a chronic outcome guaranteed.

steady state often indicates an unhealthy response (chronic inflammation), while the stable zero steady state refers to a healthy response (resolution of inflammation).

The bifurcation diagrams of a realistic model often contain many points called bifurcation points. For example, the point at which the stable and unstable steady states coalesce is defined as a saddle-node bifurcation (limit point) and is denoted by SN. Another case is if two fixed points do not disappear when they collide at the bifurcation point, and they switch their stability as the parameter is varied. In other words, there is one stable and one unstable steady state, and after they collide, the stable steady state becomes unstable and vice versa. In that case, it is called a transcritical bifurcation, a particular kind of local bifurcation denoted by Tr, see Figure 2.4. A list of the bifurcations that appear in this thesis is given in Appendix A.

The bifurcation diagrams of the real model often exhibit monostable and bistable regions. The system has a monostable region if there is a unique stable steady state in that region. For example, in Figure 2.4, there are two monostable regions; the chronic region from zero to the transcritical bifurcation point (Tr), and the healthy region beyond a saddle-node bifurcation (SN). It is clear that in the region from the transcritical bifurcation (Tr) to saddle-node bifurcation (SN), the system has two stable steady states separated by an unstable steady state. Thus, the behaviour of the system can evolve into one of two stable equilibrium points for the same parameter values. So, in this region, the system exhibits bistability. In a dynamical system, bistability means the system has two stable equilibrium points, and it can evolve to one of two stable steady

states for the same parameter values (*i.e.* switching between states requires different initial conditions) (Piedrafita *et al.*, 2010; Rombouts & Gelens, 2021). From a mathematical point of view, bistability occurs in the first and second-order system when an unstable equilibrium point lies between two different stable equilibrium points (Kuznetsov, 2013). Whenever the system parameters change so that a threshold value is crossed, the system abruptly switches between the two stable steady states, and the system may not revert to the previous state (Rombouts & Gelens, 2021). This transition is discontinuous, fast, and irreversible.

In section 2.2, we show that the steady state solutions of (2.3) are three distinct steady states, one zero when $m = g = c = 0$, which corresponds to a healthy response, and two non-zero steady states which correspond to a chronic response. As we saw earlier the zero steady state is stable provided that $\gamma_m > c_T$. Identifying and classifying the nature of chronic steady states is a more complex task; we therefore explore the model's broader dependence on parameter values via bifurcation analysis conducted in XPPAUT (as described in *e.g.* Ermentrout (2002) and Gandy & Nelson (2022)).

Figure 2.5 shows bifurcation diagrams that illustrate how the steady states of (2.3) depend upon the system's parameters, holding all unspecified parameter values at the values of Table 2.2. Solid and dashed curves represent stable and unstable steady states respectively. In Figures 2.5(a,b), we observe that the healthy steady state at zero is stable provided that $\gamma_m > c_T$. In Figure 2.5(a), the branch representing the chronic steady states arises via a transcritical bifurcation (Tr) and undergoes a saddle-node bifurcation (SN), giving rise to stable chronic solutions. In Figure 2.5(a), the saddle-node occurs for a negative value of c_T , so there exists a stable chronic steady state for all positive values of the bifurcation parameter c_T of interest here, for the parameter values of Table 2.2. In addition, Figure 2.5(a) exhibits a bistable region (B:Chr/Res) for the bifurcation parameter $c_T \in [\text{SN}, \text{Tr}]$, with both healthy and chronic outcomes, and switching between these outcomes depends on the initial conditions, and monostable with chronic outcomes guaranteed (M:Chr) for $c_T > \text{Tr}$. An increase in the value of c_T enhances the recruitment of macrophages and other immune cells to the damaged area, resulting in a prolonged inflammatory state and potential progression to chronic inflammation.

In Figure 2.5(b), we see similar (although reflected) behaviour to that of Figure 2.5(a), with the chronic steady state being stable for all values of γ_m less than SN. We can see that Figure 2.5(b) also exhibits areas of bistability (B:Chr/Res) for $\gamma_m \in [\text{Tr}, \text{SN}]$, and monostability with inflammation resolving (M:Res) for $\gamma_m > \text{SN}$, and monostability with chronic outcomes guaranteed (M:Chr) for $\gamma_m \in [0, \text{Tr}]$. For large values of γ_m , the macrophage population decays sufficiently quickly that it be eliminated in

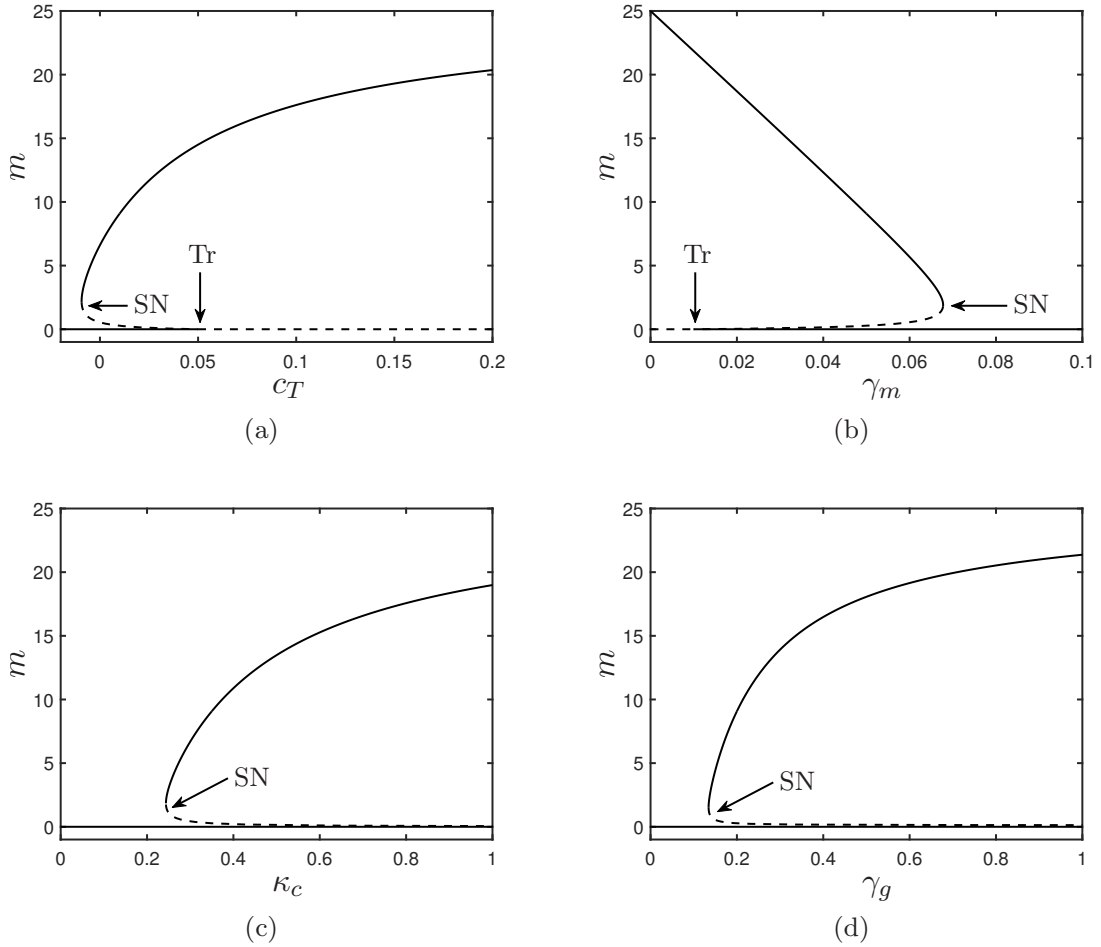


Figure 2.5: Bifurcation diagrams illustrating steady state solutions of (2.3) and their dependence upon the model's parameters. All system parameter values (other than those listed above) are held fixed to the values listed in Table 2.2. Solid and dashed lines represent stable and unstable steady states respectively; SN = saddle-node bifurcation; Tr = transcritical bifurcation.

the long-term, removing the model's sole pro-inflammatory feedback and guaranteeing a healthy outcome. Similarly, Figures 2.5(c,d) show that large values of κ_c promote chronicity as more pro-inflammatory mediators are produced, and large values of γ_g promote chronicity via rapid decay of anti-inflammatory mediators. In addition, Figures 2.5(c,d) show a healthy response when the bifurcation parameter κ_c or γ_g is less than SN. Table 2.4 summarizes all the bifurcation points mentioned in Figure 2.5.

Bifurcation analyses conducted via XPPAUT are not limited to examining single-parameter changes; they also analyse by simultaneously changing two system parameters while leaving the remaining parameters fixed (unchanged). Thus, two-parameter bifurcation diagrams can provide a clearer view of how the variation in two system parameter values affects the stability of the steady states and the position of bifurcation points. These diagrams provide valuable insights into the system's behaviour by

Bifurcation point	Bifurcation parameter
Figure 2.5 (a)	
SN	$c_T = -9.342 \times 10^{-3}$
Tr	$c_T = 5 \times 10^{-2}$
Figure 2.5 (b)	
SN	$\gamma_m = 6.776 \times 10^{-2}$
Tr	$\gamma_m = 1 \times 10^{-2}$
Figure 2.5 (c)	
SN	$\kappa_c = 2.438 \times 10^{-2}$
Figure 2.5 (d)	
SN	$\gamma_g = 1.345 \times 10^{-2}$

Table 2.4: Bifurcation points shown in Figure 2.5.

revealing monostable and bistable regions, enabling a deeper understanding of the system's behaviour and the effects of parameter interactions.

In Figure 2.6, we track the coordinates of the transcritical and saddle-node bifurcations of Figure 2.5 in two-dimensional slices of parameter space, identifying regions of parameter space in which the model is monostable with inflammation resolving (M:Res), monostable with chronic outcomes ensuing (M:Chr), or bistable (B) with both outcomes possible and the switching between these being driven by initial conditions. In Figures 2.6(a, c, d), we observe that the transcritical bifurcation (Tr) is at a constant value for all values of m_{max} , κ_c , or γ_g . Figure 2.6(a) illustrates the general trend that we obtain healthy outcomes for large values of γ_m (which result in a small macrophage population) and chronic outcomes for small values of γ_m (which result in larger macrophage populations). These regions generally straddle an intermediate region of bistability in which both outcomes are permissible. Figure 2.6(a) illustrates how the scale of this region of bistability depends upon the parameter m_{max} , which bounds the size of the macrophage population in our model. For m_{max} small, this region of bistability narrows as the chronic outcome is gradually eliminated; this is intuitive, since the macrophage population is the only source of inflammation in this model. For m_{max} larger, however, we see relatively weak qualitative dependence on this parameter; while increasing m_{max} beyond its default value of 25 here does have some effect on the size of the bistable region, we still attain these three distinct behaviours as a function of γ_m .

In Figure 2.6(b) illustrates that increasing c_T (which is related to the growth rate of the macrophage population) enhances the stability of the chronic state, and the position of the saddle-node bifurcation that bounds this exhibits an approximately linear rela-

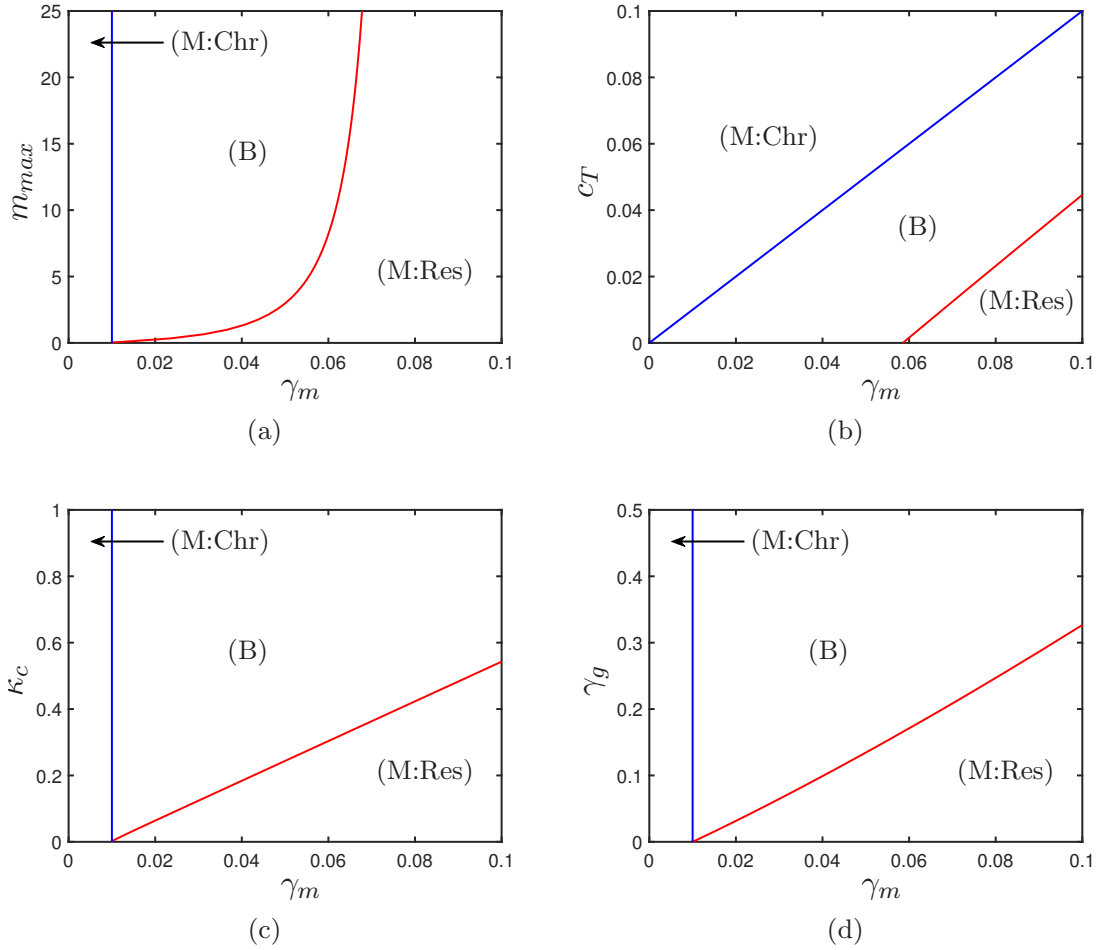


Figure 2.6: Two-parameter bifurcation diagrams illustrating steady state solutions of the model and their dependence upon the model’s parameters. Red and blue lines represent saddle-node and transcritical bifurcations respectively. “B” = bistable with both healthy and chronic outcomes permissible; “M:Res” = monostable with inflammation resolving; “M:Chr” = monostable with a chronic outcome guaranteed.

relationship between c_T and γ_m . In Figures 2.6(c,d), we observe that increasing either κ_c or γ_g (which corresponds to enhancing the pro-inflammatory feedback or reducing the anti-inflammatory feedback) has the intuitive effect of promoting the chronic state. As either of these parameters increases, the only mechanism available to return the model to a state of guaranteed resolution of damage is to increase the parameter γ_m , which acts to eliminate the pro-inflammatory feedback loop by eliminating the macrophage population entirely.

Overall, the bifurcation analysis of (2.3) for the parameters of Table 2.2 in Figure 2.6 reveals that our model exhibits three distinct behaviours (referred to as (M:Chr), (M:Res), and B) depending on changes in the bifurcation parameter. The size of macrophage populations significantly influences the dynamics of inflammation. Larger macrophage populations contribute to the enlargement of the bistable region, representing both

healthy or chronic outcomes, with switching being driven by the system's initial conditions. In addition, macrophages are our model's main source in establishing positive and negative feedback loops and increasing the concentration of pro- and anti-inflammatory mediators in the inflamed area via κ_c and γ_g , respectively. These mediators play a crucial role in either resolving inflammation or causing further damage. In particular, when the size of macrophage populations is small (indicated by large values of γ_m), the system tends towards a guaranteed healthy outcome. This is achieved by reducing the triggering of pro-inflammatory components (which results in small values of m_{max} , c_T , κ_c and γ_g), thereby eventually eliminating the stimulus of inflammation originating from the macrophage population in the damaged area.

2.4 Discussion

In this chapter, we have presented and analysed a simple baseline model of the inflammatory response that involves interactions between a single population of macrophages and groups of generic pro- and anti-inflammatory mediators. In this model, we are primarily interested in how variations in model parameters affect a switch between resolving and chronic outcomes. The resolution of inflammation occurs when monocyte-derived macrophages leave the affected tissue, the concentration of pro-inflammatory mediators subsides, and the tissues regain their integrity and function. By contrast, chronic inflammation occurs when macrophages release excessive pro-inflammatory mediators in the inflamed area, exacerbating the inflammatory response and causing further tissue damage.

In this model, our single macrophage population provides a simple switch between resolved (healthy) and chronic steady state solutions. Depending on our choice of parameters or the model's initial conditions, the model exhibits three distinct behaviours; the model is either monostable with resolution guaranteed, monostable with chronic outcomes guaranteed, or bistable with both outcomes permissible and the resulting inflammatory condition determined by initial conditions. Since the macrophage population is inflammation-promoting in this model, parameter choices that reduce the size of the macrophage population promote monostability to the resolved outcome in general. That is, to ensure resolution, we may either decrease the rate of macrophage proliferation (by reducing c_T) or increase the rate of macrophage loss (γ_m). Similarly, downscaling the rates of pro-inflammatory mediator production (κ_c) or anti-inflammatory mediator decay (γ_g) shifts the model toward a resolved outcome.

Despite the regulated and prominent role of macrophages in alerting the immune sys-

tem in case of tissue damage and the repair and remodelling of tissues, they can also indirectly negatively impact the affected tissues, exacerbating tissue injury into a chronic disease, since all macrophages exhibit pro-inflammatory effect in this model. However, we observe that the only way to achieve a resolved outcome is to ultimately eliminate the macrophage population entirely. We note that eliminating macrophages to mitigate damage is not biologically realistic, as macrophages should be present to low baseline levels even in healthy tissue; we regard this as a significant limitation of this model, which we will seek to address in the next chapter. Nonetheless, it is pertinent to note that many existing models of inflammatory dynamics use models akin to our simple model (Kumar *et al.*, 2004; Herald, 2010; Dunster *et al.*, 2014; Bayani *et al.*, 2020a), and regard the macrophage variable as describing an elevation of macrophage numbers above the healthy baseline, rather than an absolute population size. While this interpretation of the zero-state is certainly justifiable in some settings, we note that this modelling approach can potentially also come with a more limited range of dynamics than a more advanced model may emit.

We note that the macrophage description of this model is perhaps most similar to that of many published models (*e.g.* Kumar *et al.* (2004); Herald (2010); Dunster *et al.* (2014); Bayani *et al.* (2020a)) since pro- and anti-inflammatory effects are attributed to the same macrophage population. Our analysis of the model reveals a key weakness thereof, which is that eliminating chronic outcomes is only possible via the elimination of the macrophage population as a whole. This is somewhat unrealistic, since healthy outcomes in real tissues would typically include a baseline (positive) level of resident macrophages (Yona *et al.*, 2013; Jenkins & Allen, 2021; Mu *et al.*, 2021). It is well-established that macrophages are highly plastic cells with distinct functional phenotypes that play a critical role in the inflammatory response. Therefore, we aim to understand the distinct roles of macrophage phenotypes that lead to more effective treatment methods, promoting healing in chronic conditions or reducing harm to damaged tissues. In the next chapter, we look to improve on our existing model by incorporating separate descriptions of pro- and anti-inflammatory macrophages, and we examine how switching between these phenotypes affects the dynamics of the model.

Modelling The Roles of Distinct Macrophage Phenotypes

Macrophages play a crucial role in all stages of inflammation and exhibit remarkable plasticity and heterogeneity in response to various stimuli, being able to differentiate into distinct phenotypes with different functional properties. Thus, macrophages exhibit a wide range of effects (both pro- and anti-inflammatory) depending on their polarisation state or “phenotype”. Furthermore, macrophages can switch phenotypes in response to their environmental signals and tissue types, including in response to the presence of various inflammatory mediators. This diversity of functional phenotypes enables macrophages to play diverse roles in the inflammatory response as directed by environmental signals in promoting and resolving inflammation.

Macrophages are characterised as a heterogeneous group of cells with various functional states. Therefore, unambiguously categorising macrophages into distinct phenotypes is unresolved and contentious. However, macrophage phenotypes can be classified into two main distinct subtypes based on their function: pro- and anti-inflammatory macrophages. Commonly, many authors refer to pro- and anti-inflammatory macrophages as “M1” and “M2” phenotypes (or similarly “classically-activated” and “alternatively-activated” phenotypes), with pro-inflammatory macrophages often being associated with inflammation and tissue damage, while anti-inflammatory macrophages are associated with tissue repair (Martinez & Gordon, 2014; Murray *et al.*, 2014; Martin & García, 2021). What is clear is that macrophages are involved in both the promotion and resolution of inflammation, changing their role according to their environment, and that this plasticity and diversity of macrophage phenotypes is a potential therapeutic target in inflammatory diseases (Mosser *et al.*, 2021; Ross *et al.*, 2021).

In this chapter, we modify the construction of the baseline model in Chapter 2 by splitting the macrophage population into two distinct phenotypes, with primarily pro- and anti-inflammatory behaviours. The resulting model focuses on resolving inflammation by examining interactions between these subtypes and inflammatory mediators within a sterile environment. Our main goal is to understand the precise roles of these macrophage phenotypes to pave the way for finding effective treatment methods aiding in repairing damaged tissue (*i.e.* resolving inflammation) or limiting the progression of chronic disease. Comparing the results of the models in chapters 2 and 3, we can elucidate how the macrophage phenotype descriptions can influence the dynamics of models of the inflammatory response.

3.1 Model derivation

In this model, we modify our description of the macrophage population in the baseline model presented in Chapter 2, to account for two distinct phenotypes of macrophages rather than the generic macrophages: one which is fundamentally pro-inflammatory (denoted m_p^*) and one which is fundamentally anti-inflammatory (denoted m_a^*), focussing on the interactions between these macrophage phenotypes and generic pro-inflammatory mediators (c^*), and also generic anti-inflammatory mediators (g^*) within a sterile environment. In general, a healthy tissue would include a baseline population of tissue-resident macrophages that are fundamentally associated with anti-inflammatory macrophages; however, in an inflammatory context, we expect heightened macrophage recruitment, with recruited macrophages being largely associated with pro-inflammatory behaviour, with the potential to cause significant tissue damage if unchecked (Martinez & Gordon, 2014). The dependent variables that appear in this model are given in Table 3.1. Asterisks indicate dimensional quantities throughout this chapter.

Pro- and anti-inflammatory macrophages differ in triggers, cytokine release, and biological functions (Shapouri-Moghaddam *et al.*, 2018). The function of pro-inflammatory macrophages (m_p^*) is often associated with the elevated production of pro-inflammatory mediators (c^*). Therefore, m_p^* macrophages exhibit potent activity against noxious stimuli, such as diseased cells and foreign substances, and release several pro-inflammatory cytokines via κ_c^* to trigger the pro-inflammatory response (Ahamada *et al.*, 2021). The action of m_p^* macrophages is counterbalanced by the role of anti-inflammatory macrophages (m_a^*), which aim primarily to suppress inflammation and maintain tissue homeostasis. Therefore, m_a^* macrophages secrete a low

Variable	Description	Unit
g^*	Anti-inflammatory mediators	pg mm^{-3}
c^*	Pro-inflammatory mediators	pg mm^{-3}
m_p^*	Pro-inflammatory macrophages	cells mm^{-3}
m_a^*	Anti-inflammatory macrophages	cells mm^{-3}

Table 3.1: Summary of the dependent variables that appear in this model.

level of pro-inflammatory cytokines but release an elevated level of anti-inflammatory cytokines via κ_g^* to clear inflammation and initiate tissue repair (Mohammadi *et al.*, 2019). In addition, anti-inflammatory mediators (g^*) alleviate and reduce inflammatory damage by removing pro-inflammatory mediators (c^*) at rate δ^* . The main functional activities associated with these phenotypes can be summarized as “Fight” for m_p^* macrophages and “Fix” for m_a^* macrophages (Mills, 2012). This functional versatility is central for macrophages to successfully perform their homoeostatic and regulatory roles, aiming to resolve inflammation and restore tissue homoeostasis.

The functional phenotypes of macrophages evolve in response to the gradual changes in their environmental signals and molecular mediators. Due to the high plasticity of macrophages, m_p^* macrophages can differentiate into m_a^* macrophages in response to environmental signals and vice versa (Shapouri-Moghaddam *et al.*, 2018; Mohammadi *et al.*, 2019; Ahamada *et al.*, 2021). The original polarisation can also be reversible upon environmental changes. For instance, the same cell may initially participate in a pro-inflammatory reaction and later join in an anti-inflammatory reaction to resolve inflammation and tissue repair. Thus, macrophages have the ability to switch phenotypes; we parameterise this switching by α_1^* (anti-inflammatory macrophages becoming pro-inflammatory) and α_2^* (the converse). This phenotypic switching is further stimulated by the presence of pro/anti-inflammatory mediators; we introduce corresponding parameters β_1^* and β_2^* to represent the strength of this mediator dependence. Here, we model the growth of the total macrophage population as logistic, up to a maximum carrying capacity of m_{max}^* . We assume that all newly recruited macrophages are of the anti-inflammatory phenotype associated with tissue repair but, under the assumption that the tissue being modelled has a maximal capacity for the total number of macrophages, we assume that the rate of this recruitment depends on the total macrophage number, $m_a^* + m_p^*$. Since macrophages can switch phenotypes dynamically and in both directions (Porcheray *et al.*, 2005; Zhang *et al.*, 2021), this approach is necessary to ensure that total macrophage numbers do not become unbounded during the course of our simulations. The interactions incorporated in this model are illustrated

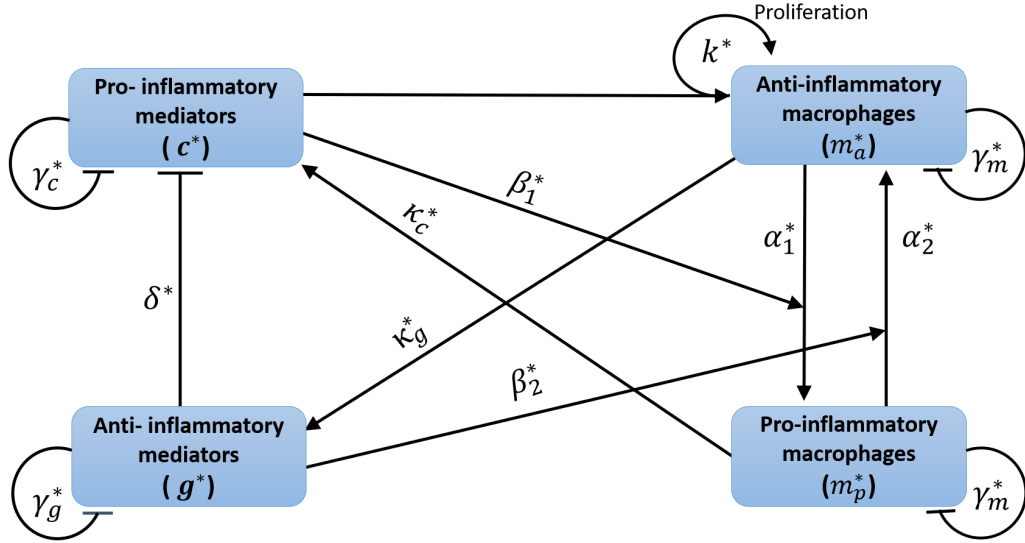


Figure 3.1: Schematic diagram representing (3.1) and illustrating component interactions between pro- and anti-inflammatory macrophages (m_p^* and m_a^*) in response to pro- and anti-inflammatory mediators (c^* and g^*), respectively. Arrows indicate positive feedbacks or supply terms; lines terminated with bars indicate negative feedbacks or loss terms.

in Figure 3.1, and give rise to the following (dimensional) ODEs:

$$\frac{dg^*}{dt^*} = \kappa_g^* m_a^* - \gamma_g^* g^*, \quad (3.1a)$$

$$\frac{dc^*}{dt^*} = \kappa_c^* m_p^* - \delta^* c^* g^* - \gamma_c^* c^*, \quad (3.1b)$$

$$\frac{dm_p^*}{dt^*} = \alpha_1^* \beta_1^* c^* m_a^* - \alpha_2^* \beta_2^* g^* m_p^* - \gamma_m^* m_p^*, \quad (3.1c)$$

$$\frac{dm_a^*}{dt^*} = k^* (c^* + c_T^*) \left(m_a^* + m_p^* \right) \left(1 - \frac{m_a^* + m_p^*}{m_{max}^*} \right) - \alpha_1^* \beta_1^* c^* m_a^* + \alpha_2^* \beta_2^* g^* m_p^* - \gamma_m^* m_a^*. \quad (3.1d)$$

The interactions presented in Figure 3.1 involve positive and negative feedback loops. The positive feedback depends on the ability of m_a^* macrophages to differentiate toward pro-inflammatory reaction m_p^* at rate α_1^* in response to different environmental stimuli, secreting pro-inflammatory cytokines via κ_c^* in response to a concentration gradient in the pro-inflammatory mediators c^* , which recruits more m_p^* macrophages to the inflamed site. On the other hand, the negative feedback operates through m_a^* macrophages and anti-inflammatory mediators g^* via κ_g^* and δ^* .

3.1.1 Parameters and non-dimensionalisation

The common dimensional parameters appearing in (2.1) and (3.1) are discussed in Section 2.1.1. Therefore, we briefly summarise the available estimates of the new dimensional parameters and comment upon how these estimates inform the corresponding choices for our baseline set of dimensionless parameters.

Transition rates between macrophage phenotypes play a crucial role in suppressing or amplifying inflammation (Zhu *et al.*, 2014; Shapouri-Moghaddam *et al.*, 2018). Torres *et al.* (2019) document that the dynamic transition of macrophage phenotypes from anti-macrophage phenotypes m_a^* to pro-macrophage phenotypes m_p^* at a rate of α_1^* lies in the range $0.01 - 1 \text{ cell mm}^{-3} \text{ day}^{-1}$, while the reverse transition of m_p^* to m_a^* at a rate of α_2^* is in the range $0.1 - 100 \text{ cell mm}^{-3} \text{ day}^{-1}$.

We nondimensionalise the system (3.1) by applying the following rescalings:

$$t^* = \frac{1}{\gamma_c^*} t, \quad c^* = \frac{\gamma_c^*}{k^*} c, \quad g^* = \frac{\gamma_c^*}{\delta^*} g, \quad m_a^* = \frac{\gamma_c^{*2}}{\delta^* \kappa_g^*} m_a, \quad m_p^* = \frac{\gamma_c^{*2}}{\delta^* \kappa_g^*} m_p, \quad (3.2)$$

to provide the following dimensionless equations:

$$\frac{dg}{dt} = m_a - \gamma_g g, \quad (3.3a)$$

$$\frac{dc}{dt} = \kappa_c m_p - c g - c, \quad (3.3b)$$

$$\frac{dm_p}{dt} = \alpha_1 c m_a - \alpha_2 g m_p - \gamma_m m_p, \quad (3.3c)$$

$$\frac{dm_a}{dt} = (c + c_T) (m_a + m_p) \left(1 - \frac{m_a + m_p}{m_{max}}\right) - \alpha_1 c m_a + \alpha_2 g m_p - \gamma_m m_a, \quad (3.3d)$$

in which we have introduced the following two additional dimensionless parameters besides the dimensionless parameter groups in (2.4):

$$\alpha_1 = \frac{\alpha_1^* \beta_1^*}{k^*}, \quad \alpha_2 = \frac{\alpha_2^* \beta_2^*}{\delta^*}. \quad (3.4)$$

The dimensionless parameters appearing in (3.3) are summarised in Table 3.2, alongside baseline values used in our simulations. We expect macrophage phenotype switching from the anti-inflammatory phenotype to the pro-inflammatory phenotype to dominate the converse direction as many inflammatory conditions are associated with increased ratios of pro-inflammatory macrophages (Zhu *et al.*, 2014; Lissner *et al.*, 2015); thus we expect $\alpha_1 \gg \alpha_2$. We solve (3.3) subject to the initial conditions of the form $m_p(0) = m_{p0} > 0$, $c(0) = c_0 > 0$, and $m_a(0) = g(0) = 0$.

Parameter	Expression	Meaning	Baseline value
κ_c	$k^* \kappa_c^* / \delta^* \kappa_g^*$	Rate of production of pro-inflammatory mediators	0.35
γ_m	γ_m^* / γ_c^*	Decay rate of macrophages	0.05
γ_g	γ_g^* / γ_c^*	Decay of anti-inflammatory mediators	0.2
c_T	$k^* c_T^* / \gamma_c^*$	Rate of macrophage proliferation in the absence of pro-inflammatory mediators	0.01
m_{max}	$\delta^* \kappa_g^* m_{max}^* / \gamma_c^{*2}$	Maximum macrophage population size	25
α_1	$\alpha_1^* \beta_1^* / k^*$	Macrophage phenotype switching (m_a to m_p)	1
α_2	$\alpha_2^* \beta_2^* / \delta^*$	Macrophage phenotype switching (m_p to m_a)	0.01

Table 3.2: Summary of the dimensionless parameters appearing in (3.3).

3.2 Identification and classification of steady state solutions

In this section, we aim to identify the steady state solutions of (3.3) and classify them by their stability. It is relatively easy to show that (3.3) has a zero steady state corresponding to a healthy response, denoted by FP_1 . However, it is generally challenging to find an analytical solution for the system of non-linear equations. Therefore, it is more appropriate to use a numerical ODE solver in Matlab to obtain the stable non-zero steady state solutions, and verify them using XPPAUT software. It appears that two additional non-zero steady states of (3.3) exist; we denote the non-zero steady state as FP_2 which represents a healthy response where the pro-inflammatory components are zero ($c = m_p = 0$) but the anti-inflammatory components remain positive ($g > 0$ and $m_a > 0$). On the other hand, the non-zero steady state in which all variables are positive represent a chronic state.

The Jacobian matrix J of (3.3) is given by

$$J = \begin{pmatrix} -\gamma_g & 0 & 0 & 1 \\ -c & -g - 1 & \kappa_c & 0 \\ -\alpha_2 m_p & \alpha_1 m_a & -\gamma_m - \alpha_2 g & \alpha_1 c \\ \alpha_2 m_p & T_{42} & T_{43} & T_{44} \end{pmatrix}, \quad (3.5)$$

where,

$$T_{42} = -\alpha_1 m_a - (m_a + m_p) \left(\frac{m_a + m_p}{m_{max}} - 1 \right), \quad (3.6)$$

$$T_{43} = \alpha_2 g - (c + c_T) \left(\frac{m_a + m_p}{m_{max}} - 1 \right) - \frac{(c + c_T) (m_a + m_p)}{m_{max}}, \quad (3.7)$$

$$T_{44} = -\gamma_m - \alpha_1 c - (c + c_T) \left(\frac{m_a + m_p}{m_{max}} - 1 \right) - \frac{(c + c_T)(m_a + m_p)}{m_{max}}. \quad (3.8)$$

To examine the stability of the zero steady state, we compute (3.5) at FP_1 , where $FP_1 = (g, c, m_p, m_a) = (0, 0, 0, 0)$, giving

$$\mathbf{J}|_{FP_1} = \begin{pmatrix} -\gamma_g & 0 & 0 & 1 \\ 0 & -1 & \kappa_c & 0 \\ 0 & 0 & -\gamma_m & 0 \\ 0 & 0 & c_T & c_T - \gamma_m \end{pmatrix}. \quad (3.9)$$

Evaluating eigenvalues of (3.9), we obtain

$$\lambda_1 = -1, \lambda_2 = c_T - \gamma_m, \lambda_3 = -\gamma_g, \lambda_4 = -\gamma_m. \quad (3.10)$$

Therefore, we can conclude that this model exhibits a healthy steady state in which all variables are equal to zero, and this steady state is stable provided that $\gamma_m > c_T$; otherwise, it is unstable. However, this model can also exhibit a further healthy steady state in which pro-inflammatory components are zero but anti-inflammatory components reach some positive levels, allowing inflammation to remain suppressed. That is, we have a second steady state in which

$$m_p = c = 0, \quad m_a = m_{max} \left(1 - \frac{\gamma_m}{c_T} \right), \quad g = \frac{m_{max}}{\gamma_g} \left(1 - \frac{\gamma_m}{c_T} \right), \quad (3.11)$$

which exists provided that $\gamma_m < c_T$. This steady state can be considered representative of a configuration in which inflammation is suppressed by a baseline population of tissue resident (anti-inflammatory) macrophages, as would typically be present in a healthy tissue. To examine the stability of the additional healthy steady state, we first compute the Jacobian (3.5) at FP_2 , where FP_2 is given by (3.11), which gives

$$\mathbf{J}|_{FP_2} = \begin{pmatrix} -\gamma_g & 0 & 0 & 1 \\ 0 & j_{22} & \kappa_c & 0 \\ 0 & j_{32} & j_{33} & 0 \\ 0 & j_{42} & j_{43} & \gamma_m - c_T \end{pmatrix}, \quad (3.12)$$

where,

$$j_{22} = \frac{m_{max}}{\gamma_g} \left(\frac{\gamma_m}{c_T} - 1 \right) - 1, \quad (3.13)$$

$$j_{32} = -\alpha_1 m_{max} \left(\frac{\gamma_m}{c_T} - 1 \right), \quad (3.14)$$

$$j_{33} = \frac{\alpha_2 m_{max}}{\gamma_g} \left(\frac{\gamma_m}{c_T} - 1 \right) - \gamma_m, \quad (3.15)$$

$$j_{42} = m_{max} \left(\frac{\gamma_m}{c_T} - 1 \right) \left(\alpha_1 - \frac{\gamma_m}{c_T} \right), \quad (3.16)$$

$$j_{43} = 2\gamma_m - c_T - \frac{\alpha_2 m_{max}}{\gamma_g} \left(\frac{\gamma_m}{c_T} - 1 \right). \quad (3.17)$$

Evaluating the eigenvalues of the Jacobian matrix (3.12), using the characteristic equation $\det(\mathbf{J} - \lambda \mathbf{I}) = 0$, we obtain the eigenvalues λ as follows:

$$\lambda_1 = -\gamma_g, \quad \lambda_2 = \gamma_m - c_T, \quad \lambda_{3,4} = \frac{(j_{22} + j_{33}) \pm \sqrt{(j_{22} - j_{33})^2 + 4\kappa_c j_{32}}}{2}. \quad (3.18)$$

Next, we determine the stability of FP_2 by examining the signs of the eigenvalues given in (3.18). We observe that λ_1 is always negative. For FP_2 as defined in (3.11) to exist, we require $\gamma_m < c_T$, consequently ensuring that λ_2 remains negative.

Moving on to λ_3 , for stability we need to show that it is always negative. This can be established by examining the inequality:

$$j_{22} + j_{33} < 0, \quad (3.19)$$

where j_{22} is derived from (3.13) and j_{33} is derived from (3.15). Substituting the expressions of j_{22} and j_{33} in (3.19), we obtain

$$\frac{m_{max}}{\gamma_g} \left(\frac{\gamma_m}{c_T} - 1 \right) - 1 + \frac{\alpha_2 m_{max}}{\gamma_g} \left(\frac{\gamma_m}{c_T} - 1 \right) - \gamma_m < 0. \quad (3.20)$$

Since we require $\gamma_m < c_T$ for FP_2 to exist, the bracketed terms in (3.20) are negative, and (3.20) is satisfied for all relevant parameter values.

Now, to determine the condition for λ_4 to be negative, we consider the inequality:

$$j_{22} + j_{33} + \sqrt{(j_{22} - j_{33})^2 + 4\kappa_c j_{32}} < 0. \quad (3.21)$$

From (3.21), we require

$$\sqrt{(j_{22} - j_{33})^2 + 4\kappa_c j_{32}} < -(j_{22} + j_{33}). \quad (3.22)$$

By squaring both sides of the inequality, we obtain

$$(j_{22} - j_{33})^2 + 4\kappa_c j_{32} < (j_{22} + j_{33})^2. \quad (3.23)$$

Expanding brackets then provides

$$j_{22}^2 - 2j_{22}j_{33} + j_{33}^2 + 4\kappa_c j_{32} < j_{22}^2 + 2j_{22}j_{33} + j_{33}^2, \quad (3.24)$$

from which we observe that stability requires

$$\kappa_c j_{32} < j_{22} j_{33}. \quad (3.25)$$

We can compute j_{22} , j_{32} , and j_{33} from (3.13), (3.14), and (3.15), respectively, to continue solving (3.25) and find the conditions for λ_4 to be negative. We simplify (3.25) as follows:

$$-\kappa_c \alpha_1 m_{max} \left(\frac{\gamma_m}{c_T} - 1 \right) < \left[\frac{m_{max}}{\gamma_g} \left(\frac{\gamma_m}{c_T} - 1 \right) - 1 \right] \left[\frac{\alpha_2 m_{max}}{\gamma_g} \left(\frac{\gamma_m}{c_T} - 1 \right) - \gamma_m \right]. \quad (3.26)$$

Expanding brackets on the right-hand side of (3.26), we obtain:

$$\frac{\alpha_2 m_{max}^2}{\gamma_g^2} \left(\frac{\gamma_m}{c_T} - 1 \right)^2 + m_{max} \left(\frac{\gamma_m}{c_T} - 1 \right) \left(\frac{-\gamma_m}{\gamma_g} - \frac{\alpha_2}{\gamma_g} \right) + \gamma_m + \kappa_c \alpha_1 m_{max} \left(\frac{\gamma_m}{c_T} - 1 \right) > 0. \quad (3.27)$$

Therefore, λ_4 is a negative if $\gamma_m < c_T$ and the following condition is satisfied:

$$\frac{\alpha_2 m_{max}^2}{\gamma_g^2} \left(\frac{\gamma_m}{c_T} - 1 \right)^2 + m_{max} \left[\alpha_1 \kappa_c - \frac{\gamma_m + \alpha_2}{\gamma_g} \right] \left(\frac{\gamma_m}{c_T} - 1 \right) + \gamma_m > 0. \quad (3.28)$$

Hence, by setting the conditions for all eigenvalues given in (3.18) to be negative, we have shown that the healthy non-trivial steady state FP_2 is stable when the conditions for λ_4 are satisfied, which are $\gamma_m < c_T$ and (3.28). Since we require $\gamma_m/c_T - 1 < 0$ in order for the steady state of (3.11) to exist, a sufficient condition for the stability of the steady state FP_2 is given by:

$$\alpha_1 \kappa_c - \frac{\gamma_m + \alpha_2}{\gamma_g} < 0. \quad (3.29)$$

Simplifying (3.29), we obtain:

$$\alpha_1 \gamma_g \kappa_c < \gamma_m + \alpha_2. \quad (3.30)$$

We note that the terms appearing on the left-hand side of (3.30) are all pro-inflammatory (with α_1 representing growth of the pro-inflammatory macrophage population, κ_c representing production of pro-inflammatory mediators and γ_g reducing the influence of anti-inflammatory mediators), while the terms on the right-hand side of (3.30) are essentially anti-inflammatory (with α_2 stimulating growth of the anti-inflammatory macrophage population and γ_m acting to suppress the macrophage population as a whole). Broadly, we therefore expect (3.28) to yield a stable steady state provided that pro-inflammatory interactions are weak in comparison to anti-inflammatory effects.

3.3 Numerical simulations

All computational simulations were carried out using Matlab (ODE solver ode45). The numerical simulations of (3.3) exhibit two distinct healthy responses and a chronic outcome, as shown in Figure 3.2.

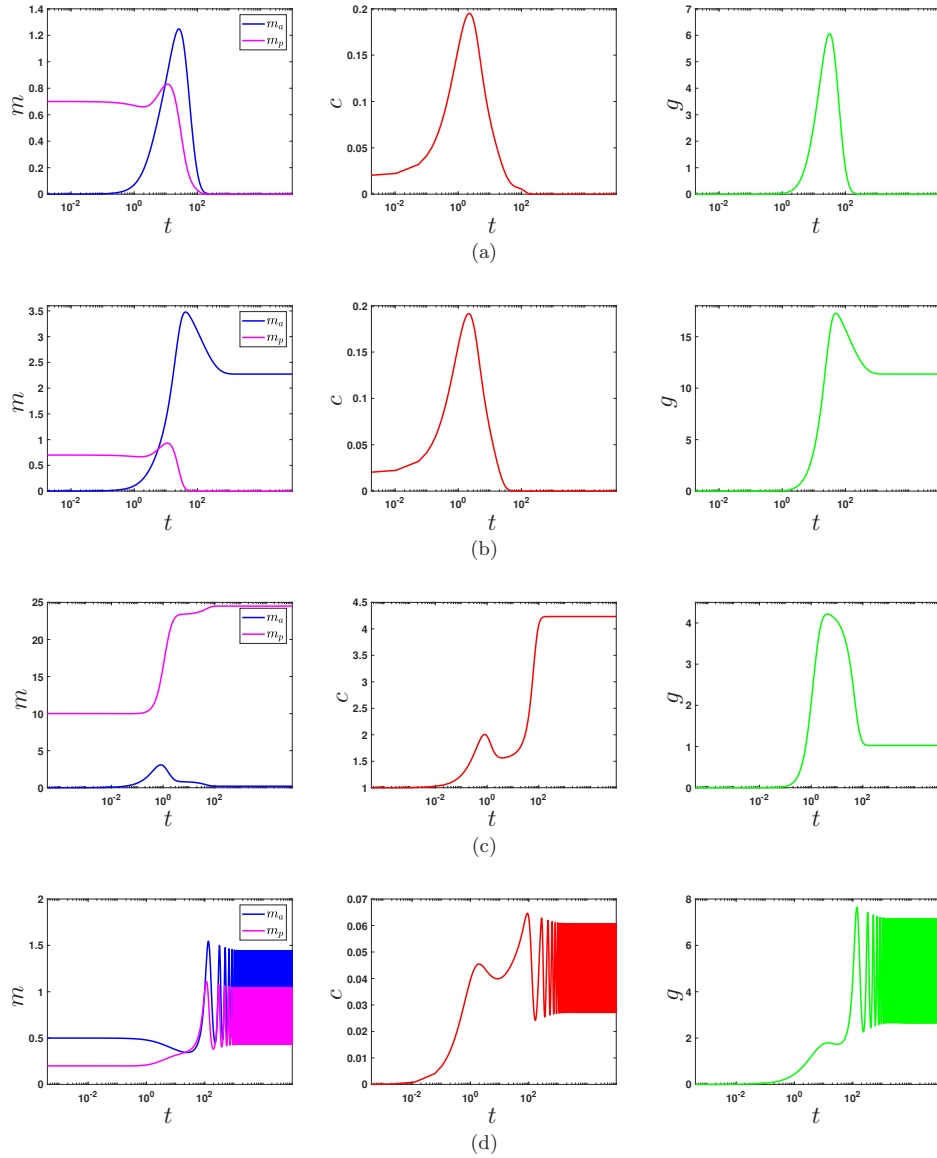


Figure 3.2: Numerical simulations of (3.3) reveal that the model can exhibit both chronic and healthy responses. In (a), we initialise the model with an initial stimulus of pro-inflammatory components ($m_p(0) = 0.7$, $c(0) = 0.02$ and $m_a(0) = g(0) = 0$), for the parameters of Table 3.2, showing that the model attains a healthy steady state in which all variables eventually become zero. In (b), an alternative healthy steady state is observed, where the pro-inflammatory components become zero ($m_p = c = 0$), while anti-inflammatory components reach some positive levels ($m_a > 0$ and $g > 0$). This state is achieved by using the same initial conditions as in (a), but with a higher stimulus of macrophage recruitment by setting $\gamma_m < c_T$, where $c_T = 0.055$, while keeping the rest of the parameters as provided in Table 3.2. For both (c) and (d), we set $\alpha_1 = 1.7$, leaving the other parameters unchanged as detailed in Table 3.2. In (c), we initialise the model with ($m_p(0) = 10$, $c(0) = 1$ and $m_a(0) = g(0) = 0$), while in (d) ($m_p(0) = 0.2$, $m_a(0) = 0.5$ and $c(0) = g(0) = 0$). In (c), the model attains a chronic steady state; in (d) we observe chronic oscillations.

In Section 3.2, we established that the zero steady state, denoted as FP_1 , is stable if and only if $\gamma_m > c_T$ as defined in (3.10). As illustrated in Figure 3.2(a), the stable zero steady state corresponds to a healthy response in which all variables eventually converge to zero.

The presence of anti-inflammatory macrophages (m_a) and anti-inflammatory mediators (g) within healthy tissues is a prerequisite for suppressing pro-inflammatory reactions (m_p and c) and maintaining tissue homeostasis and overall health. In Section 3.2, we documented that a non-zero steady state, denoted as FP_2 , can remain stable provided that $\gamma_m < c_T$ (as defined in (3.11)) and the condition stated in (3.28) is met. Consequently, when these conditions are satisfied, an alternative healthy steady state can be achieved, characterized by the complete absence of pro-inflammatory components ($m_p = c = 0$), while anti-inflammatory components reach some positive levels ($m_a > 0$ and $g > 0$), as shown in Figure 3.2(b). As a result, the dynamics shown in Figure 3.2(b) provide more biologically realistic results than that in Figure 3.2(a). This is because g and m_a must remain present in the body to fulfil their vital biological roles rather than being assumed to be eliminated for the attainment of a healthy state.

Increasing the transition rate towards pro-inflammatory macrophages by setting $\alpha_1 = 1.7$ in Figure 3.2 (c) and (d) can result in chronic outcomes. In such cases, all variables reach some positive levels, leading to persistent inflammation. In Figure 3.2(c), we can observe that the model attains a highly-inflamed configuration, where $m_p \gg m_a$, and c reaches an elevated level. This configuration enhances the pro-inflammatory feedback from m_p , leading to a significant increase in c and sustained high-level inflammation, which causes more damage. Figure 3.2 (d) illustrates that the model can exhibit a chronic outcome characterized by oscillatory behaviour (which could be likened to inflammatory conditions that exhibit relapsing–remitting characteristics), in which all variables reach non-zero levels. However, these variables do not converge to a stable steady state but rather fluctuate over time, indicating that the system follows a periodic pattern. This suggests the presence of Hopf bifurcation.

3.4 Bifurcation analysis

Macrophages are a heterogeneous group of cells with various functional states in the inflammatory response. Therefore, it is essential to understand the underlying mechanisms of macrophage functional phenotypes, including m_a and m_p subtypes, which play a crucial role in resolving inflammation. Analysing the bifurcation structure of models of the inflammatory response can help us more effectively develop potential

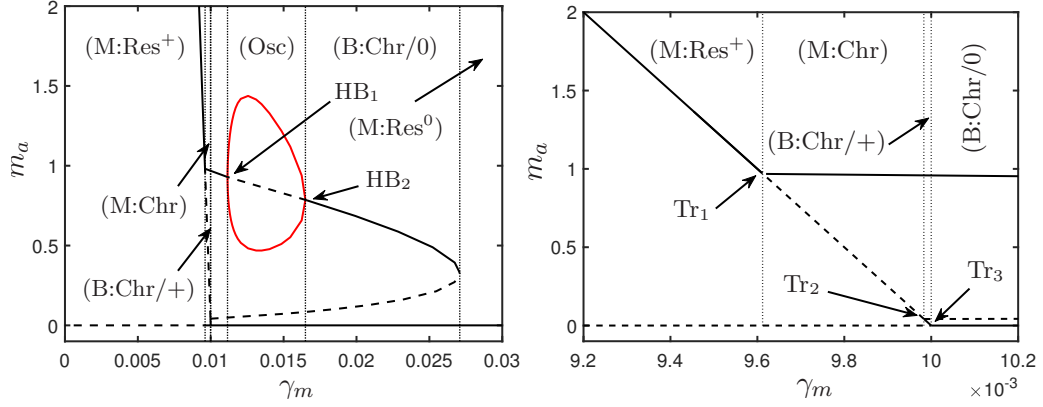


Figure 3.3: Bifurcation analysis of (3.3) for the parameter values of Table 3.2, showing how the stability of the steady states changes as γ_m vary. The figure on the right illustrates the confined region defined by the transcritical bifurcations depicted in the Figure on the left. Solid and dashed lines represent stable and unstable solutions respectively; red line represents a periodic orbit. “B” indicates that the model is bistable with both healthy and chronic outcomes permissible, while “M” denotes monostability; the corresponding steady state solutions being that in which inflammation resolves and all variables reach zero (labelled “Res⁰” or “0”), that in which inflammation resolves but anti-inflammatory components are positive (labelled “Res⁺” or “+”; see (3.11)), or chronic states (labelled “Chr”). “Osc” denotes oscillatory (chronic) solutions.

therapeutic targets for inflammation.

Figure 3.3 shows how the stability of the steady states of (3.3) changes as γ_m varies, for the baseline parameter values of Table 3.2. The over-arching key observation here (in comparison with the corresponding figures for the simple homogenised model presented in Chapter 2; Figure 2.6) is that accounting separately for distinct macrophage phenotypes avails a much more complex array of possible outcomes. As described above, this model supports two different types of resolved outcomes: that in which all variables are zero (labelled “Res⁰” or “0” in Figure 3.3); or that given by (3.11) (labelled “Res⁺” or “+” in Figure 3.3), in which the macrophage population reaches a positive steady state value, but inflammation is suppressed by the sustained presence of the anti-inflammatory macrophage and mediator populations. Biologically, the latter of these represents a more realistic healthy configuration. Which of these resolved states is permissible is controlled only by the parameters that govern the overall macrophage population dynamics, *i.e.* c_T , which represents baseline macrophage recruitment in the absence of inflammation, and γ_m , which is the rate of macrophage loss (as macrophages either die or vacate the tissue of interest). Figure 3.3 shows a transcritical bifurcation lying at $\gamma_m = c_T = 0.01$, which is independent of the model’s other parameters. For $\gamma_m > c_T$, the zero state is always stable and the steady state of (3.11) does not exist.

For $\gamma_m < c_T$, the zero state is unstable and the steady state of (3.11) is stable apart from in a narrow region of parameter space in which this solution is also destabilised by the model's other pro-inflammatory interactions according to (3.28). Holding all parameters apart from γ_m fixed, (3.28) provides a quadratic equation in γ_m , the roots of which provide two further transcritical bifurcations as the stability of the Res^+ state changes; these transcritical bifurcations also give rise to branches of chronic solutions. These chronic solutions persist as γ_m is slowly increased, until we reach the limit point represented by SN; beyond this point, γ_m is sufficiently large that the only possible outcome is the zero state. In Figure 3.3, we observe that there is also the potential for the branch of chronic solutions to undergo Hopf bifurcations that give rise to stable periodic orbits, represented by red lines.

Figure 3.4 illustrates bifurcation diagrams of (3.3) in terms of the parameters given in Table 3.2. The zero steady state is stable for $\gamma_m > c_T$ as defined in (3.10). In Figure 3.4(a), the model demonstrates a guaranteed healthy outcome where all inflammatory components are zero, indicated as "M:Res⁰", when γ_g is less than the saddle-node bifurcation (occurring at $\text{SN}_1 = 0.2992$). Within the region bounded by two saddle-node bifurcations, SN_1 and SN_2 (where $\text{SN}_2 = 0.632$), the model demonstrates multiple outcomes, including a healthy zero state and varying levels of chronic inflammation (low and high). The model becomes bistable beyond SN_2 , where γ_g is sufficiently large.

In Figure 3.4(b), a healthy outcome is achieved when κ_c is less than the saddle-node bifurcation (at $\text{SN}_1 = 0.5236$), represented as "M:Res⁰". However, an excessive production of κ_c can result in sustained inflammation. Multiple outcomes are observed when κ_c is bounded between the saddle-node bifurcation and the Hopf bifurcation ($[\text{SN}_1, \text{HB}_2] = [0.5236, 0.6043]$), and oscillations occurring as κ_c approaches the vicinity of the Hopf bifurcation region. Beyond the saddle-node bifurcation (at $\text{SN}_2 = 4.177$), the model is bistable, with either the zero state or a chronic state permissible, which is denoted as (B:Chr/0).

The behaviour of steady state solutions in Figure 3.4(c) closely resembles that observed in Figure 3.4(b). As previously mentioned, as the bifurcation parameters (γ_g , κ_c and α_1) increase, an overproduction of pro-inflammatory mediators from m_p macrophages leads to persistent inflammation. In Figure 3.4(a–c), we observe that these chronic solutions persist as the bifurcation parameters (γ_g , κ_c and α_1) are gradually increased, resulting in the model exhibiting a bistable region where both healthy zero state and severe chronic inflammation are possible.

In Figure 3.4(d), α_2 plays a role in the inflammatory response opposite to that of α_1 . For the model to attain a healthy outcome, the value of α_2 must be higher than the

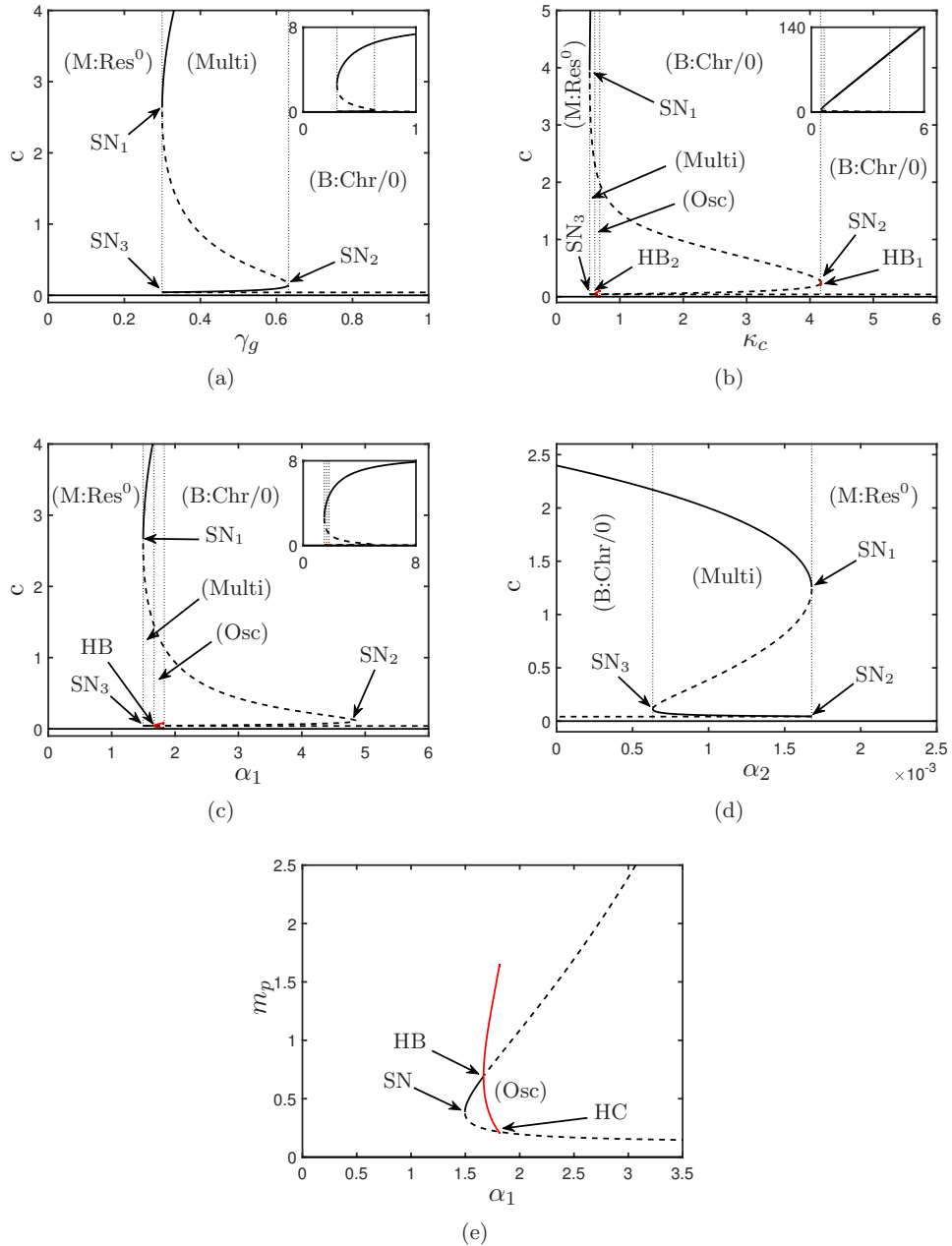


Figure 3.4: Bifurcation diagrams illustrating steady state solutions of (3.3) for the parameters given in Table 3.2. Black solid and dashed lines represent stable and unstable steady-state solutions, respectively. The red line represents a periodic orbit. In (a-d), “M:Res⁰” denotes monostable with inflammation resolving and all variables reach zero; “B:Chr/0” indicates that the model is bistable with both healthy and chronic outcomes permissible; ‘multi’ denotes that the model exhibits multiple outcomes, including healthy and low- and high-chronic outcomes; “Osc” denotes oscillatory (chronic) solutions. In (e), SN indicates a saddle-node bifurcation, HB represents a Hopf bifurcation, and HC denotes a Homoclinic bifurcation.

saddle-node bifurcation, denoted as SN₁ where SN₁ = 0.001678.

Bifurcation point	Bifurcation parameter
Figure 3.4 (a)	
SN ₁	$\gamma_g = 2.992 \times 10^{-1}$
SN ₂	$\gamma_g = 6.32 \times 10^{-1}$
SN ₃	$\gamma_g = 2.992 \times 10^{-1}$
Figure 3.4 (b)	
SN ₁	$\kappa_c = 5.236 \times 10^{-1}$
SN ₂	$\kappa_c = 4.177$
SN ₃	$\kappa_c = 5.236 \times 10^{-1}$
HB ₁	$\kappa_c = 4.172$
HB ₂	$\kappa_c = 6.043 \times 10^{-1}$
Figure 3.4 (c)	
SN ₁	$\alpha_1 = 1.496$
SN ₂	$\alpha_1 = 4.849$
SN ₃	$\alpha_1 = 1.496$
HB	$\alpha_1 = 1.668$
Figure 3.4 (d)	
SN ₁	$\alpha_2 = 1.678 \times 10^{-3}$
SN ₂	$\alpha_2 = 6.328 \times 10^{-4}$
SN ₃	$\alpha_2 = 1.678 \times 10^{-3}$

Table 3.3: Bifurcation points shown in Figure 3.4. SN indicates a saddle-node bifurcation and HB represents a Hopf bifurcation.

It is worth noting that, at particular values of the bifurcation parameter, there is the potential for the branch of chronic solutions to undergo Hopf bifurcations that give rise to stable periodic orbits. This is illustrated in Figure 3.4(e), where the oscillatory region expands. However, a branch of periodic solutions may suddenly end as the periodic orbit curve collides with the saddle point, resulting in a homoclinic bifurcation point (HC) and the disappearance of the periodic orbit curve. Table 3.3 summarizes all the bifurcation points shown in Figure 3.4.

In Figure 3.5, we track the coordinates of the saddle-node and Hopf bifurcations of Figure 3.4 in two-dimensional slices of parameter space, identifying regions of parameter space in which the model is monostable with inflammation resolving (M:Res⁰) or bistable (B:Chr/0) with both healthy and chronic outcomes possible, and the switching between these being driven by initial conditions. In Figure 3.5(a), it's clear that a narrow healthy outcome region is present when κ_c has a low value. Likewise, a low value of α_1 results in a narrow healthy outcome region, even when κ_c is large. This observa-

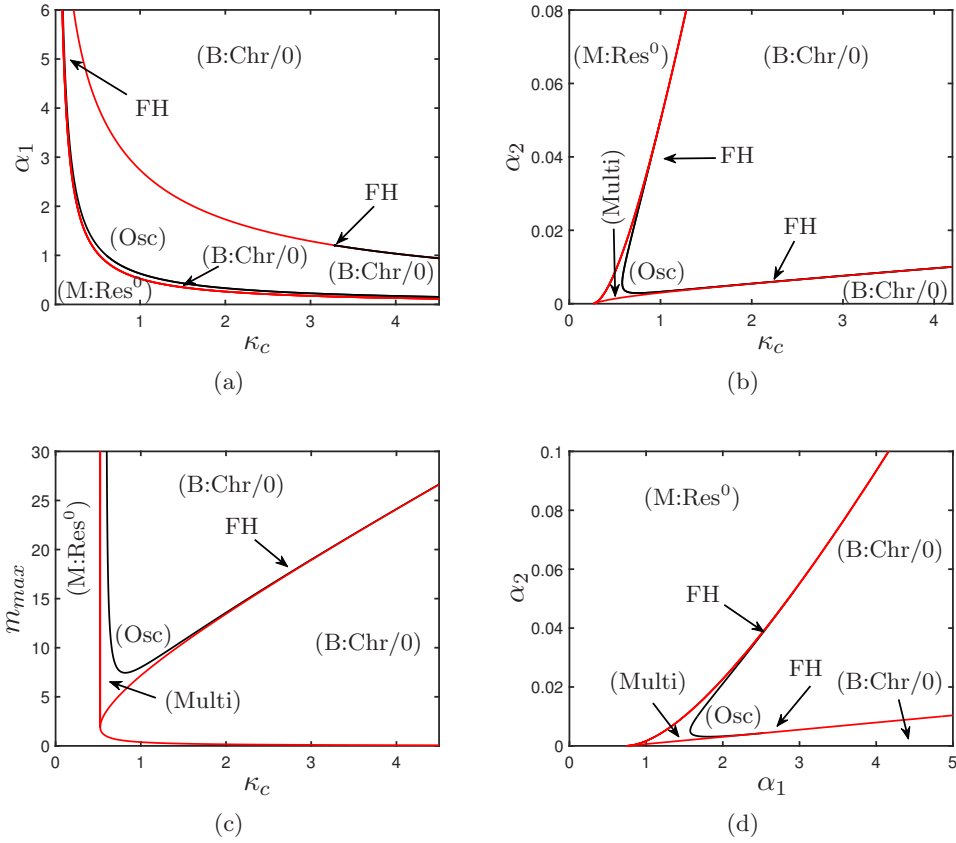


Figure 3.5: Two-parameter bifurcation diagrams illustrating solutions of (3.3) for the parameters given in Table 3.2. Red lines represent saddle-node bifurcations and black lines represent Hopf bifurcations. “M:Res⁰” denotes monostability with inflammation resolving and all variables reach zero, while “B:Chr/0” indicates that the model is bistable with both healthy and chronic outcomes permissible. “multi” denotes that the model exhibits multiple outcomes. “Osc” denotes oscillatory (chronic) solutions. “FH” indicates a Fold-Hopf bifurcation.

tion suggests that the bistability region’s scale expands as both κ_c and α_1 increase. In a dynamical system’s two-dimensional slices of parameter space, a Fold-Hopf bifurcation (FH) occurs when the saddle-node bifurcation (also known as the Fold Bifurcation) curve intersects tangentially with the Hopf bifurcation curve, as shown in Figure 3.5(a). The system undergoes a qualitative change at this point, as the Hopf curve and corresponding oscillatory solutions vanish while the saddle-node bifurcation branch persists.

Figure 3.5(b) suggests that the healthy monostability region arises when κ_c is small; otherwise, the model is bistable. Increasing α_2 expands this region, causing the saddle-node and Hopf bifurcation curves to shift to the right. Moreover, the oscillatory region is limited and confined between two saddle-node bifurcation curves.

Figure 3.5(c) illustrates that the resolution of inflammation, labelled as (M:Res⁰), can

occur with a low value of κ_c regardless of the value of m_{max} . Moreover, the region of oscillations labelled "Osc" is highly dependent on the size of the macrophage population and is eliminated when m_{max} is sufficiently small.

As previously mentioned, α_2 plays a significant role in promoting the resolution of inflammation by increasing the production of anti-inflammatory mediators from m_a macrophages, which mitigate the action of pro-inflammatory mediators. Intuitively, the effects of α_1 and α_2 are converse to one another. Figure 3.5(d) illustrates the effects of α_1 and α_2 in determining the region of inflammation outcomes; decreasing α_1 or increasing α_2 has the effect of expanding of monostability region with healthy solution guaranteed, labelled as (M:Res⁰).

Of particular interest in this model are the parameters α_1 and α_2 , which control the rates of macrophage phenotype switching (from m_a to m_p , and m_p to m_a , respectively). As discussed above, we expect $\alpha_1 \gg \alpha_2$ in general. Figures 3.6(a,b) illustrate the effects of α_1 and α_2 on the bifurcation structure of this model, with variations in these two parameters affecting changes in the stability of the Res⁺ state via (3.28) and also the position of the saddle-node that represents the switch from chronicity to the zero state for large γ_m . Intuitively, the effects of α_1 and α_2 are converse to one another. For all other parameters fixed, and assuming that $\gamma_m < c_T$ so that the Res⁺ state exists, increasing α_1 or decreasing α_2 has the effect of expanding the interval of γ_m values within which (3.28) is violated, so that the Res⁺ solution is unstable; we therefore see an expanding window in which the model is monostable with a chronic solution guaranteed (M:Chr in the figure). For sufficiently small α_1 or sufficiently large α_2 , the model's pro-inflammatory facets are so weak that the Res⁺ state is never destabilised and the model is monostable and guaranteed to attain the Res⁺ (healthy) configuration.

The parameters α_1 and α_2 also affect the chronic state by altering the position of the saddle-node bifurcation shown in Figure 3.3; as illustrated by the red lines in Figures 3.6(a,b). Decreasing α_1 or increasing α_2 weakens the model's pro-inflammatory feedbacks (in comparison to anti-inflammatory feedbacks) and shifts the saddle-node to the left in Figure 3.3, narrowing the corresponding region of bistability, until the saddle-node meets the transcritical bifurcations given by (3.28), when chronic solutions are eliminated. Conversely, increasing α_1 or decreasing α_2 shifts the balance of feedbacks towards pro-inflammation and the saddle-node shifts to the right in Figure 3.3, resulting in a larger window of bistability, including for larger values of γ_m . It is interesting to note that the values of α_1 and α_2 also have a significant influence over the potential for oscillatory outcomes (which are present immediately above the black line in Figure 3.6(a), and in the enclosed region labelled "Osc" in Figure 3.6(b)). In par-

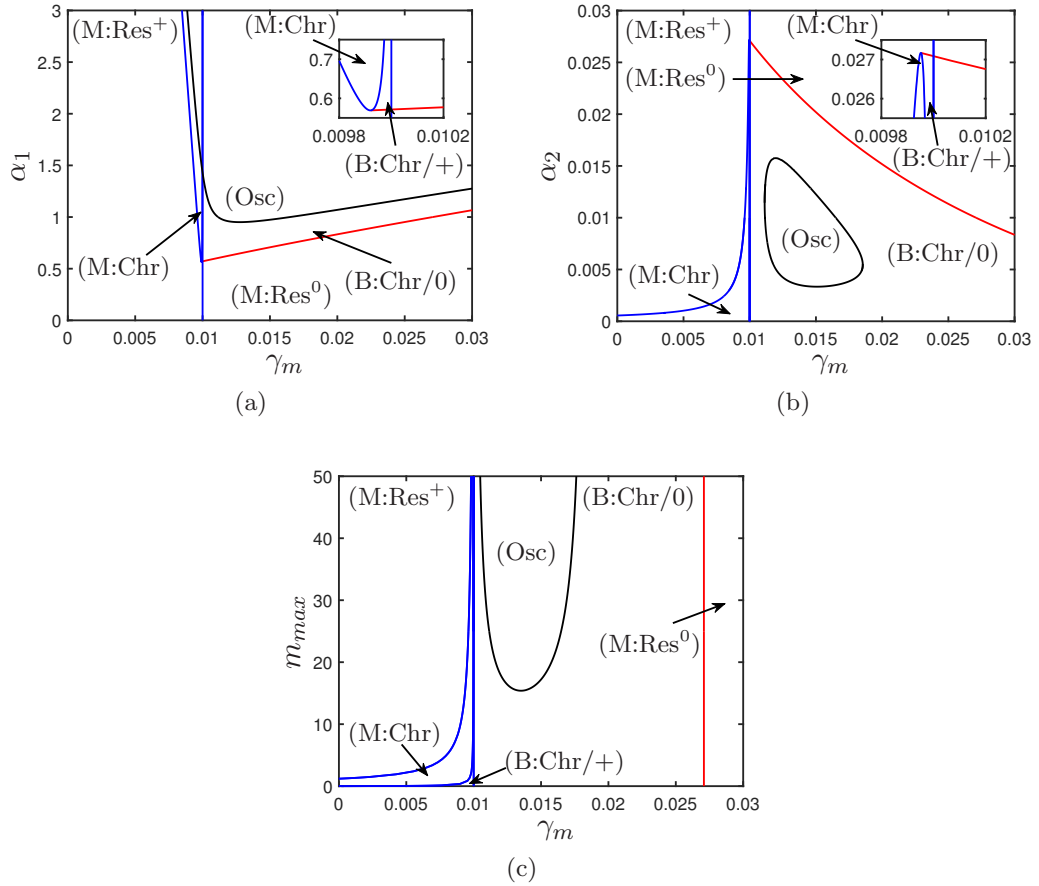


Figure 3.6: Two-parameter bifurcation diagrams illustrating steady state solutions of the model and their dependence upon the model’s parameters, for the parameter values of Table 3.2. Red lines represent saddle-node bifurcations, blue lines represent transcritical bifurcations, and black lines represent Hopf bifurcations. “B” indicates that the model is bistable with both healthy and chronic outcomes permissible, while “M” denotes monostability; the corresponding steady state solutions being those in which inflammation resolves and all variables reach zero (labelled “Res⁰” or “0”), those in which inflammation resolves but anti-inflammatory components are positive (labelled “Res⁺” or “+”; see (3.11)), or chronic states (labelled “Chr”). “Osc” denotes oscillatory (chronic) solutions.

ticular, we note that very small values of α_2 can eliminate oscillations entirely, which suggests that bidirectional phenotype switching specifically underpins the existence of these oscillations, which were not observed in the simple model in Chapter 2 or in the previous models of Dunster *et al.* (2014) that include only one macrophage phenotype. The potential for such oscillations to exist depends strongly upon the size of the macrophage population under consideration; as Figure 3.6(c) shows, the region of oscillatory behaviour grows as m_{max} is increased, and is eliminated entirely for m_{max} sufficiently small. These chronic solutions persist as γ_m is slowly increased, until we reach

the saddle-node bifurcation represented by the red lines in Figures 3.6(a–c); beyond this point, γ_m is sufficiently large that the only possible outcome is the zero state.

3.5 Discussion

In this chapter, we modified the construction of the simple baseline model presented in Chapter 2 by splitting the macrophage population into two distinct phenotypes, with primarily pro- and anti-inflammatory behaviours, the latter being reminiscent of tissue-resident macrophages. We note that this in itself is still an over-simplification of a realistic inflammatory environment *in vivo*, in which macrophage populations are numerous and still not universally categorised Gordon *et al.* (2014). One key result of this modelling approach is that the model now provides a healthy (resolved) configuration with positive macrophage numbers; *i.e.* a configuration in which pro-inflammatory macrophages and mediators are absent, but anti-inflammatory macrophages remain present to sustain the healthy configuration of the tissue. The existence of this resolved state is dependent upon the parameters that govern the size of the macrophage population; if $\gamma_m < c_T$, the zero-state is unstable, and the positive healthy state exists, with stability governed by (3.28). Therefore, the results of this model are more biologically acceptable than those presented in the simple baseline model in Chapter 2.

Figures 3.4, 3.5, and 3.6 illustrated the full range of dynamics of this model, revealing that the model also exhibits oscillatory solutions not observed in the simple model in Chapter 2 (which could be considered reminiscent of inflammatory conditions with relapsing-remitting characteristics). The existence of these oscillations is entirely reliant on the choice of the “two phenotype” modelling approach, and is also most evident when the total macrophage population (m_{max}) is large, so that there is scope for large disparity between the sizes of the pro- and anti-inflammatory macrophage populations. The rates of macrophage phenotype switching impact upon these dynamics in a largely intuitive manner: parameter choices that reduce the size of the pro-inflammatory macrophage populations (α_1 small, α_2 large, or κ_c small) can eliminate chronic outcomes entirely; choices that increase the scope for large populations of pro-inflammatory macrophages (α_1 small, α_2 large, or κ_c small) can expand regions of bistability or chronicity and avail more complex outcomes such as oscillations.

The inflammatory response’s severity depends on the size of m_p macrophage populations and α_1 . If either of these factors is large, it can lead to excessive inflammation and tissue damage. It’s also important to identify and address the underlying cause of the rise in the size of m_p macrophage populations since it’s essential to prevent the

development of chronic diseases. Therefore, maintaining a balance between α_1 and mechanisms that reduce the size of m_p macrophage populations is crucial for promoting a healthy outcome and resolving inflammation.

We note that the inflammatory response is a complex biological process that involves numerous immune cells. As such, a limitation of the model presented here is that we incorporate only macrophages, and omit other immune cells that play key roles in determining inflammatory outcomes. In the following chapter, we expand upon the model presented here to also include neutrophils, which are typically the first immune cells to arrive at the inflammation site, and also play significant roles in releasing relevant inflammatory mediators. In Chapter 4, we examine the extent to which the results of the model presented here are sensitive to the inclusion of an additional neutrophil population.

Incorporating The Role of Neutrophils

Neutrophils are the most abundant inflammatory cells in the body's immune system. They enhance the inflammatory response by releasing chemicals that attract more macrophages to the inflamed site. Thus, neutrophils and macrophages play a pivotal role as the primary immune cells in the inflammatory response, including removing dead cells and debris and engulfing foreign particles through phagocytosis. Neutrophil cells can undergo programmed cell death, also known as apoptosis, which is a natural process to regulate the inflammatory response. However, under certain circumstances, neutrophils can undergo necrosis, releasing their toxic contents. This can exacerbate the intensity of the inflammatory response, causing further damage to the surrounding host tissue, particularly if macrophages are unable to efficiently clear the necrotic cells.

In this chapter, we expand upon the biological scope of the inflammation model in Chapter 3 by introducing two additional groups of neutrophils: active neutrophils and apoptotic neutrophils. We aim to gain a better understanding of the roles played by macrophage phenotypes in the removal of apoptotic neutrophils, with the aim of preventing the onset of a persistent chronic inflammatory response that can be triggered by the leakage of the toxic content of necrotic cells into surrounding healthy cells. To achieve this, we use numerical simulations and bifurcation analysis to investigate how variation in the system's key parameters influences its outcomes, contributing to developing potential therapeutic targets for chronic inflammation.

4.1 Model derivation

In this model, we build upon the previous inflammation model presented in Chapter 3 by incorporating active and apoptotic neutrophils with both anti- and pro-inflammatory actions. Thus, this model focuses on the interactions between two subtypes of macrophage phenotypes, two groups of neutrophil cells and groups of generic pro- and anti-inflammatory mediators evolving over time (t^*) (with stars denoting dimensional variables), namely: pro-inflammatory macrophages $m_p^*(t^*)$, anti-inflammatory macrophages $m_a^*(t^*)$, active neutrophils $n^*(t^*)$, apoptotic neutrophils $a^*(t^*)$, generic pro-inflammatory mediators $c^*(t^*)$ and generic anti-inflammatory mediators $g^*(t^*)$. These interactions occur at the cellular level, focusing on the inflammation affecting the body over time by identifying the conditions that promote tissue damage in the absence of pathogens and highlighting its biological significance.

Neutrophils are the most abundant leukocytes in the body's immune system, and play a crucial role in the early stages of the inflammatory response, usually being the first-responding immune cells to the site of inflammatory damage due to their rapid movement and small size (Butterfield *et al.*, 2006; Kolaczkowska & Kubes, 2013; Rosales, 2018). Active neutrophils (n^*) are recruited to the site of inflammatory damage in response to high levels of pro-inflammatory mediators; we denote the corresponding rate of recruitment by χ_n^* . During the initial phase of inflammation, active neutrophils combat initial damage and foreign particles by phagocytosis, cytokine release, and secretion of toxic content. As neutrophils age, they eventually die through apoptosis; we denote the corresponding rate of apoptosis by ν^* . Apoptotic neutrophils ultimately undergo secondary necrosis naturally (at rate γ_a^*), releasing their toxic contents and providing a further source of pro-inflammatory mediators (*i.e.* worsening the inflammatory damage). We parameterise this additional source term by rate parameter κ_a^* , but note that this source is known to saturate as the number of apoptotic neutrophils increases, and hence (following (Dunster *et al.*, 2014)) we also introduce a corresponding saturation constant β_a^* below. In order to mitigate against potential damage from apoptotic neutrophils, macrophages phagocytose apoptotic neutrophils before they can undergo necrosis. While phagocytosis of apoptotic cells is a key macrophage function in general, we expect phagocytosis to be predominantly driven by tissue-resident macrophages (Schulz *et al.*, 2019; Jenkins & Allen, 2021), which we associate with our anti-inflammatory macrophage population here. We introduce the rate parameter ϕ^* to parameterise phagocytosis of apoptotic neutrophils by anti-inflammatory macrophages, and also denote the relative phagocytic ability of pro-inflammatory macrophages by dimensionless parameter $\phi_2 \ll 1$.

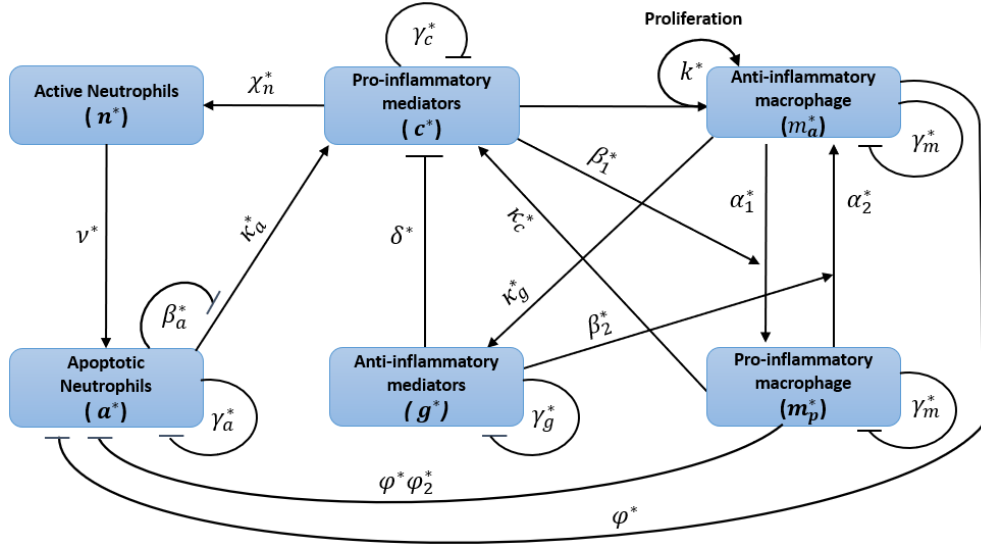


Figure 4.1: Schematic diagram representing (4.1) and illustrating the interactions incorporated in this model, healthy neutrophils (n^*) and apoptotic neutrophils (a^*), with associated parameters. Arrows indicate positive feedbacks or supply terms; lines terminated with bars indicate negative feedbacks or loss terms.

The interactions featuring in this model are shown in Figure 4.1 and provide the following ODE system:

$$\frac{dn^*}{dt^*} = \chi_n^* c^* - \nu^* n^*, \quad (4.1a)$$

$$\frac{da^*}{dt^*} = \nu^* n^* - \phi^* (m_a^* + \phi_2 m_p^*) a^* - \gamma_a^* a^*, \quad (4.1b)$$

$$\frac{dg^*}{dt^*} = \kappa_g^* m_a^* - \gamma_g^* g^*, \quad (4.1c)$$

$$\frac{dc^*}{dt^*} = \kappa_c^* m_p^* + \kappa_a^* \gamma_a^* \left(\frac{a^{*2}}{\beta_a^{*2} + a^{*2}} \right) - \delta^* c^* g^* - \gamma_c^* c^*, \quad (4.1d)$$

$$\frac{dm_p^*}{dt^*} = \alpha_1^* \beta_1^* c^* m_a^* - \alpha_2^* \beta_2^* g^* m_p^* - \gamma_m^* m_p^*, \quad (4.1e)$$

$$\frac{dm_a^*}{dt^*} = k^* (c^* + c_T^*) (m_a^* + m_p^*) \left(1 - \frac{m_a^* + m_p^*}{m_{max}^*} \right) - \alpha_1^* \beta_1^* c^* m_a^* + \alpha_2^* \beta_2^* g^* m_p^* - \gamma_m^* m_a^*. \quad (4.1f)$$

We note that the above model incorporates a deliberately simple description of the neutrophil population and its roles, providing a minimal sub-model with single positive and negative feedback loops. In the single positive feedback loop, pro-inflammatory mediators initially recruit active neutrophils to the damaged site, which later become

apoptotic neutrophils at rate v^* and undergo necrosis, leading to the production of more pro-inflammatory mediators via κ_a^* , which further attract more active neutrophils to the damaged tissues. The negative feedback loop describes macrophages' ability to remove apoptotic neutrophils before they release toxic contents into healthy cells. The previous works of Dunster *et al.* (2014) and Bayani *et al.* (2020a) additionally included a source of pro-inflammatory mediators from active neutrophils; however, this feedback is much weaker than that of apoptotic neutrophils and is hence omitted here for ease. Furthermore, these works also considered a more complex recruitment term for neutrophils that is explicitly down-regulated by anti-inflammatory mediators. We neglect this here in order to facilitate direct comparison with the previous model introduced in Chapter 3.

4.1.1 Parameters and non-dimensionalisation

In Section 3.1.1, we reviewed the common dimensional parameters that appeared in (3.1). Here, we briefly introduce the available estimates for the new dimensional parameters incorporated in this model, which are listed in Table 4.1, along with their respective value ranges. Furthermore, we comment upon how these estimates inform the corresponding choices for our baseline set of dimensionless parameters.

Again, we nondimensionalise (4.1) by applying the scalings of (3.2) and also scale neutrophil populations according to

$$n^* = \frac{\chi_n^*}{k^*} n, \quad a^* = \frac{\chi_n^*}{k^*} a, \quad (4.2)$$

to obtain the following dimensionless equations:

$$\frac{dn}{dt} = c - v n, \quad (4.3a)$$

$$\frac{da}{dt} = v n - \phi (m_a + \phi_2 m_p) a - \gamma_a a, \quad (4.3b)$$

$$\frac{dg}{dt} = m_a - \gamma_g g, \quad (4.3c)$$

$$\frac{dc}{dt} = \kappa_c m_p + \kappa_a \gamma_a \left(\frac{a^2}{\beta_a^2 + a^2} \right) - c g - c, \quad (4.3d)$$

$$\frac{dm_p}{dt} = \alpha_1 c m_a - \alpha_2 g m_p - \gamma_m m_p, \quad (4.3e)$$

$$\frac{dm_a}{dt} = (c + c_T) (m_a + m_p) \left(1 - \frac{m_a + m_p}{m_{max}} \right) - \alpha_1 c m_a + \alpha_2 g m_p - \gamma_m m_a, \quad (4.3f)$$

Parameter	Meaning	Range of values and units	References
χ_n^*	Maximal rate of neutrophil influx	$10^6 - 10^7$ cell pg^{-1} day $^{-1}$	Kim <i>et al.</i> (2008)
ν^*	Rate of neutrophil apoptosis	$0.1 - 72$ day $^{-1}$	Summers <i>et al.</i> (2010) Minucci <i>et al.</i> (2020)
γ_a^*	Rate of necrosis of apoptotic neutrophils	$9.6 - 48$ day $^{-1}$	Marée <i>et al.</i> (2005)
ϕ^*	Rate of phagocytosis of apoptotic neutrophils by m_a macrophages	$10^{-3} - 10^{-1}$ cell $^{-1}$ mm^3 day $^{-1}$	Dunster <i>et al.</i> (2014) Bayani <i>et al.</i> (2020a) Nelson <i>et al.</i> (2023)
κ_a^*	Production of c on necrosis of apoptotic neutrophils	pg mm^{-3}	
β_a^*	Saturation constant	cell mm^{-3}	

Table 4.1: Summary of the new dimensional parameter values incorporated in (4.1).

in which we have introduced the following additional (to (2.4) and (3.4) dimensionless parameters:

$$\nu = \frac{\nu^*}{\gamma_c^*}, \quad \phi = \frac{\phi^* \gamma_c^*}{\delta^* \kappa_g^*}, \quad \gamma_a = \frac{\gamma_a^*}{\gamma_c^*}, \quad \kappa_a = \frac{k^* \kappa_a^*}{\gamma_c^*}, \quad \beta_a = \frac{\beta_a^* k^*}{\chi_n^*}. \quad (4.4)$$

We solve (4.3) subject to the initial conditions $m_p(0) = m_{p0} > 0$, $c(0) = c_0 > 0$, and $m_a(0) = g(0) = n(0) = a(0) = 0$.

The newly introduced dimensionless parameters appearing in (4.3) are summarised in Table 4.2 (see also Table 3.2), alongside baseline values used in our simulations. In a previous model of type 1 diabetes, Marée *et al.* (2005) estimate the rate at which macrophages phagocytose apoptotic cells to be in the range 10^{-7} – 10^{-5} mL cell $^{-1}$ h $^{-1}$. We note that this measure does not explicitly incorporate macrophage phenotype information. Inferring the dimensionless parameter ϕ from such a measure is difficult due to uncertainty in other relevant dimensional parameters that appear in (4.4); however, previous works have generally considered ϕ to lie approximately in the range 10^{-3} – 10^{-1} (Dunster *et al.*, 2014; Bayani *et al.*, 2020a; Dunster *et al.*, 2023; Nelson *et al.*, 2023). Since the role of phagocytosing apoptotic neutrophils primarily falls to tissue-resident macrophages (Schulz *et al.*, 2019; Jaggi *et al.*, 2020; Jenkins & Allen, 2021), which we associate with the anti-inflammatory macrophage phenotype in our model, we assume $\phi_2 \ll 1$. Here, we take $\phi = 0.1$ as our baseline choice for phagocytosis of apoptotic neutrophils by macrophages of the m_a phenotype.

Since neutrophils are known to have a shorter lifespan than macrophages (Akgul *et al.*,

Parameter	Expression	Meaning	Baseline value
ϕ	$\phi^* \gamma_c^* / \delta^* \kappa_g^*$	Rate of phagocytosis of apoptotic neutrophils by m_a macrophages	0.1
ϕ_2	—	Relative rate of phagocytosis of apoptotic neutrophils by m_p compared to that of m_a	0.01
ν	ν^* / γ_c^*	Rate of neutrophil apoptosis	0.1
κ_a	$k^* \kappa_a^* \gamma_a^* / \gamma_c^{*2}$	Production of c on necrosis of apoptotic neutrophils	2
γ_a	γ_a^* / γ_c^*	Rate of necrosis of apoptotic neutrophils	1
β_a	$\beta_a^* k^* / \chi_n^*$	Saturation constant	0.5

Table 4.2: Summary of the newly introduced dimensionless parameters appearing in (4.3), with baseline values used in simulations.

2001; Parihar *et al.*, 2010), it is intuitive that $\nu > \gamma_m$ in general. We therefore choose $\nu = 0.1$ in Table 4.2, but also investigate the role of ν more widely in Section 4.4 below. Once neutrophils become apoptotic, they are rapidly lost via secondary necrosis, on a similar timescale to the rate of decay of inflammatory mediators (Haslett, 1999; Dunster *et al.*, 2014). We therefore set $\gamma_a = \gamma_a^* / \gamma_c^* = 1$ in Table 4.2.

The remaining mediator production rate parameter, κ_a , is not readily available from existing literature, due partly to a reasonably complex dependence on numerous dimensional model parameters (as given in (4.4)) for which values are uncertain. It is known, however, that the concentration of pro-inflammatory mediators released on necrosis of apoptotic neutrophils is large in comparison to that from active cells (Lawrence & Gilroy, 2007). In light of this, we choose $\kappa_a > \kappa_c$, and set $\kappa_a = 2$ in Table 4.2.

4.2 Identification and classification of steady state solutions

Here, we aim to identify the steady state solutions of (4.3) and classify them by their stability. Since we model neutrophils as entirely pro-inflammatory in nature, healthy steady states must have $n = a = 0$, with $c = m_p = 0$ as described in Chapter 3. It is simple to show that (4.3) has a zero steady state corresponding to a healthy outcome where all variables converge to zero, which we denote as FP_1 . We compute the Jacobian

matrix for (4.3), denoted as \mathbf{J} , which is defined as follows:

$$\mathbf{J} = \begin{pmatrix} -\nu & 0 & 0 & 1 & 0 & 0 \\ \nu & T_{22} & 0 & 0 & -a\phi\phi_2 & -a\phi \\ 0 & 0 & -\gamma_g & 0 & 0 & 1 \\ 0 & T_{42} & -c & -g-1 & \kappa_c & 0 \\ 0 & 0 & -\alpha_2 m_p & \alpha_1 m_a & -\gamma_m - \alpha_2 g & \alpha_1 c \\ 0 & 0 & \alpha_2 m_p & T_{64} & T_{65} & T_{66} \end{pmatrix}, \quad (4.5)$$

where,

$$T_{22} = -\phi(m_a + \phi_2 m_p) - \gamma_a, \quad (4.6)$$

$$T_{42} = \frac{2a\kappa_a}{a^2 + \beta_a^2} - \frac{2a^3\kappa_a}{(a^2 + \beta_a^2)^2}, \quad (4.7)$$

$$T_{64} = -\alpha_1 m_a - (m_a + m_p) \left(\frac{m_a + m_p}{m_{max}} - 1 \right), \quad (4.8)$$

$$T_{65} = \alpha_2 g - (c + c_T) \left(\frac{m_a + m_p}{m_{max}} - 1 \right) - \frac{(c + c_T)(m_a + m_p)}{m_{max}}, \quad (4.9)$$

$$T_{66} = -\gamma_m - \alpha_1 c - (c + c_T) \left(\frac{m_a + m_p}{m_{max}} - 1 \right) - \frac{(c + c_T)(m_a + m_p)}{m_{max}}. \quad (4.10)$$

To examine the stability of the zero steady state, we evaluate the Jacobian matrix \mathbf{J} , at $\text{FP}_1 = (n, a, g, c, m_p, m_a) = (0, 0, 0, 0, 0, 0)$, which gives

$$\mathbf{J}|_{\text{FP}_1} = \begin{pmatrix} -\nu & 0 & 0 & 1 & 0 & 0 \\ \nu & -\gamma_a & 0 & 0 & 0 & 0 \\ 0 & 0 & -\gamma_g & 0 & 0 & 1 \\ 0 & 0 & 0 & -1 & \kappa_c & 0 \\ 0 & 0 & 0 & 0 & -\gamma_m & 0 \\ 0 & 0 & 0 & 0 & c_T & c_T - \gamma_m \end{pmatrix}. \quad (4.11)$$

Computing the eigenvalues (λ) of the Jacobian matrix at FP_1 , as given in (4.11), provides:

$$\lambda_1 = -1, \quad \lambda_2 = -\gamma_a, \quad \lambda_3 = -\gamma_g, \quad \lambda_4 = -\gamma_m, \quad \lambda_5 = -\nu, \quad \lambda_6 = c_T - \gamma_m. \quad (4.12)$$

As evident from (4.12), we observe that the healthy steady state in which all variables converge to zero is stable when $\gamma_m > c_T$, while it becomes unstable otherwise. This is consistent with the corresponding calculation of Chapter 3; see (3.10).

Numerical simulations of (4.3) reveal an additional non-zero steady state corresponding to a healthy response, assuming the pro-inflammatory components are zero ($n = a = c = m_p = 0$), while the anti-inflammatory components remain positive ($g > 0$ and $m_a > 0$), allowing inflammation to remain suppressed. That is, we have second healthy steady state, denoted as FP_2 , in which

$$n = a = m_p = c = 0, \quad m_a = m_{max} \left(1 - \frac{\gamma_m}{c_T}\right), \quad g = \frac{m_{max}}{\gamma_g} \left(1 - \frac{\gamma_m}{c_T}\right), \quad (4.13)$$

which exists provided that $\gamma_m < c_T$. To examine the stability of the second healthy steady state, we compute the Jacobian (4.5) at FP_2 , where FP_2 is given by (4.13), which gives

$$J|_{FP_2} = \begin{pmatrix} -\nu & 0 & 0 & 1 & 0 & 0 \\ \nu & j_{22} & 0 & 0 & 0 & 0 \\ 0 & 0 & -\gamma_g & 0 & 0 & 1 \\ 0 & 0 & 0 & j_{44} & \kappa_c & 0 \\ 0 & 0 & 0 & j_{54} & j_{55} & 0 \\ 0 & 0 & 0 & j_{64} & j_{65} & \gamma_m - c_T \end{pmatrix}, \quad (4.14)$$

where,

$$j_{22} = \phi m_{max} \left(\frac{\gamma_m}{c_T} - 1\right) - \gamma_a, \quad (4.15)$$

$$j_{44} = \frac{m_{max}}{\gamma_g} \left(\frac{\gamma_m}{c_T} - 1\right) - 1, \quad (4.16)$$

$$j_{54} = -\alpha_1 m_{max} \left(\frac{\gamma_m}{c_T} - 1\right), \quad (4.17)$$

$$j_{64} = m_{max} \left(\frac{\gamma_m}{c_T} - 1\right) \left(\alpha_1 - \frac{\gamma_m}{c_T}\right), \quad (4.18)$$

$$j_{55} = \frac{\alpha_2 m_{max}}{\gamma_g} \left(\frac{\gamma_m}{c_T} - 1\right) - \gamma_m, \quad (4.19)$$

$$j_{65} = 2\gamma_m - c_T - \frac{\alpha_2 m_{max}}{\gamma_g} \left(\frac{\gamma_m}{c_T} - 1\right). \quad (4.20)$$

Evaluating the eigenvalues of the Jacobian matrix (4.14), we obtain the eigenvalues λ as follows:

$$\begin{aligned} \lambda_1 &= -\gamma_g, \quad \lambda_2 = -\nu, \quad \lambda_3 = \gamma_m - c_T, \quad \lambda_4 = \phi m_{max} \left(\frac{\gamma_m}{c_T} - 1\right) - \gamma_a, \\ \lambda_5 &= \frac{(j_{44} + j_{55}) + \sqrt{(j_{44} - j_{55})^2 + 4\kappa_c j_{54}}}{2}, \quad \lambda_6 = \frac{(j_{44} + j_{55}) - \sqrt{(j_{44} - j_{55})^2 + 4\kappa_c j_{54}}}{2}. \end{aligned} \quad (4.21)$$

We observe that when $n = a = 0$, the healthy steady states of this model are otherwise identical to the model in Chapter 3; that is, there is one healthy steady state with all variables equal to zero, which is stable provided $\gamma_m > c_T$, and a second healthy steady state as given in (4.13), which exists and is stable for parameter choices that satisfy the following condition:

$$\frac{\alpha_2 m_{max}^2}{\gamma_g^2} \left(\frac{\gamma_m}{c_T} - 1 \right)^2 + m_{max} \left[\alpha_1 \kappa_c - \frac{\gamma_m + \alpha_2}{\gamma_g} \right] \left(\frac{\gamma_m}{c_T} - 1 \right) + \gamma_m > 0. \quad (4.22)$$

We note that, in addition to the healthy steady states of this model, and for positive values of κ_a and β_a , there also exist two steady states in which the macrophage populations reach zero and chronic inflammation is sustained by neutrophils alone, given by

$$m_a = m_p = g = 0, \quad a = \hat{a}, \quad c = \gamma_a \hat{a}, \quad n = \frac{\gamma_a \hat{a}}{\nu}, \quad (4.23)$$

where,

$$\hat{a}^2 - \kappa_a \hat{a} + \beta_a^2 = 0. \quad (4.24)$$

Solving (4.24) via the quadratic formula provides

$$\hat{a} = \frac{\kappa_a \pm \sqrt{\kappa_a^2 - 4\beta_a^2}}{2}. \quad (4.25)$$

Real solutions to (4.25) exist when $\kappa_a^2 > 4\beta_a^2$; *i.e.* when neutrophil feedbacks are strong in comparison to those of macrophages, in which case the model is much less sensitive to macrophage dynamics. For parameter values of interest here, numerical stability analysis reveals that the two roots of (4.25) are always saddle points and are hence unlikely to be attained biologically. We therefore largely omit these steady states from our discussions below (although noting their existence can be helpful in explaining where more physiologically relevant branches of our bifurcation diagrams terminate in the bifurcation analysis that follows). Furthermore, numerical simulations reveal that this model has scope to support multiple stable chronic steady states, for some parameters.

4.3 Numerical Simulations

Our primary focus throughout the analysis is to determine whether the model converges to steady states, which represent the resolution of inflammatory damage, as shown in Figure 4.2 or chronic inflammation, as illustrated in Figure 4.3.

In this model, we observe that the healthy steady states are identical to those discussed in Chapter 3. The model attains a zero steady state, corresponding to the resolution

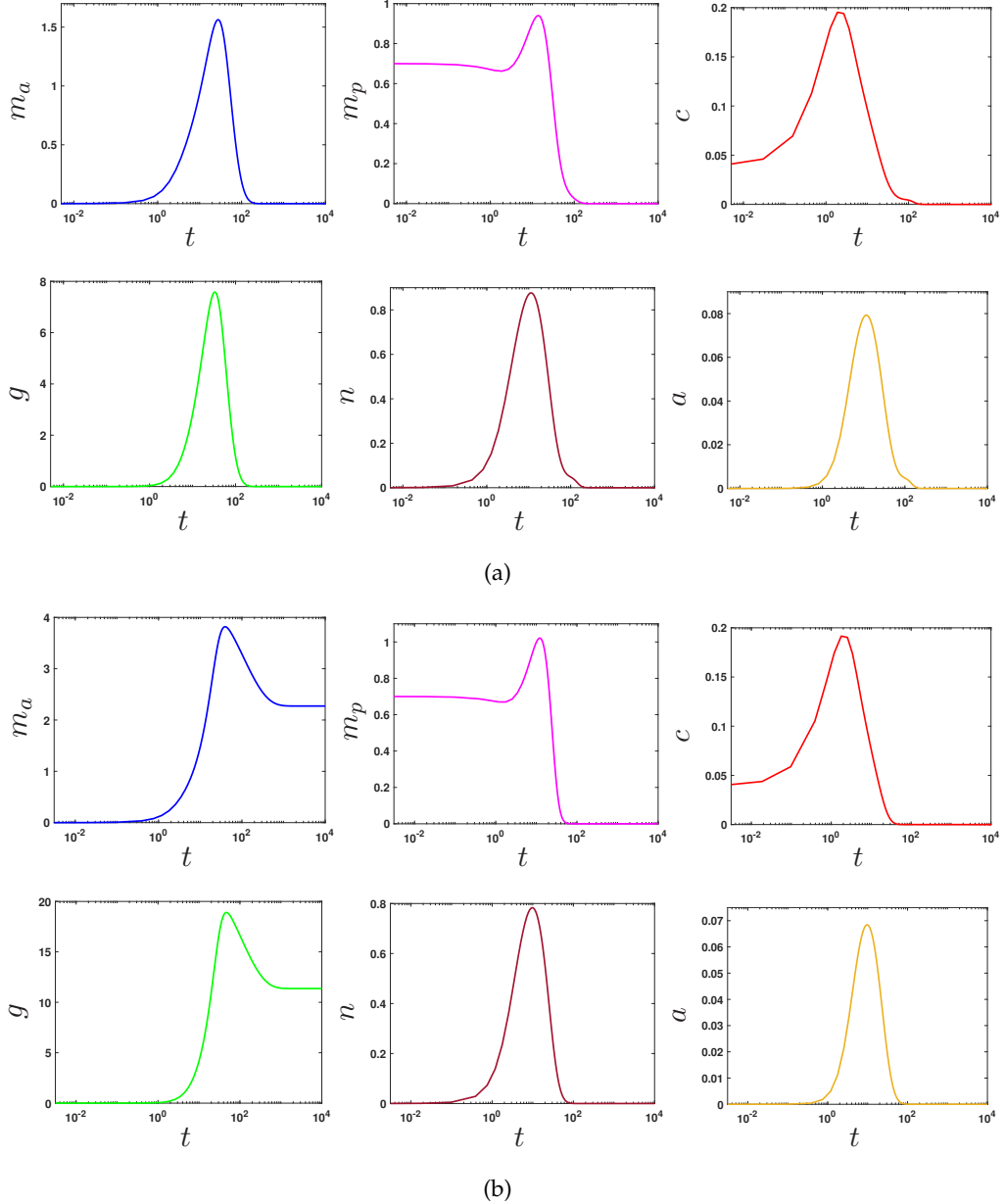


Figure 4.2: Numerical simulations of (4.3) illustrate that the model exhibits two distinct steady state solutions, both of which correspond to healthy outcomes. In (a), we initialise the model with $m_p(0) = 0.7$, $c(0) = 0.04$ and $m_a(0) = g(0) = n(0) = a(0) = 0$ to demonstrate a healthy response for the parameters of Table 4.2, where all variables converge to zero. In (b), we maintain the same initial conditions as in (a) and set the parameter c_T to 0.055, while keeping the other parameters as listed in Table 4.2, which allows the model to attain a second healthy steady state as given in (4.13).

of inflammation, in which all immune cells and chemical mediators' levels reach zero over time, as shown in Figure 4.2(a). Additionally, the model achieves a second healthy steady state where the pro-inflammatory components become zero ($m_p = c = n = a = 0$), while the anti-inflammatory components reach positive levels ($m_a > 0$ and $g > 0$),

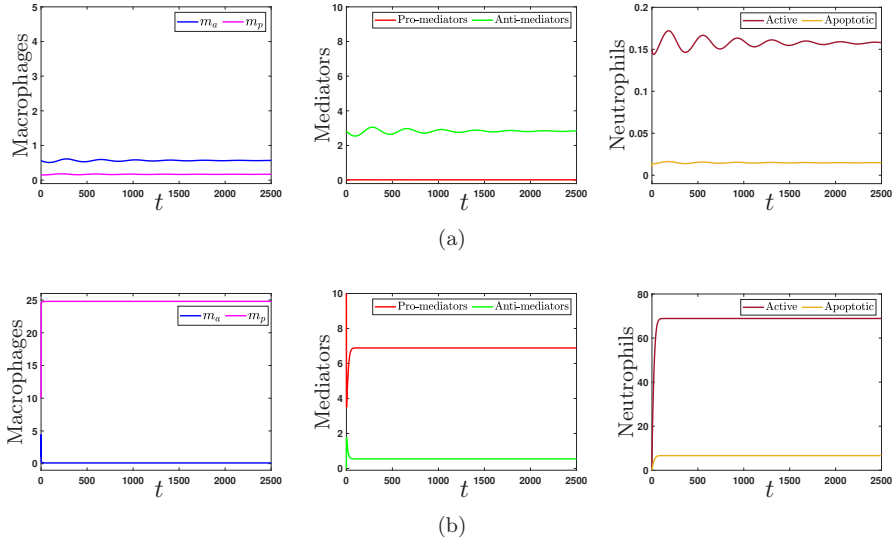


Figure 4.3: Convergence to two distinct chronic steady states for $\gamma_m = 0.025$ and all other parameters as in Table 4.2, for two differing choices of initial conditions. In (a), the model achieves a chronic configuration with low neutrophil numbers and comparatively high numbers of anti-inflammatory macrophages/mediators. In (b), very large numbers of pro-inflammatory macrophages result in more pro-inflammatory mediators, more neutrophils and less phagocytosis of apoptotic neutrophils, resulting in a more severe chronic outcome.

as depicted in Figure 4.2(b).

In general, we observe two possible chronic outcomes (as shown for $\gamma_m = 0.025$ in Figure 4.3), where all immune cells and mediators' levels settle to positive values, allowing inflammation to persist and cause further tissue damage. Firstly, the model may attain a configuration in which m_p is low and m_a is sufficiently large that phagocytosis of apoptotic neutrophils by anti-inflammatory macrophages can mitigate against the pro-inflammatory feedback from neutrophils reasonably successfully, resulting in sustained low-level inflammation (as shown in Figure 4.3(a)). These solutions are reminiscent of the chronic solutions of Chapter 3. Alternatively, the model may attain a configuration in which m_p is very large in comparison to m_a , which results in not only more pro-inflammatory mediator production, but also greatly reduced phagocytosis of apoptotic neutrophils. The model can therefore attain a steady state with much greater levels of pro-inflammatory mediators and both active and apoptotic neutrophils (as shown in Figure 4.3(b)). These solutions represent new, highly inflamed configurations sustained by the presence of neutrophils.

4.4 Bifurcation analysis

In Figure 4.4, we illustrate a bifurcation diagram for (4.3), for the parameter values of Table 4.2. We observe that low-level chronic outcomes such as that of Figure 4.3(a) exhibit a bifurcation structure that heavily resembles the chronic solutions of the model covered in Chapter 3 (see Figure 3.3); that is, for varying γ_m , these chronic solutions are bounded above by a saddle-node bifurcation and bounded below by the lowest root of (4.22), which provides a transcritical bifurcation whose location is independent of all neutrophil-related parameters. In addition to these chronic solutions, we have a branch of additional severely inflamed configurations, such as that of Figure 4.3(b), in which neutrophil numbers are extremely high. This branch, shown in magenta in Figure 4.4, is once again bounded above by a saddle-node bifurcation in γ_m , and provides stable configurations for all γ_m values below this saddle-node coordinate. In order to distinguish these chronic configurations below, we introduce the nomenclature “Chrⁿ” to denote the severely inflamed chronic configuration sustained by neutrophils, and continue to use “Chr” to label chronic configurations analogous to those of the previous model presented in Chapter 3. The coexistence of these chronic states (together with the healthy Res⁰ and Res⁺ configurations described above) provide a more complex array of classifications of parameter space than was observed in the model introduced in Chapter 3, including regions of multistability (with more than two stable objects present), bistable regions involving the Chrⁿ solution, and regions in which low-level oscillations and high-level chronic inflammation co-exist, as illustrated in Figure 4.4. (We note that three transcritical bifurcations exist at or close to $\gamma_m = c_T$, where the Res⁰ and Res⁺ configurations change stability. While we have omitted labellings of these narrow intermediate regions of Figure 4.4 for clarity, these can be inferred directly from Figure 3.3, with the Chrⁿ state superimposed).

In Figure 4.5, we track the coordinate of the saddle node bifurcation that lies on the Chrⁿ branch (shown in magenta in Figure 4.4) as a function of α_1 and α_2 . This allows us to divide parameter space into two regions: one in which highly-inflamed Chrⁿ solutions exist (shown in red), and one in which the model qualitatively recovers the model of Chapter 3 (shown in green). We note that for sufficiently small α_1 or sufficiently large α_2 the Chrⁿ solution is eliminated entirely (as we move parameters into the green regions of Figures 4.5), and the remaining saddle-node curves (for solutions analogous to the model covered in Chapter 3) can collide with the transcritical bifurcations of (4.22), eliminating the potential for chronic outcomes entirely.

It is interesting mathematically to note that the macrophage and mediator dynamics of this model recover the previous model discussed in Chapter 3 in the limit $\chi_n^* \rightarrow 0$, in

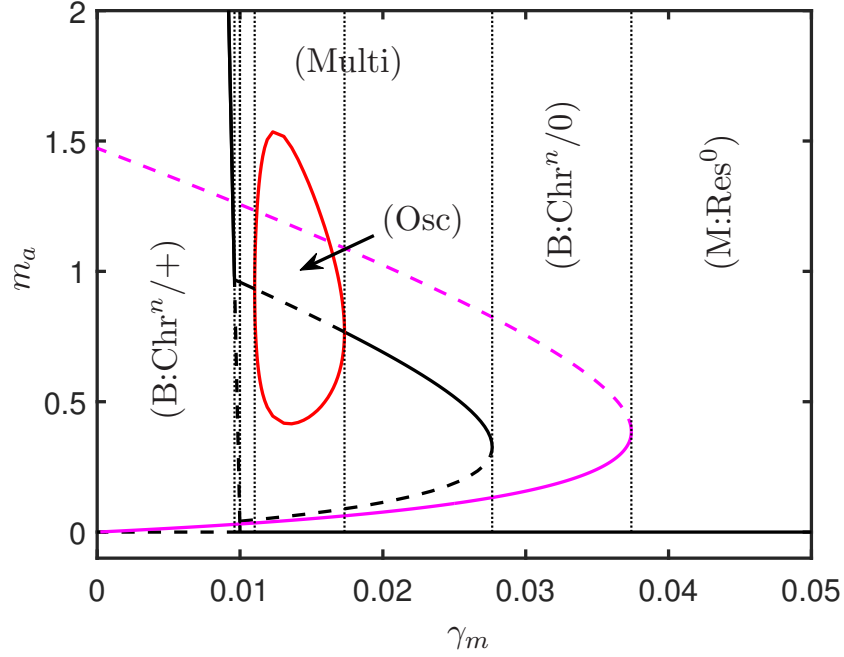


Figure 4.4: Bifurcation diagrams for (4.3), for the parameter values of Table 4.2. The magenta curve corresponds to the chronic steady state of Figure 4.3(b), in which the system attains a severely inflamed configuration with very high neutrophil numbers. (We label this chronic state “Chrⁿ” in order to distinguish it from the chronic states of that of the model presented in Chapter 3.) The remaining curves correspond qualitatively to the branches of Figure 3.3 for the model covered in Chapter 3.

which neutrophil recruitment is eliminated entirely. (We note that this is not a biologically relevant limit to consider, as a typical inflammatory environment involves significantly more rapid recruitment of neutrophils than macrophages in the short term (Butterfield *et al.*, 2006; Kolaczowska & Kubes, 2013; Rosales, 2018). Nonetheless, this observation provides a useful tool in our mathematical analysis). In dimensionless terms, the limit $\chi_n^* \rightarrow 0$ corresponds to taking $\beta_a \rightarrow \infty$ (due to (4.4)), which suppresses the pro-inflammatory feedback from apoptotic neutrophils in (4.3d).

Figure 4.6(a) illustrates how the locations of the bifurcations shown in Figure 4.4 depend upon β_a . In particular, we observe that in the limit $\beta_a \rightarrow \infty$, the two saddle-node bifurcations of Figure 4.4 approach one-another and converge upon the saddle-node coordinate of Figure 3.3 for the model covered in Chapter 3. In this limit, the macrophage and mediator dynamics decouple from the neutrophil equations in (4.3), and equations (4.3c–4.3f) attain identical steady states to the model in Chapter 3. Since the dimensionless parameter β_a does not explicitly govern neutrophil recruitment in (4.3) (instead parameterising the strength of the neutrophil feedback) low levels of pro-inflammatory mediators (c) do still trigger neutrophil recruitment, even in the limit $\beta_a \rightarrow \infty$, but these neutrophils do not effect the macrophage/mediator dynamics. For

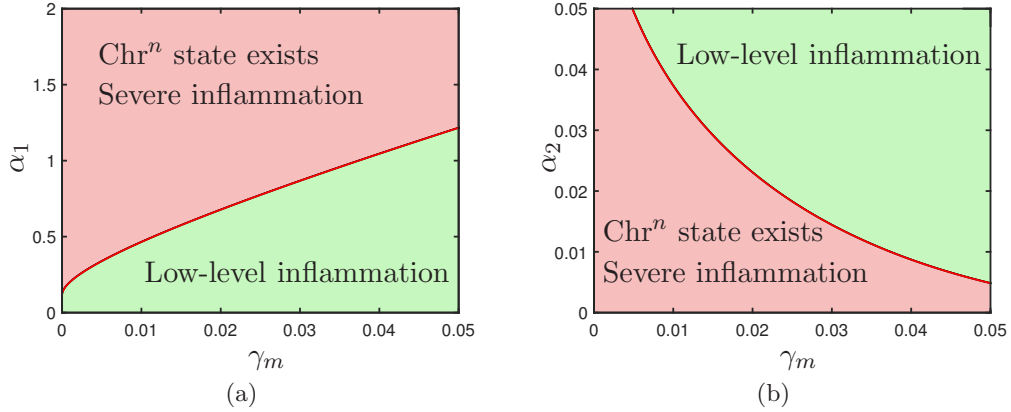


Figure 4.5: Bifurcation diagrams for (4.3), for the parameter values of Table 4.2. In (a,b), we track the coordinate of the saddle-node bifurcation on the Chr^n branch (shown in magenta in Figure 4.4) as a function of the macrophage phenotype switching parameters α_1 and α_2 , dividing parameter space into two regions: one in which highly-inflamed Chr^n exists (shown in red), and one in which the model qualitatively recovers the model of Chapter 3, which is associated with low-level inflammation (shown in green).

this reason, the region of monostability to the Res^+ state that model in Chapter 3 exhibits for γ_m small (see Figure 3.3) is replaced by a region of bistability involving both the Res^+ state and the Chr^n state in this model. Due to the persistent presence of neutrophils, the Chr^n state never interacts with the Res^+ state (for which $n = 0$), and hence is not destabilised for small γ_m .

In Figure 4.6(b), we show an enlargement of Figure 4.6(a) for β_a small — a biologically relevant limit to consider, since neutrophil pro-inflammatory feedbacks are generally considered to be much greater than those of macrophages (Tecchio *et al.*, 2014). The figure illustrates that the low-level solutions analogous to the model in Chapter 3 include chronic outcomes for values of γ_m lying between the transcritical bifurcation corresponding to the lowest root of (4.22) (blue curve) and a saddle node bifurcation (solid red curve), with this region also including oscillatory solutions bounded by two Hopf bifurcations. As β_a decreases, the saddle node moves to the right in the figure, resulting in low-level chronic outcomes for larger γ_m , and the upper Hopf bifurcation moves likewise, resulting in a growing window of oscillatory solutions, until the Hopf and saddle-node ultimately collide at a Bogdanov–Takens bifurcation. Additionally, the severely-inflamed Chr^n solution is stable to the left of its corresponding saddle-node bifurcation, shown as a dashed red curve in Figure 4.6(b).

In Figures 4.6(c) and 4.6(d), we illustrate how these curves evolve as we manipulate α_1 and α_2 . In these figures, we plot only the transcritical bifurcation corresponding to the smallest root of (4.22) (dashed lines) and the saddle node bifurcation (solid lines) that

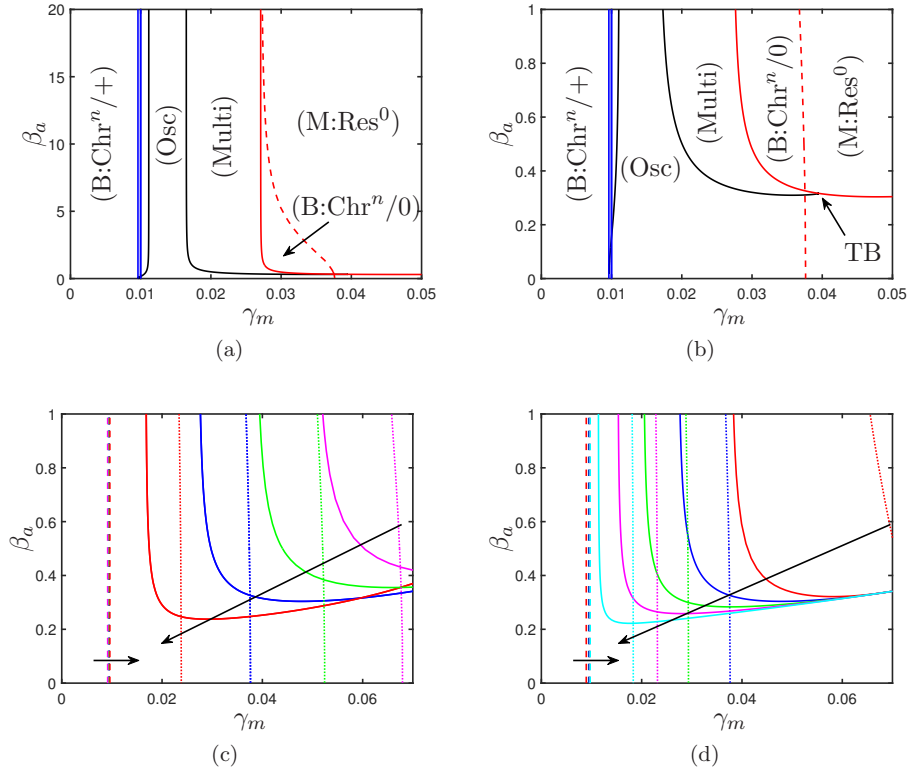


Figure 4.6: Two-parameter bifurcation diagrams illustrating solutions of (4.3) for the parameters given in Table 4.2. In (a), we track the positions of relevant bifurcations as a function of β_a . Red, black and blue curves represent saddle-node, Hopf and transcritical bifurcations respectively; the dashed red curve represents the saddle-node bifurcation on the Chr^n branch shown in magenta in Figure 4.4. In the limit $\beta_a \rightarrow \infty$, macrophage dynamics become independent of neutrophils and the Chr^n state collapses onto the chronic state of the model in Chapter 3. In (b) we show an enlarged version of Figure 4.6(b) for $\beta_a \leq 1$. The severely inflamed Chr^n solution is stable to the left of the dashed red curve; the remaining solutions correspond approximately to the model presented in Chapter 3. In (c,d) we illustrate how these curves shift as we vary the macrophage phenotype switching parameters α_1 and α_2 respectively. Here we plot only the saddle-node curve corresponding to the Chr^n state (dotted), the saddle-node curve that bounds the low-level chronic region above (solid lines) and the transcritical bifurcation that bounds this region below via (4.22) (dashed lines), omitting intermediate bifurcations for clarity. Reducing α_1 or increasing α_2 moves these curves in the direction of the arrows shown, reducing the scope for chronic solutions. In (c), illustrated curves are for $\alpha_1 = 0.75$ (red), $\alpha_1 = 1$ (blue), $\alpha_1 = 1.25$ (green) and $\alpha_1 = 1.5$ (magenta). In (d), illustrated curves are for $\alpha_2 = 0.005$ (red), $\alpha_2 = 0.01$ (blue), $\alpha_2 = 0.015$ (green), $\alpha_2 = 0.02$ (magenta) and $\alpha_2 = 0.025$ (cyan). “B” indicates that the model is bistable with both healthy and chronic outcomes permissible, while “M” denotes monostability; the corresponding steady state solutions being that in which inflammation resolves and all variables reach zero (labelled “Res⁰” or “0”), that in which inflammation resolves but anti-inflammatory components are positive (labelled “+”; see (4.13)), or chronic states (labelled “Chr” or “Chrⁿ”). “Osc” denotes oscillatory (chronic) solutions. “TB” indicates a Bogdanov–Takens bifurcation.

together bound regions of chronic outcomes analagous to model presented in Chapter 3 (including oscillations), along with the saddle-node corresponding to the Chr^n branch (dotted lines). We observe that either decreasing α_1 or increasing α_2 has the effect of shifting the transcritical bifurcation of (4.22) slightly to the right in the figures, while the saddle-node curves both move to the left; that is, the window of bistability is narrowed in both of these scenarios, with the potential for chronic outcomes being reduced as we manipulate phenotypic switching in a manner that favours greater numbers of anti-inflammatory macrophages at the expense of fewer pro-inflammatory macrophages.

Figure 4.7 more closely examines the relationship between the additional neutrophil-driven dynamics of this model and the rates of macrophage phenotype switching, α_1 and α_2 . In Figure 4.7, we take $\gamma_m = 0.025$ and $\beta_a = 0.5$ as our baseline values, as this combination of parameters has been identified to facilitate chronic outcomes in Figure 4.4, and seek to elucidate the local sensitivity to neutrophil-related parameters in tandem with macrophage phenotype switching. Since we have observed above that the influence of the two macrophage phenotype switching parameters (α_1 and α_2) are essentially the converse of one another, we focus here upon α_1 in isolation and infer similar (converse) conclusions upon α_2 . For varying α_1 , we examine how the locations of bifurcation points vary as we manipulate β_a (which captures the strength of neutrophil feedbacks relative to those of macrophages), ϕ (the rate at which anti-inflammatory macrophages remove apoptotic neutrophils), and ν (the rate of neutrophil apoptosis). We note that ϕ and ν have been identified as key parameters that effect the switch from healthy to chronic outcomes in previous works (Dunster *et al.*, 2014; Bayani *et al.*, 2020a).

In Figure 4.7(a), we show a bifurcation diagram illustrating the role of α_1 . Here, since $\gamma_m > c_T$, the healthy steady state at zero (Res^0) is stable and the Res^+ state of (4.13) doesn't exist. Additionally, for sufficiently large values of α_1 , chronic steady states corresponding to low-level inflammation (*cf.* model in Chapter 3) and severe inflammation (akin to Figure 4.3(b)) exist, both of which are bounded below by a saddle-node bifurcation. While the severely-inflamed Chr^n solution is stable for all α_1 values beyond the relevant saddle node, the branch of low-level inflammatory steady states can be destabilised via a Hopf bifurcation, giving rise to oscillatory solutions that grow in amplitude until they collide with a nearby saddle and are eliminated via a homoclinic bifurcation (HC). Figure 4.7(b) illustrates how these chronic solutions depend upon β_a . In particular, we note that a reduction in β_a results in the Hopf bifurcation (and corresponding homoclinic bifurcation; not plotted) converging toward the neighbouring saddle node on the low-inflammation branch until these points collide at a Bogdanov–

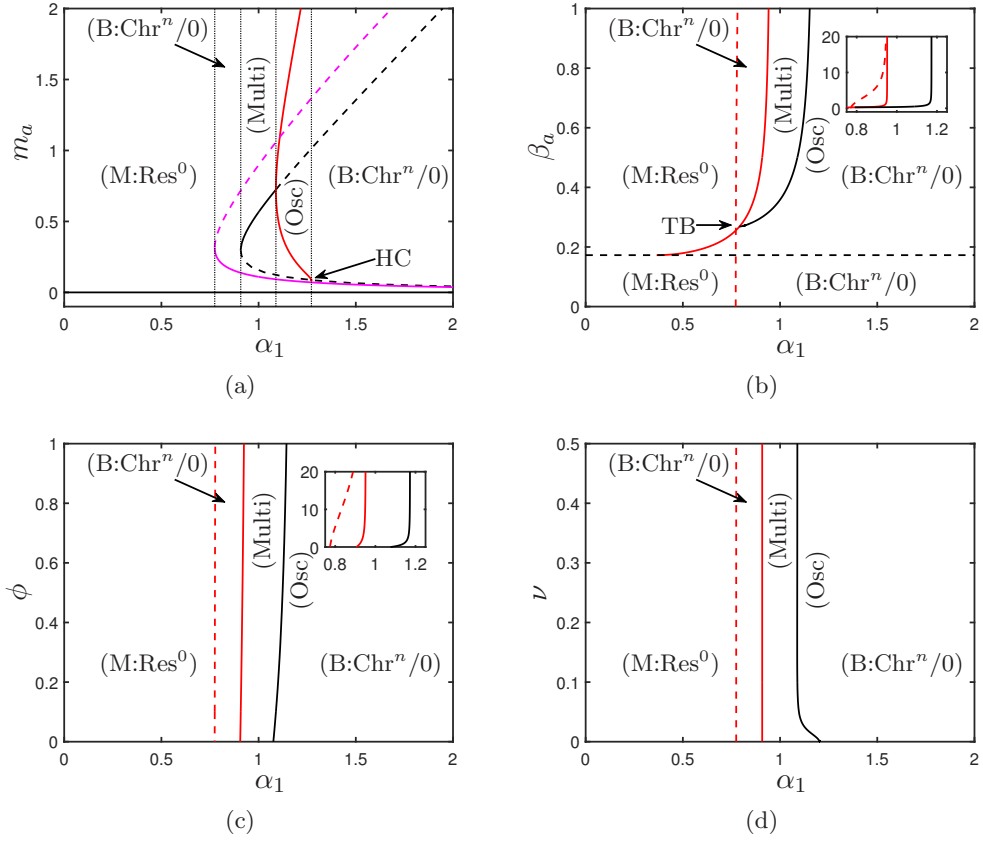


Figure 4.7: Bifurcation diagrams illustrating solutions of (4.3) for $\gamma_m = 0.025$ and all remaining parameters as given in Table 4.2. In (a), the magenta curve corresponds to the chronic steady state of Figure 4.3(b), in which the system attains a severely inflamed configuration with very high neutrophil numbers, labelled as “Chrⁿ”. The remaining curves correspond qualitatively to the branches of Figure 3.4(c) for the model covered in Chapter 3, where the chronic steady states (solid black curve) represent low-level inflammation, as shown in Figure 4.3(a), and labelled as “Chr”. In (b-d), we track the positions of relevant bifurcations depicted in (a) as a function of α_1 . Red, black and blue curves represent saddle-node, Hopf and transcritical bifurcations respectively; the dashed red curve represents the saddle-node bifurcation on the Chrⁿ branch shown in magenta in (a); the dashed black curve shown in (b) which is given (4.23,4.25) represents a saddle point. “B” indicates that the model is bistable with both healthy and chronic outcomes permissible, while “M” denotes monostability; the corresponding steady state solution being that in which inflammation resolves and all variables reach zero (labelled “Res⁰” or “0”). “Chrⁿ” denotes the severely-inflamed chronic state sustained by high neutrophil numbers. “Osc” denotes oscillatory (chronic) solutions. “HC” indicates a homoclinic bifurcation. “TB” indicates a Bogdanov–Takens bifurcation.

Takens point at $\beta_a = \beta_a^{TB} \simeq 0.28$. As we continue to decrease β_a , this saddle node then collides (at $\beta_a \simeq 0.1866$) with one of the saddle points given by (4.23,4.25) and is eliminated, rendering the severely-inflamed Chrⁿ state the sole chronic configuration.

In Figures 4.7(c) and 4.7(d), we examine the model's sensitivity to the rates of neutrophil phagocytosis by macrophages (ϕ) and apoptosis (ν). Interestingly, we observe that the model is much less sensitive to these parameters than it is to parameters related to phenotype switching. While previous models that included only a single macrophage population exhibited strong dependence upon these parameters, our results here suggest that actually manipulation of these parameters could instead be thought of as a convenient proxy for capturing phenotypic switching within a homogenised model that omits a more detailed description of disparate macrophage populations.

4.5 Discussion

In this model, we supplemented the model presented in Chapter 3 with an additional pro-inflammatory feedback loop via a population of neutrophils, recruited in the presence of pro-inflammatory mediators. As neutrophils age, they ultimately become apoptotic and, if not successfully phagocytosed by macrophages before they lyse, provide a strong source of further pro-inflammatory mediators on lysis. While phagocytic ability is a key attribute of macrophages in general, we primarily attributed this role to our anti-inflammatory phenotype in this model since phagocytic activity is known to be primarily linked to tissue-resident macrophage populations (Schulz *et al.*, 2019; Jenkins & Allen, 2021).

Our analysis revealed that the additional feedback loop in this model resulted in a diverse range of potential steady states that includes the two resolved outcomes of the model discussed in Chapter 3, chronic outcomes similar to those in the previous model in Chapter 3 in which inflammation is sustained but at a reasonably low level, a new chronic state in which inflammation is severe and sustained by very high numbers of both neutrophils and pro-inflammatory macrophages, and also various unstable states including those of (4.23,4.25). Furthermore, the model continues to exhibit oscillatory solutions as in the model of Chapter 3. We have shown (in Figure 4.4) that the dynamics of this model are essentially those of the model of Chapter 3 but with the new severely-inflamed chronic state overlaid, in a manner that is strongly dependent upon the model's parameters.

In the limit $\beta_a \rightarrow \infty$ (in which the influence of neutrophils is vanishingly small compared to that of macrophages), this model qualitatively reduces to the model covered in Chapter 3. For $\beta_a \sim \mathcal{O}(1)$, the additional severely-inflamed chronic state can exist depending on (in particular) the rates of macrophage phenotype switching. For α_1

large or α_2 small, for which we promote the pro-inflammatory macrophage population, the severely-inflamed state exists and the model has scope to be multistable with the potential for healthy outcomes, low-level inflammation or severe inflammation for the same parameters. In the opposing limit, the model recovers the model of Chapter 3.

While previous models (Kumar *et al.*, 2004; Lelekov-Boissard *et al.*, 2009; Herald, 2010; Penner *et al.*, 2012; Dunster *et al.*, 2014; Bianca *et al.*, 2015; Bangsgaard *et al.*, 2017; Bayani *et al.*, 2020a,b) that have only included a single homogenised macrophage population have highlighted the rates of neutrophil apoptosis (ν) and phagocytosis of apoptotic neutrophils (ϕ) as key in determining the switch between chronic outcomes and resolution (and therefore points of potential focus for therapeutic intervention), our analysis of this model reveals that the model has only weak sensitivity to these parameters in comparison to phenotype switching via α_1 and α_2 . This further highlights the fact that explicitly incorporating distinct macrophage phenotypes in future models of inflammation is key in fully describing resultant dynamics, and also indicates that manipulation of macrophage polarisation states could itself be a viable therapeutic target.

We note that the question of how to categorise macrophage phenotypes is a contentious one, especially given that the diversity and complexity of documented macrophage polarisation states is expanding (Murray *et al.*, 2014). We have here chosen to focus on two opposing polarisation states, the first anti-inflammatory (which could be equated with resident macrophages that exist in a wide range of tissues, or the traditionally labelled M2 phenotype), and the second pro-inflammatory (which could be equated with the M1 phenotype). This is doubtlessly an over-simplification in itself; however, this approach enabled us to expose how model outcomes (such as the existence of a second healthy steady state in which inflammation is suppressed by a continual presence of anti-inflammatory macrophages) and dynamics (including oscillations) depend upon our models' inclusion of distinct macrophage phenotypes. We believe that models that exhibit this additional healthy outcome, which is dependent on a resident macrophage population, are physiologically more realistic than those with only a trivial healthy state. An alternative approach to modelling macrophage phenotypes is to consider these as lying on a continuous spectrum of pro/anti-inflammatory activity, perhaps utilising a model based on partial differential equations. This could potentially allow the capture of more subtle macrophage phenotypes that no doubt play a role in multiple disease states (Tabas & Bornfeldt, 2016; Chauhan *et al.*, 2016; Hesketh *et al.*, 2017; Atri *et al.*, 2018). We explore this idea further in the following chapter.

Modelling The Continuum of Macrophage Phenotypes

Macrophages are a key component of the inflammatory response; they protect the body by eliminating harmful foreign particles and repairing damaged tissues. Once macrophages acquire a functional phenotype, they can continue to change their phenotypes in response to novel environmental influences, and this process is known as polarization (Murray, 2017). Numerous factors can be involved in macrophage polarization to produce a diverse and extensive range of functional phenotypes (Martinez *et al.*, 2008; Murray *et al.*, 2014; Juhas *et al.*, 2015). Therefore, there is no definitive classification stating the exact number of macrophage phenotypes, and their classification remains the subject of ongoing research and debate. In chapters 3 and 4, we classified macrophages into two distinct phenotypes based on whether their functional activity is pro- or anti-inflammatory. However, this binary classification is an oversimplified description and cannot represent the majority of macrophage phenotypes due to the heterogeneity and plasticity of macrophages (Martinez & Gordon, 2014; Murray *et al.*, 2014; Martin & García, 2021).

Here, we describe a more advanced model in which macrophage phenotypes are considered to lie on a continuous spectrum of inflammatory activity, with a range of intermediate phenotypes lying between the fully pro-inflammatory and fully anti-inflammatory classifications of chapters 3 and 4. As a result, our corresponding model takes the form of a system of partial differential equations. As in previous chapters, we analyse the model via numerical simulation in Matlab and bifurcation analysis in XPPAUT, the latter being achieved via a semi-discretisation of the PDE model to construct a corresponding ODE approximation that is tractable for bifurcation analysis.

5.1 Model derivation

We model macrophages on a continuous spectrum of phenotypes, classified according to their levels of pro/anti-inflammatory activity. We denote the number of macrophages by $m^*(t^*, p)$, where t^* represents time and stars are used to distinguish dimensional variables from their dimensionless counterparts below. The independent variable $p \in [-1, 1]$ here parameterises macrophage phenotypes, with $p = 1$ corresponding to a fully pro-inflammatory phenotype and $p = -1$ corresponding to a fully anti-inflammatory phenotype. Additionally, we introduce variables $c^*(t^*)$ and $g^*(t^*)$ to represent concentrations of generic pro- and anti-inflammatory mediators present in the tissue of interest; thus, c^* and g^* together describe the inflammatory landscape upon which macrophages reside. We expect macrophages to switch phenotype dynamically in response to changes in the inflammatory context, with high levels of inflammation (c^* high, g^* low) driving a shift toward pro-inflammatory macrophage phenotypes, and low levels of inflammation (c^* low, g^* high) promoting a shift to the anti-inflammatory phenotypes typically found in resident macrophage populations in healthy tissues (Davies *et al.*, 2013).

We model phenotype switching via two convective fluxes, q^{+*} and q^{-*} , which shift macrophages toward pro-inflammatory and anti-inflammatory phenotypes respectively. We expect pro-inflammatory mediators, c^* , to drive macrophages to become more pro-inflammatory, and expect the strength of the corresponding flux to be largest for fully anti-inflammatory macrophages (with $p = -1$), with macrophages at the fully pro-inflammatory end of the phenotype spectrum ($p = 1$) not to be affected at all. Thus, we write

$$q^{+*} = \alpha_1^* c^* (1 - p) m^*. \quad (5.1)$$

Similarly, anti-inflammatory mediators, g^* , drive phenotypic switching in the opposing direction, with the greatest effect on macrophages when $p = 1$. We write

$$q^{-*} = -\alpha_2^* g^* (1 + p) m^*. \quad (5.2)$$

Here, the parameters α_1^* and α_2^* describe the rates of phenotypic switching in response to environmental cues from mediators. We also note that these choices of flux terms constrain macrophages to the domain $p \in [-1, 1]$, since q^{+*} is zero when $p = 1$ and q^{-*} is zero when $p = -1$.

Following the model in Chapter 2, we assume that macrophages proliferate logistically up to some maximum population size m_{max}^* and decay at constant rate γ_m^* , and that the rate of proliferation is enhanced in the presence of pro-inflammatory mediators.

Thus, we have the following partial differential equation that governs the macrophage population:

$$\frac{\partial m^*}{\partial t^*} + \frac{\partial}{\partial p} (\alpha_1^* c^* (1-p) m^* - \alpha_2^* g^* (1+p) m^*) = k^* (c^* + c_T^*) R(p) m_T^* \left(1 - \frac{m_T^*}{m_{max}^*}\right) - \gamma_m^* m^*, \quad (5.3)$$

in which $k^* c_T^*$ is the baseline rate of macrophage proliferation in the absence of pro-inflammatory mediators, $R(p)$ is a function specifying which phenotypic configuration newly acquired macrophages reside in (chosen below), and $m_T^*(t^*)$ is the total number of macrophages present in the system at a given time, given by:

$$m_T^*(t^*) = \int_{-1}^1 m^*(t^*, p) dp. \quad (5.4)$$

To prescribe mediator dynamics, we take the interactions given in the model of Chapter 2 as a guide, noting that macrophages can produce both pro- and anti-inflammatory mediators (in a manner that depends on their phenotype). Our mediator dynamics are governed by the following ordinary differential equations:

$$\frac{dg^*}{dt^*} = \kappa_g^* \int_{-1}^1 f_1(p) m^* dp - \gamma_g^* g^*, \quad (5.5)$$

$$\frac{dc^*}{dt^*} = \kappa_c^* \int_{-1}^1 f_2(p) m^* dp - \delta^* c^* g^* - \gamma_c^* c^*, \quad (5.6)$$

in which κ_g^* and κ_c^* parameterise rates of mediator production, γ_g^* and γ_c^* parameterise rates of mediator decay, δ^* represents a mitigating effect of anti-inflammatory mediators against pro-inflammatory mediators, and the functions $f_1(p)$ and $f_2(p)$ describe how the rates of production of each group of mediators varies as a function of macrophage phenotype. For simplicity, we assume linear dependences for the latter, *i.e.*

$$f_1(p) = \frac{1-p}{2}, \quad f_2(p) = \frac{1+p}{2}; \quad (5.7)$$

that is, macrophages that are in a fully pro-inflammatory configuration ($p = 1$) produce no anti-inflammatory mediators at all and, likewise, macrophages that are fully anti-inflammatory ($p = -1$) produce no pro-inflammatory mediators.

We solve the system (5.3–5.7) subject to initial conditions representing an initially positive population of macrophages and some appropriate mediator concentrations. We therefore prescribe

$$m = m_0^*(p), \quad c^* = c_0^*, \quad g^* = g_0^* \quad \text{at } t^* = 0. \quad (5.8)$$

The interactions featured in this model are illustrated in Figure 5.1. Macrophage phenotype is a dynamic process regulated by the microenvironment. Due to macrophages'

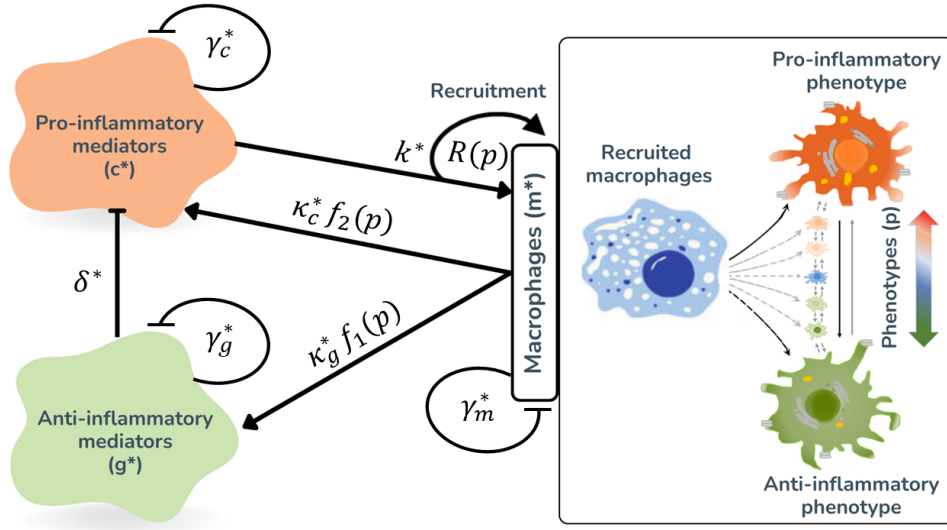


Figure 5.1: Schematic diagram representing (5.3–5.7) and illustrating the interactions between a single population of macrophages ($m^*(t^*, p)$), which involves a continuous spectrum of phenotypes, ranging from a fully anti-inflammatory to a fully pro-inflammatory phenotype, with generic groups of pro- and anti-inflammatory mediators ($c^*(t^*)$ and $g^*(t^*)$, respectively). Arrows indicate positive feedback or supply terms, while lines terminated with bars indicate negative feedback or loss terms.

remarkable adaptability, they can alter their phenotype to a continuous spectrum of phenotypes in response to environmental cues. As a result, the same macrophage cells have the ability to perform various functions in response to inducers, including cytokine production, phagocytosis, and tissue repair and remodelling. We assume that both fully anti- and pro-inflammatory macrophages represent the two extremes of the phenotypic continuum while omitting the role of neutrophils introduced in Chapter 4 to simplify the model.

5.1.1 Nondimensionalisation

To simplify our analysis below, we nondimensionalise (5.3–5.8) by introducing the following scalings:

$$t^* = \frac{1}{\gamma_c^*} t, \quad g^* = \frac{\gamma_c^*}{\delta^*} g, \quad c^* = \frac{\gamma_c^*}{k^*} c, \quad m^* = \frac{\gamma_c^{*2}}{\delta^* \kappa_g^*} m, \quad (5.9)$$

which yields the following system of dimensionless equations:

$$\frac{\partial m}{\partial t} + \frac{\partial}{\partial p} (\alpha_1 c (1-p) m - \alpha_2 g (1+p) m) = (c + c_T) R(p) m_T \left(1 - \frac{m_T}{m_{max}} \right) - \gamma_m m, \quad (5.10)$$

$$\frac{dg}{dt} = \int_{-1}^1 f_1(p)m dp - \gamma_g g, \quad (5.11)$$

$$\frac{dc}{dt} = \kappa_c \int_{-1}^1 f_2(p)m dp - c g - c, \quad (5.12)$$

with

$$m_T(t) = \int_{-1}^1 m(t,p) dp. \quad (5.13)$$

In (5.10–5.12) above, we have introduced the following dimensionless parameter groupings:

$$\gamma_g = \frac{\gamma_g^*}{\gamma_c^*}, \quad \gamma_m = \frac{\gamma_m^*}{\gamma_c^*}, \quad \kappa_c = \frac{\kappa_c^* k^*}{\kappa_g^* \delta^*}, \quad c_T = \frac{k^* c_T^*}{\gamma_c^*} \quad (5.14)$$

$$\alpha_1 = \frac{\alpha_1^*}{k^*}, \quad \alpha_2 = \frac{\alpha_2^*}{\delta^*}, \quad m_{max} = \frac{\delta^* \kappa_g^* m_{max}^*}{\gamma_c^{*2}}. \quad (5.15)$$

We solve (5.10–5.13) subject to the initial conditions:

$$m = m_0(p), \quad c = c_0, \quad g = g_0 \quad \text{at } t = 0. \quad (5.16)$$

5.1.2 Parameters

We note that theoretical studies of inflammation, in general, suffer from difficulties in accurately inferring corresponding model parameters due to limitations in available experimental data. This is due to a variety of factors, including a lack of suitable non-invasive experimental protocols, the fact that parameter values would be likely to have significant variability between differing inflammatory conditions and affected tissues, and the fact that many patients with inflammatory conditions are late to report to medical professionals, limiting the extent to which the onset of the acute inflammatory phase can be interrogated. Furthermore, we note that inferring rate parameters, in particular, would require temporal data that is difficult to obtain *in vivo*. In light of these limitations, it is more practical to estimate the orders of magnitude of corresponding dimensionless parameter groupings based on our knowledge of which mechanisms dominate. Our approach is to construct a baseline set of parameter values (given in Table 5.1) which reflects available knowledge around dominant mechanisms, and to then analyse the impact of variations in these parameters via numerical simulation and bifurcation analysis. Where possible, we configure our baseline parameter choices to be consistent with the parameters listed in Table 2.2 in order to facilitate comparison of the PDE model discussed here with related ODE model discussed in Chapter 2.

The decay rates of individual mediators are reasonably well documented, but can vary according to the medical context in question. The half-lives of the pro-inflammatory

cytokines IL-1 β , IL-8 and TNF α have been indicated to lie in the range 18.2 – 24 min, while the anti-inflammatory cytokine IL-1RA decays more slowly with a half-life in the range 4 – 6 h (Liu *et al.*, 2021). In our model, this could suggest that $\gamma_g = \gamma_g^*/\gamma_c^* \ll 1$. However, some cytokines (*e.g.* IL-6) can have both pro- and anti-inflammatory effects (Liu *et al.*, 2021), suggesting that $\gamma_g \sim 1$ in some contexts. Here, following the model of Chapter 2, we take $\gamma_g = 0.2$ as our default value in Table 5.1.

Identifying accurate values for the parameters that govern macrophage population dynamics is difficult in general, since these depend upon the scale of the affected tissue. However, the rate of macrophage loss (γ_m^*) has been documented (in the context of wound healing) to lie in the range 0.2 – 1.41 per day (Waugh & Sherratt, 2007; Cooper *et al.*, 2015), indicating that macrophage loss occurs at a slower rate than decay of pro-inflammatory mediators; we hence set $\gamma_m = \gamma_m^*/\gamma_c^* < 1$ in Table 5.1. Accurately prescribing the rate of proliferation/recruitment of the macrophage populations in isolation is hindered by the fact that macrophage proliferation rates are known to depend on background levels of inflammatory mediators (Jenkins & Allen, 2021). In (5.10), we assume that macrophage proliferation rates take a linear dependence upon pro-inflammatory mediator concentrations (*i.e.* of the form $c + c_T$) and, under the expectation that proliferation rates should appreciably increase in the presence of pro-inflammatory mediators, we expect c_T to be small in comparison to the scale over which c varies. We therefore set $c_T = 0.01$ in Table 5.1. Likewise, since the maximal macrophage population size will depend heavily on the size of the tissue of interest, we follow the model of Chapter 2 in choosing $m_{max} = 25$ as a baseline value in Table 5.1.

We expect macrophage phenotype switching toward the pro-inflammatory end of the spectrum (α_1) to dominate the converse direction (α_2) as many inflammatory conditions are associated with increased ratios of pro-inflammatory macrophages (Zhu *et al.*, 2014; Lissner *et al.*, 2015); thus we expect $\alpha_1 \gg \alpha_2$.

The remaining mediator production rate parameter, κ_c , is not readily available from existing literature. Following the model of Chapter 2, we choose $\kappa_c = 0.35$ as our baseline value; however, we note that our definition of κ_c here varies slightly from that of the model of Chapter 2, since its interpretation here is inherently linked to the manner in which the mediator production functions $f_2(p)$ and, indirectly, $f_1(p)$ are prescribed. Here, we choose $f_1(p)$ and $f_2(p)$ to be $\mathcal{O}(1)$ functions, and vary the strength of the production of mediators via κ_c . Variations of all parameter values around these baseline values are examined throughout our analyses below.

Parameter	Expression	Meaning	Baseline value
κ_c	$k^* \kappa_c^* / \delta^* \kappa_g^*$	Rate of production of pro-inflammatory mediators	0.35
γ_m	γ_m^* / γ_c^*	Decay rate of macrophages	0.05
γ_g	γ_g^* / γ_c^*	Decay of anti-inflammatory mediators	0.2
c_T	$k^* c_T^* / \gamma_c^*$	Rate of macrophage proliferation in the absence of pro-inflammatory mediators (c)	0.01
m_{max}	$\delta^* \kappa_g^* m_{max}^* / \gamma_c^{*2}$	Maximum macrophage population size	25
α_1	$\alpha_1^* \beta_1^* / k^*$	Macrophage phenotype switching (anti- to pro-inflammatory phenotype)	1
α_2	$\alpha_2^* \beta_2^* / \delta^*$	Macrophage phenotype switching (pro- to anti-inflammatory phenotype)	0.01

Table 5.1: Summary of the dimensionless parameters appearing in the model. Parameter values are estimated as described in Section 5.1.2.

5.2 Numerical scheme

We solve the system (5.10–5.13) numerically via a method of lines approach, by discretising in the phenotype variable, p , to obtain a system of ODEs which we solve via in-built ODE solvers in Matlab and XPPAUT.

We discretise in p by introducing $N + 1$ equally-spaced meshpoints p_j given by

$$p_j = -1 + j \, dp \quad \text{for } j = 0, \dots, N, \quad (5.17)$$

where $dp = 2/N$ is the corresponding meshpoint spacing. Furthermore, we write $m_j(t) \simeq m(t, p_j)$ to represent the approximation of the macrophage variable at a given phenotype meshpoint.

We approximate the flux terms in (5.10) via standard, first-order finite difference approximations. To ensure numerical stability, we take an upwinding approach in which we choose forward or backward finite difference approximations depending on the direction of the flux. Since the term containing $\alpha_1 c$ represents flux in the positive p -direction, we employ a backward difference approximation for the derivative evaluated on meshpoint j , writing

$$\frac{\partial}{\partial p} ((1-p)m) \Big|_{p=p_j} = \frac{1}{dp} ((1-p_j)m_j - (1-p_{j-1})m_{j-1}) + \mathcal{O}(dp), \quad (5.18)$$

for all $j = 1, \dots, N$. Conversely, since the term containing $\alpha_2 g$ represents flux in the

negative p -direction, we employ the following forward difference approximation:

$$\frac{\partial}{\partial p} ((1+p)m) \Big|_{p=p_j} = \frac{1}{dp} ((1+p_{j+1})m_{j+1} - (1+p_j)m_j) + \mathcal{O}(dp), \quad (5.19)$$

for all $j = 0, \dots, N-1$. On the boundaries, we adapt (5.18) and (5.19) to reflect that $m = 0$ for all points outside of the domain $p \in [-1, 1]$, writing

$$\frac{\partial}{\partial p} ((1-p)m) \Big|_{p=p_0} = \frac{1}{dp} (1-p_0)m_0 + \mathcal{O}(dp), \quad (5.20)$$

$$\frac{\partial}{\partial p} ((1+p)m) \Big|_{p=p_N} = -\frac{1}{dp} (1+p_N)m_N + \mathcal{O}(dp). \quad (5.21)$$

We evaluate the integrals in (5.11) and (5.12) via trapezium rule, writing

$$\int_{-1}^1 f_i(p)m dp \simeq \frac{dp}{2} \left(f_i(p_0)m_0 + f_i(p_N)m_N + 2 \sum_{j=1}^{N-1} f_i(p_j)m_j \right) \equiv F_i(t), \quad (5.22)$$

for $i = 1, 2$. Similarly, we evaluate $m_T(t)$ according to

$$m_T(t) \simeq \frac{dp}{2} \left(m_0 + m_N + 2 \sum_{j=1}^{N-1} m_j \right). \quad (5.23)$$

We note that the approximations arising from the trapezium rule in (5.22) and (5.23) are, in isolation, second-order; however, the accuracy of our numerical method overall is limited to first-order due to the errors associated with (5.18–5.21). We restrict to first-order finite difference schemes in (5.18–5.21) for simplicity here, and confirm sufficient numerical accuracy by examining results for differing choices of N when constructing and testing corresponding numerical codes.

Under the approximations above, the system (5.10–5.13) gives rise to the following system of $N + 3$ ODEs at leading order:

$$\begin{aligned} \frac{dm_0}{dt} &= -\frac{\alpha_1 c}{dp} ((1-p_0)m_0) + \frac{\alpha_2 g}{dp} ((1+p_1)m_1 - (1+p_0)m_0) \\ &\quad + (c + c_T) R(p_0)m_T \left(1 - \frac{m_T}{m_{max}} \right) - \gamma_m m_0, \end{aligned} \quad (5.24)$$

$$\begin{aligned} \frac{dm_j}{dt} &= -\frac{\alpha_1 c}{dp} ((1-p_j)m_j - (1-p_{j-1})m_{j-1}) + \frac{\alpha_2 g}{dp} ((1+p_{j+1})m_{j+1} - (1+p_j)m_j) \\ &\quad + (c + c_T) R(p_j)m_T \left(1 - \frac{m_T}{m_{max}} \right) - \gamma_m m_j, \quad \text{for } j = 1, \dots, N-1, \end{aligned} \quad (5.25)$$

$$\begin{aligned} \frac{dm_N}{dt} &= -\frac{\alpha_1 c}{dp} ((1-p_N)m_N - (1-p_{N-1})m_{N-1}) + \frac{\alpha_2 g}{dp} (- (1+p_N)m_N) \\ &\quad + (c + c_T) R(p_N)m_T \left(1 - \frac{m_T}{m_{max}} \right) - \gamma_m m_N, \end{aligned} \quad (5.26)$$

$$\frac{dg}{dt} = F_1(t) - \gamma_g g, \quad (5.27)$$

$$\frac{dc}{dt} = \kappa_c F_2(t) - cg - c, \quad (5.28)$$

with m_T as given in (5.23). Throughout this chapter, numerical simulations and bifurcation analyses are based upon implementations of the system (5.23–5.28) in Matlab and XPPAUT with $N = 100$. In Matlab, this ODE system is solved using the in-built solver `ode45`. In XPPAUT, we implement the adaptive, implicit solver `CVODE` as described in Ermentrout (2002). In both cases, convergence tests have been performed across a range of N values to ensure that our choice of N does not adversely affect the accuracy of our results. In Matlab, we trialled values of N in the range $N \in [60, 500]$. In XPPAUT, we are limited by the capabilities of the software to $N \leq 253$ (since XPPAUT can handle a maximum of 256 ODEs in total). For $N = 100$, we found that both the numerical simulations in Matlab and the bifurcation analysis in XPPAUT captured the Matlab numerical results for higher choices of N with good accuracy. Hence, we chose $N = 100$ for all of the remainder of our analysis.

5.3 Results

In the following sections, we use a combination of numerical simulations conducted in Matlab and bifurcation analyses conducted in XPPAUT to analyse the system (5.10–5.13). In both cases, the corresponding codes involve a finite difference discretisation in the phenotype variable p , which converts our PDE system into a system of ODEs that can be simulated using standard in-built solvers. More details of the numerical scheme are given in Section 5.2. Throughout, we are interested in whether (for a given set of parameter values) the system emits a positive steady state that represents chronic inflammation, returns to a ‘healthy’ steady state in which pro-inflammatory components are zero, or provides more complex dynamics such as oscillatory solutions (which could be likened to inflammatory conditions that exhibit relapsing–remitting characteristics). We will observe that, often, the system may exhibit multiple of these potential solutions for a fixed parameter set, with the switch between outcomes being governed by initial conditions. We will also draw comparisons of the results of this PDE model against the model of Chapter 2, which has less detailed descriptions of macrophage phenotypes, to elucidate the extent to which our conclusions may be sensitive to the modelling approach.

5.3.1 Stability of the zero state

It is trivial to see that the system (5.10–5.13) has a steady state at $m = g = c = 0$. Since this steady state contains no pro-inflammatory components, we regard this configuration as one type of resolved outcome. In order to determine the stability of this steady state, we linearise (5.10–5.13) by introducing the following scalings:

$$m(t, p) = \varepsilon \hat{m}(t, p), \quad g(t) = \varepsilon \hat{g}(t), \quad c(t) = \varepsilon \hat{c}(t), \quad (5.29)$$

and write

$$m_T = \varepsilon \int_{-1}^1 \hat{m}(t, p) \, dp = \varepsilon \hat{m}_T. \quad (5.30)$$

At $\mathcal{O}(\varepsilon)$, (5.10–5.12) reduce to

$$\frac{\partial \hat{m}}{\partial t} = c_T R(p) \hat{m}_T - \gamma_m \hat{m}, \quad (5.31)$$

$$\frac{d\hat{g}}{dt} = \int_{-1}^1 f_1(p) \hat{m} \, dp - \gamma_g \hat{g}, \quad (5.32)$$

$$\frac{d\hat{c}}{dt} = \kappa_c \int_{-1}^1 f_2(p) \hat{m} \, dp - \hat{c}. \quad (5.33)$$

For the linear choices of $f_1(p)$ and $f_2(p)$ given in (5.7), we can simplify the integrals in (5.32) and (5.33) by noting the following (in which we write $f(p)$ in place of $f_1(p)$ or $f_2(p)$ for compactness):

$$\begin{aligned} \int_{-1}^1 f(p) \hat{m} \, dp &= \frac{1}{2} \int_{-1}^1 (1 \pm p) \hat{m} \, dp \\ &= \frac{1}{2} \int_{-1}^1 \hat{m} \, dp \pm \frac{1}{2} \int_{-1}^1 p \hat{m} \, dp \\ &= \frac{1}{2} \hat{m}_T \pm \frac{1}{2} \left(p \hat{m}_T \Big|_{-1}^1 - \int_{-1}^1 \hat{m}_T \, dp \right). \end{aligned} \quad (5.34)$$

Noting that \hat{m}_T is independent of p , the bracketed terms in (5.34) cancel and we have

$$\int_{-1}^1 f(p) \hat{m} \, dp = \frac{1}{2} \hat{m}_T. \quad (5.35)$$

Since (5.35) reveals that (5.32) and (5.33) depend only upon \hat{m}_T , rather than \hat{m} itself, it is helpful to reformulate (5.31) in terms of \hat{m}_T and eliminate \hat{m} entirely. We note that

$$\begin{aligned} \frac{d\hat{m}_T}{dt} &= \frac{d}{dt} \int_{-1}^1 \hat{m} \, dp \\ &= \int_{-1}^1 \frac{\partial \hat{m}}{\partial t} \, dp \end{aligned}$$

$$= \int_{-1}^1 c_T R(p) \hat{m}_T - \gamma_m \hat{m} \, dp, \quad (5.36)$$

in which the final equality comes from (5.31). Restricting attention to the case $R(p) = 1$ for ease, (5.36) then provides

$$\frac{d\hat{m}_T}{dt} = c_T \int_{-1}^1 \hat{m}_T \, dp - \gamma_m \int_{-1}^1 \hat{m} \, dp = (2c_T - \gamma_m) \hat{m}_T, \quad (5.37)$$

in which we have again noted that \hat{m}_T is independent of p .

With (5.37) replacing (5.31), and with (5.32) and (5.33) rewritten according to (5.35), (5.31–5.33) can be expressed as the following linear system:

$$\frac{d}{dt} \begin{pmatrix} \hat{m}_T \\ \hat{g} \\ \hat{c} \end{pmatrix} = \underbrace{\begin{pmatrix} 2c_T - \gamma_m & 0 & 0 \\ \frac{1}{2} & -\gamma_g & 0 \\ \frac{\kappa_c}{2} & 0 & -1 \end{pmatrix}}_{\mathbf{J}} \begin{pmatrix} \hat{m}_T \\ \hat{g} \\ \hat{c} \end{pmatrix}. \quad (5.38)$$

Since the Jacobian matrix \mathbf{J} is triangular, its eigenvalues are given by its diagonal entries. For the zero state to be stable, we require all the eigenvalues of \mathbf{J} to have negative real part. Thus, the zero state is stable provided that

$$c_T < \frac{\gamma_m}{2}. \quad (5.39)$$

The stability of the zero state is therefore determined by the underlying growth/decay dynamics of the macrophage population in the absence of inflammatory stimuli, with c_T representing the rate of growth of the macrophage population in the absence of pro-inflammatory mediators, and γ_m being the rate of loss of macrophages as they vacate the tissue or die.

5.3.2 Analysis for $R(p) = 1$

For simplicity, we begin our numerical analysis with consideration of the case $R(p) = 1$, for which all macrophage phenotypes are recruited uniformly. While this is not necessarily a biologically realistic assumption, it provides a useful starting point for our mathematical analysis; we examine the impact of non-uniform choices of $R(p)$ in Section 5.3.3 below.

Figure 5.2 illustrates some typical solutions to (5.10–5.13). Here, we hold all parameters fixed at the values of Table 5.1 but vary γ_g to illustrate the range of permissible solutions. For $\gamma_g = 1$ (Figure 5.2(a)), the system attains a steady state configuration in which pro-inflammatory mediator concentrations are high, anti-inflammatory

mediator concentrations are low, and macrophages are polarised entirely toward pro-inflammatory phenotypes. This configuration represents a chronic inflammatory outcome. Reducing γ_g to its default value of 0.2 (Figure 5.2(b)), results in higher levels of anti-inflammatory mediators which stimulates macrophage phenotype switching toward anti-inflammatory phenotypes (via the flux term arising from (5.2)). Here, the system attains a stable oscillatory configuration (periodic orbit) with macrophages mostly polarised toward anti-inflammatory activity but also with periodic surges of more pro-inflammatory phenotypes that prevent the inflammation being mitigated against entirely. Levels of pro-inflammatory mediators are lower than in Figure 5.2(a) due to the upscaled role of the anti-inflammatory mediators and macrophages, but the solution is nonetheless chronic. In Figure 5.2(c), we set $\gamma_g = 0.01$ and observe that, while pro-inflammatory mediator concentrations are initially sufficiently high to drive macrophages toward pro-inflammatory phenotypes, rapid accumulation of anti-inflammatory mediators then reverses the direction of phenotypic switching, moving macrophages toward anti-inflammatory configurations. Here, pro-inflammatory mediator concentrations eventually reach zero and the macrophage population ultimately leaves the tissue entirely as the macrophage decay term via γ_m outweighs the growth term (c_T) in (5.10); the system reaches the zero state, which is stable for these parameter choices according to (5.39). We regard this configuration as a healthy outcome in which inflammation is resolved entirely.

We note that, in Figure 5.2, we have illustrated typical outcomes by varying one of our model parameters (γ_g in this case). Equally, for some parameters, we could illustrate similar results by holding parameters fixed and varying our initial conditions, the model often being bistable for many parameter choices. In order to elucidate how our model's solutions depend on each of our parameters more fully, we perform bifurcation analysis in XPPAUT to track the coordinates of steady states and oscillatory solutions as a function of each parameter. (See Section 5.2 for further details of the numerical scheme used.)

In the bifurcation diagrams presented in this section, we use the following abbreviations to indicate the model's behaviour: (Res) indicates that the only stable solution is the steady state at zero, where inflammation resolves and all variables reach zero; (Chr) denotes that the only stable solution is a single chronic steady state corresponding to chronic inflammation; (B) indicates that the model is bistable with both resolving and chronic steady states permissible; (Multi) represents that the model permits more than two stable steady states, one of which is the zero state; (Chr:2) means that the model has two stable chronic steady states and the zero state is unstable; Osc denotes oscil-

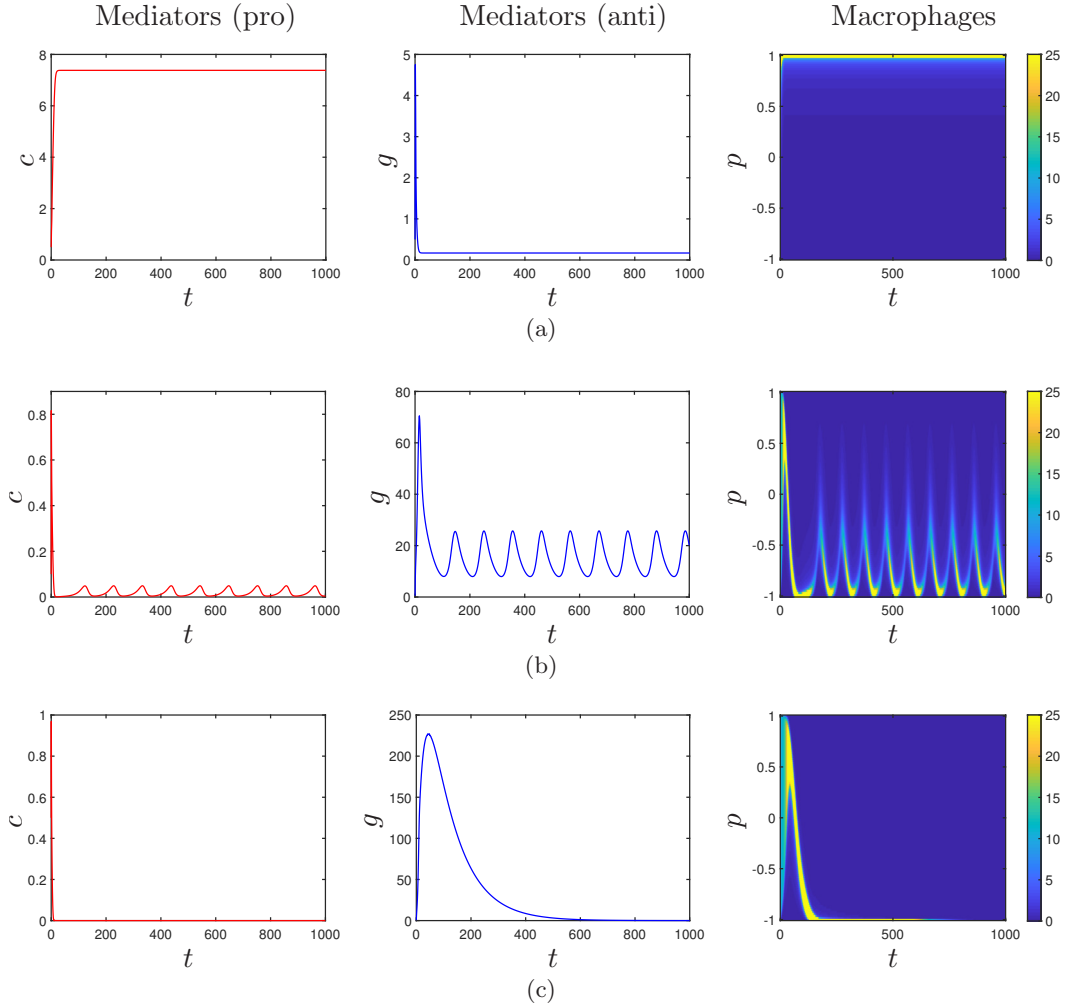


Figure 5.2: Numerical simulations of (5.10–5.13) subject to initial conditions $c(0) = g(0) = 0.5$ and $m(0, p) = 10$ for (a) $\gamma_g = 1$, (b) $\gamma_g = 0.2$ and (c) $\gamma_g = 0.01$, $R(p) = 1$ and all unspecified parameters as given in Table 5.1.

latory (chronic) solutions; (Res/Osc) indicates that the model converges to either the zero state or an oscillatory solution; (B/Osc) denotes that the model converges to either the zero state, a unique chronic state, or an oscillatory solution.

Figure 5.3 illustrates bifurcation diagrams for each of our seven model parameters, holding all unspecified parameters at the values given in Table 5.1. The vertical axes in the figures show pro-inflammatory mediator concentrations, c , which is a proxy for the severity of chronically inflamed states. The inset figures in the top-right of each panel provide an indication of the corresponding macrophage phenotypes for each branch; colouring represents the ‘median’ macrophage phenotype, calculated according to

$$p_{median} = \min \hat{p} \in [-1, 1] : \int_{-1}^{\hat{p}} m \, dp \geq \frac{m_T}{2}, \quad (5.40)$$

with configurations for which $m_T = 0$ coloured black. Dark blue or dark red colourings

indicate that the distribution of macrophage phenotypes is mostly anti-inflammatory or mostly pro-inflammatory, respectively.

For the parameter values of Table 5.1, the model permits resolution via convergence to the zero state (as per (5.39), labelled “Res” in Figure 5.3), or chronic oscillatory outcomes as shown in Figure 5.2(b) (labelled “Osc” in Figure 5.3). In general, we observe that changes in parameter values that stimulate macrophage numbers, either directly (γ_m smaller, or c_T larger) or indirectly via pro-inflammatory mediators (κ_c larger), can act to overwhelm oscillations, eliminating them via a Hopf bifurcation and often giving rise to a chronic steady state. Furthermore, increasing c_T and/or reducing γ_m can destabilise the zero state via a transcritical bifurcation corresponding to (5.39), resulting in a configuration of the model in which a chronic steady state outcome is guaranteed (demarcated by “Chr” in Figure 5.3). Conversely, increasing γ_m or decreasing c_T (both of which reduce the size of the macrophage population) results in a growth of the amplitude of oscillatory solutions, until the periodic orbit ultimately collides with a neighbouring saddle (with $c \simeq 0$) and is hence eliminated via a homoclinic bifurcation. For sufficiently large choices of γ_m , in particular, the only permissible solution is one of resolution, the zero state being the only stable solution here. Intuitively, we may make converse conclusions regarding stimulation or repression of anti-inflammatory mediators, in comparison to those of pro-inflammatory mediators: for γ_g small, we have large numbers of anti-inflammatory mediators and chronic outcomes are eliminated; oscillations exist for values of γ_g lying between a Hopf bifurcation and a homoclinic bifurcation; and moderate to large choices of γ_g (for which anti-inflammatory mediator contributions are lesser) reveal regions of bistability or multistability (labelled “B” and “Multi” in Figure 5.3) in which there are two or more stable steady states and the system may attain either resolved or chronic steady-state outcomes.

The existence of oscillatory solutions requires a reasonably large macrophage population, oscillations being eliminated entirely for m_{max} small, see Figure 5.3(b). Furthermore, we observe that oscillatory solutions generally correspond to macrophage configurations that comprise primarily anti-inflammatory phenotypes; large numbers of pro-inflammatory macrophage phenotypes generally correspond to the existence of stable chronic steady states.

The phenotype switching parameters, α_1 and α_2 , play a joint role in controlling many of the above observations. For α_1 fixed at its default value of Table 5.1, varying α_2 reveals a window of α_2 -values in which oscillations exist, bounded between two Hopf bifurcations. (See Figure 5.3(d).) For α_2 fixed at its default value, smaller choices of α_1 result in a bistable configuration in which the model attains either the zero state or

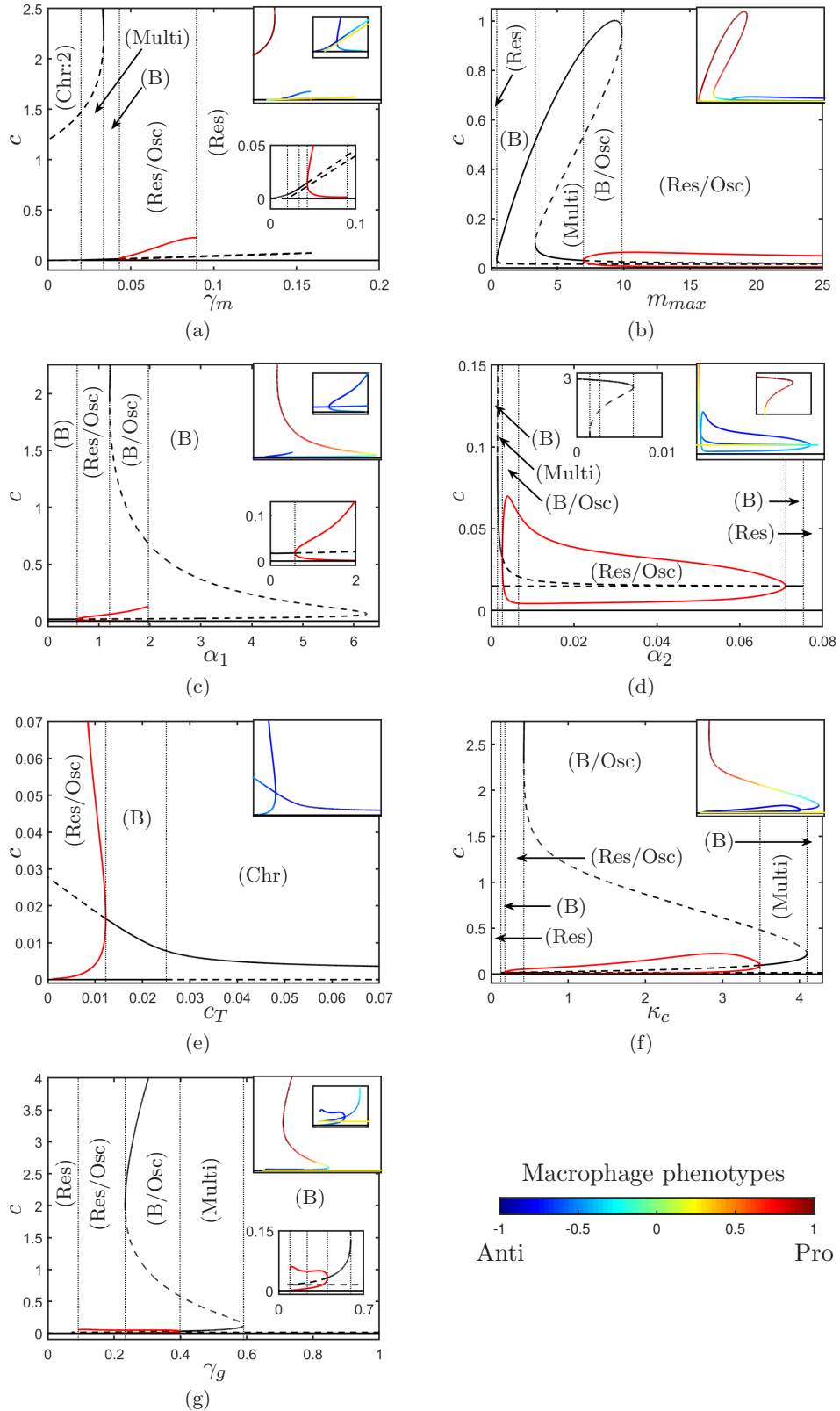


Figure 5.3: Bifurcation diagrams illustrating solutions of (5.10–5.13). All unspecified parameters are as in Table 5.1. Solid/dashed curves represent stable/unstable solutions; black and red represent steady states and periodic orbits respectively. Inset: the same curves, but instead coloured according to the median macrophage phenotype given by (5.40).

a weakly-inflamed chronic state that is mitigated by macrophage polarisation toward anti-inflammatory phenotypes. Meanwhile, a larger choice of α_1 can give rise to a new chronic state in which pro-inflammatory mediator concentrations are much higher and macrophages are primarily polarised toward pro-inflammatory phenotypes (as shown in Figure 5.3(c)). In order to fully understand the joint effect of these two parameters (and others), it is helpful to track the coordinates of the bifurcations observed above in two-dimensional slices of parameter space, as illustrated in Figure 5.4.

Figure 5.4 reveals a reasonably complex interdependence between our model parameters, illustrating numerous areas of parameter space in which model outcomes are distinct. In Figure 5.4(a,b), we expose how the macrophage phenotype switching parameters (α_1 and α_2) act in tandem with the rate of macrophage decay (γ_m) to control the location of corresponding bifurcations. From (5.39), we know that the zero state (which corresponds to resolution of inflammation) is destabilised via a transcritical bifurcation at $\gamma_m = 0.02$ (for the parameter values of Table 5.1). This transcritical bifurcation is shown as blue curves in Figures 5.4(a,b). To the left of these curves, γ_m is relatively small and the macrophage population is relatively large, and the model is relatively sensitive to phenotype switching via α_1 and α_2 , which together determine the number of chronic steady states that exist. For α_1 small or α_2 large, macrophage polarisation is driven primarily toward anti-inflammatory phenotypes and there exists a unique chronic state corresponding to relatively low-level inflammation. For α_1 large or α_2 small, macrophage phenotype switching in the direction of pro-inflammatory phenotypes is stronger and we may obtain a second chronic steady state corresponding to more severe inflammation (*i.e.* with c larger). (See, also, Figure 5.3(c,d).) For γ_m larger, so that the zero state is stable, α_1 and α_2 effect a switch in the existence/stability of chronic steady states, moving the model between configurations of guaranteed resolution (α_1 small or α_2 large) or bistability with both chronic and resolved outcomes permissible (α_1 large or α_2 small). This joint role of α_1 and α_2 is further elucidated in Figure 5.4(c), in which we track bifurcations in (α_1, α_2) -space. For intermediate values of γ_m , α_1 and α_2 , we find Hopf bifurcations that can give rise to oscillations as shown above in Figures 5.2(b) and 5.3.

In Figure 5.4(d), we draw similar conclusions regarding the parameters that control the sizes of the two mediator concentrations (*i.e.* κ_c , which controls the rate of growth of the pro-inflammatory mediators, and γ_g , which controls the rate of decay of the anti-inflammatory mediators). Intuitively, for κ_c and γ_g both small, the pro-inflammatory mediator population is small and the anti-inflammatory mediator population is large and the model attains a configuration in which resolution of inflammation is guaran-

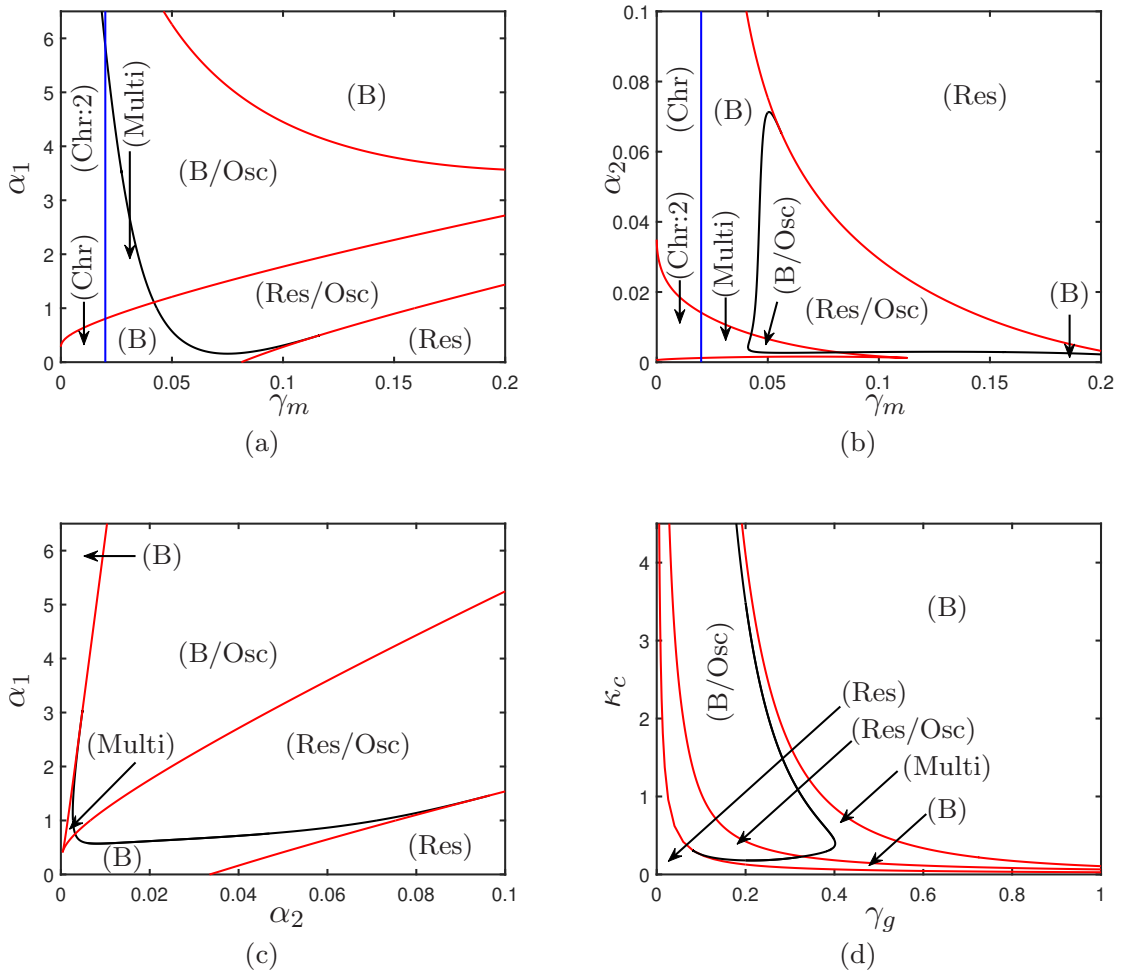


Figure 5.4: Bifurcation diagrams illustrating bifurcations of (5.10–5.13) in two-dimensional slices of parameter space. Red curves represent saddle-node bifurcations; black curves represent Hopf bifurcations; blue curves represent transcritical bifurcations. All unspecified parameters are as given in Table 5.1.

ted. When these parameters are both large, chronic steady states are promoted and the model attains a bistable configuration (noting that the resolved state at zero is always stable here due to the values of γ_m and c_T satisfying (5.39)). Intermediate choices of κ_c and γ_g can give rise to oscillatory solutions or additional chronic states as we have already observed in Figure 5.3(f,g).

5.3.3 The effect of variations in $R(p)$

We, here, investigate the extent to which our choice of recruitment function $R(p) = 1$ above influences the observed dynamics. That is, we seek to understand the manner in which the existence or stability of healthy and chronic outcomes depends upon the polarisation state of newly recruited macrophages. Here, we take $R(p)$ to be of a Gaussian-like shape given by

$$R(p) = \exp\left(-\frac{(p-\mu)^2}{\sigma^2}\right), \quad (5.41)$$

where $\mu \in (-1,1)$ parameterises the ‘mean phenotype’ of newly recruited macrophages and σ captures the level of variability in recruited macrophage phenotypes. In the limit $\mu \rightarrow 1$, newly recruited macrophages are primarily polarised toward pro-inflammatory activity, whereas the limit $\mu \rightarrow -1$ corresponds to recruitment of primarily anti-inflammatory phenotypes. We note that in the limit $\sigma \rightarrow \infty$ we have $R(p) \rightarrow 1$, and we recover the previous case of Section 5.3.2.

In Figure 5.5, we show bifurcation diagrams akin to Figure 5.3(a) but with $R(p)$ as given by (5.41), for a range of μ and σ values. Here, we treat the rate of macrophage loss γ_m as our bifurcation parameter and examine how the number and nature of steady states and the positions of related bifurcations are influenced by changes in $R(p)$. In Figure 5.3(a), for $R(p) = 1$ we observed that the healthy state is stable for $\gamma_m > 0.02$ (as per (5.39)), and for sufficiently large values of γ_m this is the only stable configuration. Additionally, two branches of chronic configurations exist for smaller choices of γ_m : a stable branch of low-level chronic solutions exists for $\gamma_m \lesssim 0.043$ and is then destabilised via a Hopf bifurcation giving rise to low-level oscillations supported by a primarily anti-inflammatory macrophage population; meanwhile, a second branch of higher-level chronic inflammation (supported by a largely pro-inflammatory macrophage population) exists for values of γ_m below a corresponding saddle-node bifurcation (at $\gamma_m \simeq 0.033$). As Figure 5.5(g-i) show, we recover these results in the limit $\sigma \rightarrow \infty$. For $\sigma \sim \mathcal{O}(1)$, the three fundamental branches of solutions above persist, but may shift in parameter space and/or exhibit stability changes.

Taking the limit $\sigma \rightarrow 0$, so that the distribution of recruited macrophage phenotypes becomes increasingly narrow, results in some small changes to the location of the transcritical bifurcation that bounds the stability of the healthy steady state. However, this appears to be an artefact of having no normalising constant in (5.41) – a deliberate choice here to ensure that $R(p) \rightarrow 1$ as $\sigma \rightarrow \infty$. As we gradually reduce σ , we slightly slow the total rate of recruitment of new macrophages, and hence slightly en-

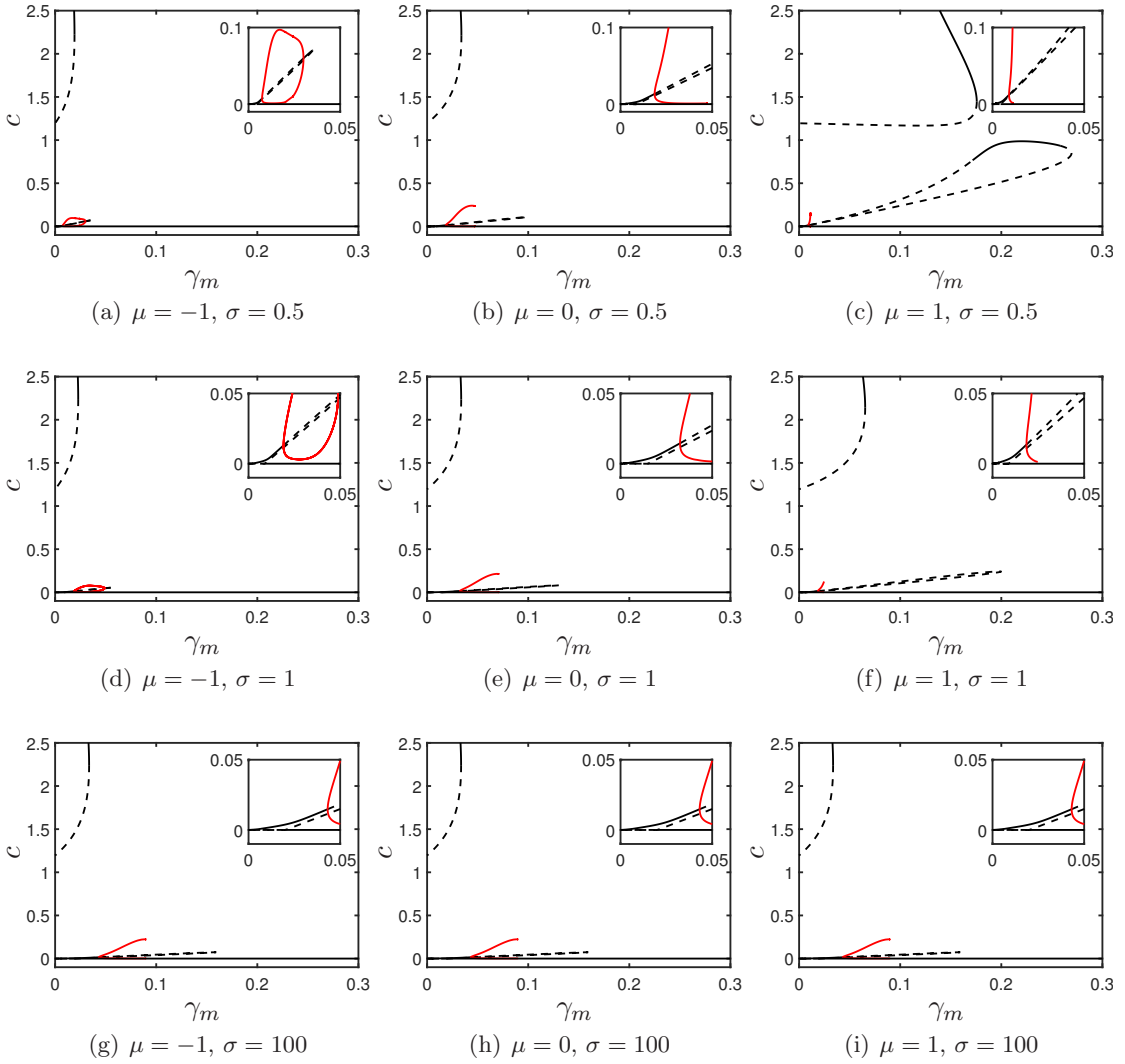


Figure 5.5: Bifurcation diagrams illustrating solutions of (5.10–5.13) with $R(p)$ given by (5.41), for varying choices of μ and σ . All unspecified parameters are as in Table 5.1. Solid/dashed black curves represent stable/unstable steady state solutions. Solid red curves represent stable periodic orbits. (Unstable periodic orbits are omitted in (c) for clarity.)

hance the stability of the healthy state (shifting the transcritical bifurcation to the left in Figure 5.5). This behaviour is symmetrical in variations of μ .

Changes to the healthy steady state and its corresponding transcritical bifurcation are relatively slight in comparison to the influence of $R(p)$ upon chronic states. Intuitively, polarisation of recruited macrophages toward pro-inflammatory activity has the effect of promoting chronic configurations. In the case of the higher-level chronic state of Figure 5.3, the saddle node that provides the upper bound in γ_m for this branch shifts toward larger γ_m -values as $\mu \rightarrow 1$, rendering this state permissible for a broader range of choices of γ_m . Additionally, the limit $\mu \rightarrow 1$ can also drive stability changes on the

low-level chronic branch, as shown for $\sigma = 0.5$ in Figure 5.5(c). Here two additional (subcritical) Hopf bifurcations are introduced, providing additional stable steady-state solutions (and unstable periodic orbits, not plotted) in regions of parameter space in which restoration of the healthy state was previously guaranteed.

In Figure 5.6, we track the γ_m -coordinates of the bifurcations shown in Figure 5.5 as we vary σ , for $\mu = -1$ (dashed lines) and $\mu = 1$ (solid lines). At the top of the figure, as $\sigma \rightarrow \infty$, all bifurcation curves converge to the corresponding γ_m -coordinates of the bifurcations in Figure 5.3(a). As we reduce σ , the extent to which the dashed and solid lines diverge from one-another reflects the extent to which the model is sensitive to the prescription of $R(p)$. Shown in blue in Figure 5.6, the position of the transcritical bifurcation that determines the stability of the healthy zero state has very weak dependence on σ ; furthermore, its position is identical for $\mu = -1$ and $\mu = 1$. The healthy state is unstable to the left of the illustrated blue curve, guaranteeing chronic outcomes here. As we move from $\mu = -1$ toward $\mu = 1$, the saddle-node bifurcation that bounds the high-level branch of chronic solutions (shown in magenta) traverses left to right, availing an expanding region of stable, high-level chronic solutions as σ reduces. Meanwhile, for $\sigma \sim \mathcal{O}(1)$, the low-level chronic branch expands as $\mu \rightarrow 1$ or shrinks as $\mu \rightarrow -1$. As shown in Figure 5.3(a), solutions on the low-level chronic branch are mostly unstable in the limit $\sigma \rightarrow \infty$; however, for $\mu \sim 1$, reducing σ ultimately results in a pair of new subcritical Hopf bifurcations which bound a region of additional stable steady states on this low-level branch. These additional stable states exist below the corresponding black curve in Figure 5.6. These additional Hopf bifurcations collide with the corresponding saddle-node branch via fold–Hopf bifurcations at the points labelled “FH” in Figure 5.6.

In Figure 5.7, we show two-parameter bifurcation diagrams that correspond to taking a horizontal cross-section through Figure 5.6 at $\sigma = 0.5$. For ease of tracking the existence of the various solutions that underlie these figures, we note that taking vertical cross-sections through the three panels in Figure 5.7 at $\mu = 0$ provides one-parameter bifurcation diagrams that qualitatively correspond to those shown for $R(p) = 1$ in Figures 5.3(a,c,d). In Figure 5.7(a), we observe (as was the case for $R(p) = 1$) that for γ_m large the model guarantees resolution regardless of the choice of μ , since the rate of loss of macrophages is sufficient to remove the macrophage population entirely, and hence eliminate damage. For smaller γ_m , there are various chronic solutions that coexist with the zero state provided that γ_m is above the transcritical bifurcation shown in blue in the figure; below this transcritical bifurcation curve chronic outcomes are guaranteed. The magenta curve in Figure 5.7(a) represents the saddle-node bifurcation on the high-

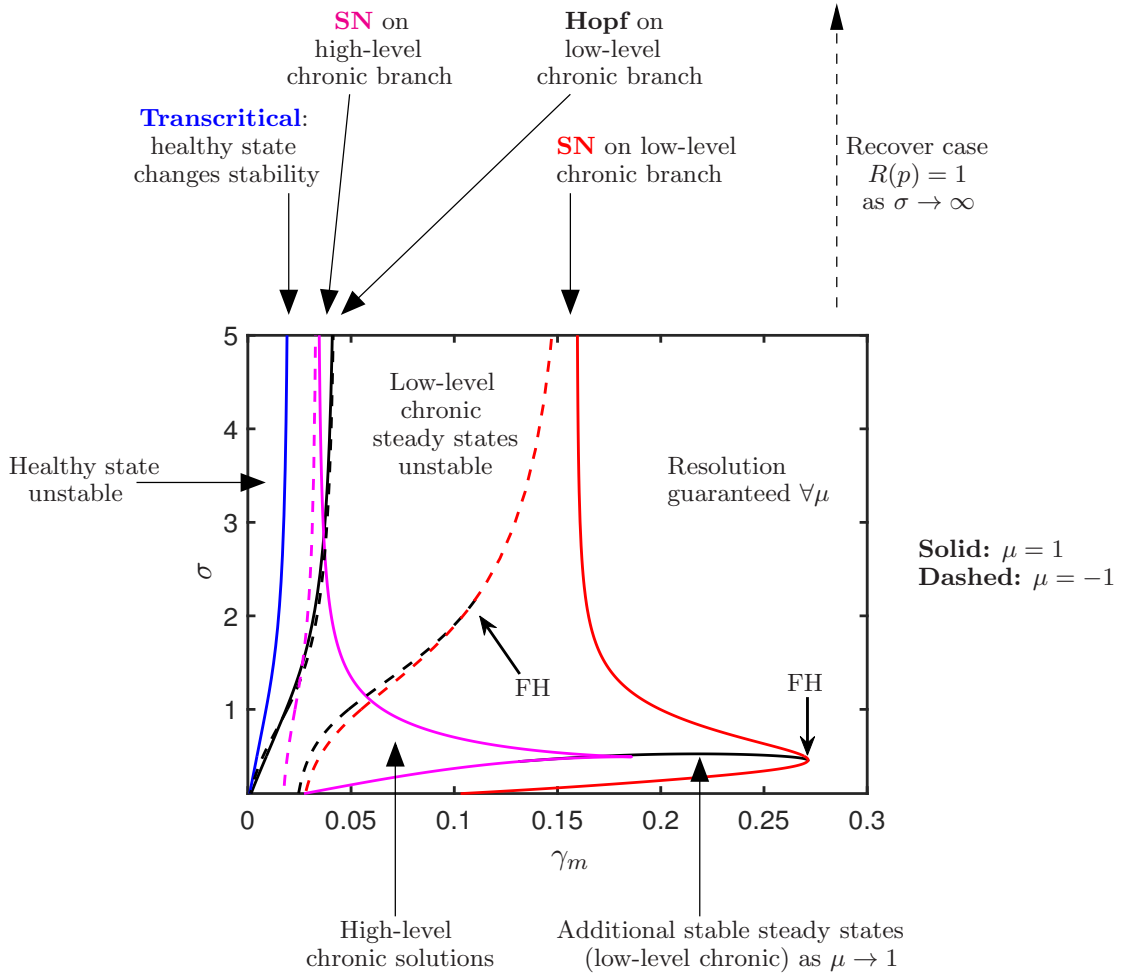


Figure 5.6: Bifurcation diagram illustrating how the bifurcations of Figure 5.3(a) move as we vary μ and σ in (5.41). As $\sigma \rightarrow \infty$, we recover the bifurcation coordinates of Figure 5.3(a), for $R(p) = 1$. Solid and dashed curves illustrate the positions of bifurcations for $\mu = 1$ and $\mu = -1$ respectively. Red and magenta curves represent distinct sets of saddle-node bifurcations; black curves represent Hopf bifurcations. The blue curve represents the position of the transcritical bifurcation where the zero state changes stability, and is identical for $\mu = \pm 1$. FH = fold-Hopf bifurcation.

level chronic branch (also plotted in magenta in Figure 5.6); a stable highly-inflamed chronic state exists below this magenta curve. The principal effects of varying the recruited macrophage phenotype (μ) are as follows: i) as $\mu \rightarrow 1$, the highly-inflamed state exists for a greater range of γ_m -values, pushing the model toward more-severe chronic outcomes; ii) for $\mu \sim 1$, additional low-level chronic solutions are created, bounded by a neighbouring curve of Hopf bifurcations; iii) as $\mu \rightarrow -1$, the model is driven towards resolution for a widening range of γ_m -values, with additional low-level chronic steady states and oscillatory solutions being confined to an increasingly narrow γ_m -range.

In Figures 5.7(b,c), we track these bifurcation points as functions of the macrophage

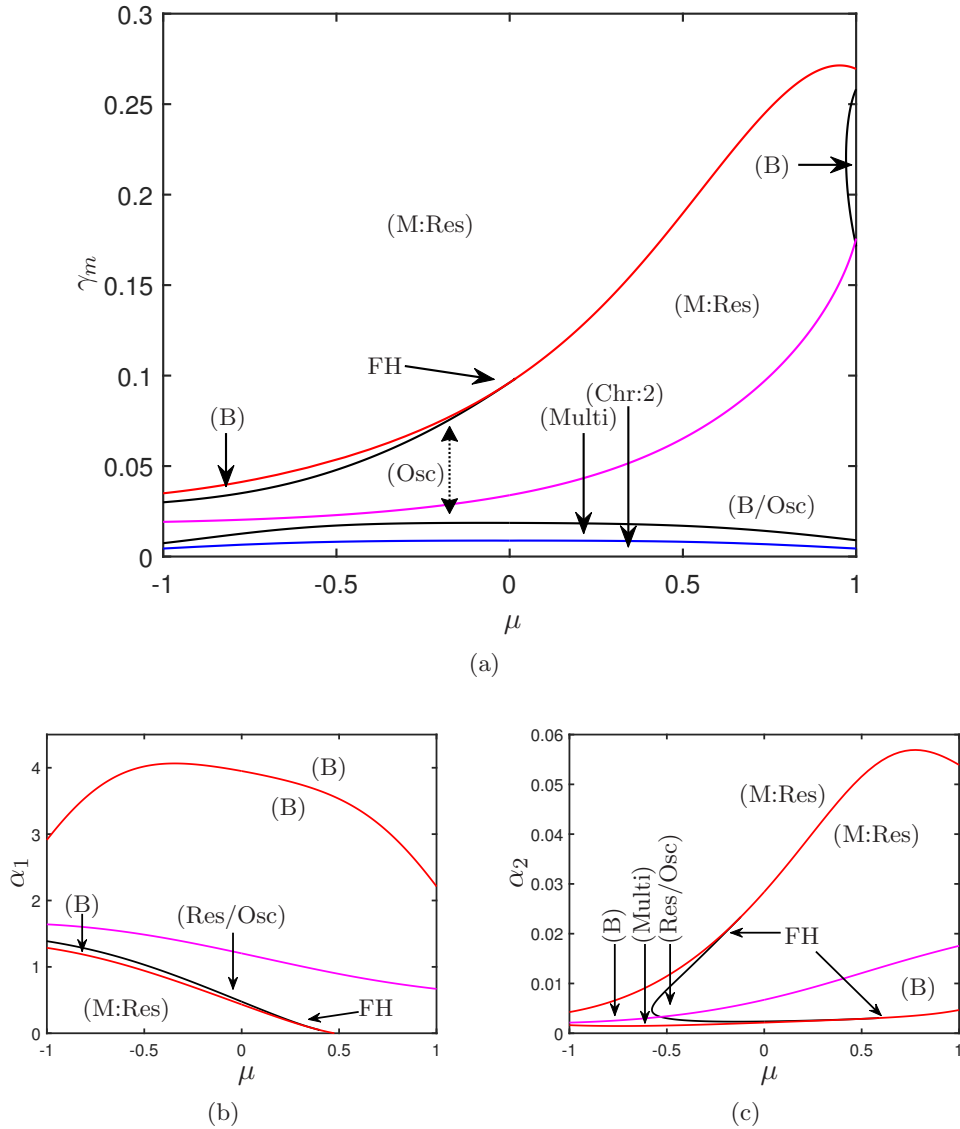


Figure 5.7: Two-parameter bifurcation diagrams illustrating the bifurcations of Figure 5.6 for $\sigma = 0.5$. Red and magenta curves represent saddle-node bifurcations on the low-level and high-level branches of Figure 5.5 respectively; black curves represent Hopf bifurcations. The blue curve represents the position of the transcritical bifurcation where the zero state changes stability. FH = fold-Hopf bifurcation.

phenotype switching parameters α_1 and α_2 . Since these figures use our baseline values for other parameters (in particular $\gamma_m = 0.05$), the zero state is stable throughout, and this is independent of μ , α_1 and α_2 here. The highly-inflamed chronic state is stable above the magenta curve in Figure 5.7(b) and below the magenta curve in Figure 5.7(c). Again, we see similar effects to above when varying μ ; *i.e.* recruited macrophages being polarised toward pro-inflammatory phenotypes ($\mu \rightarrow 1$) stimulates chronic outcomes on the highly-inflamed branch (in particular), and the converse ($\mu \rightarrow -1$) promotes resolution. (We note that the saddle-node bifurcation represented by the upper red

curve in Figure 5.7(b) effects only the number of unstable steady states. This is also the case for the two saddle-node bifurcations shown in red in Figure 5.7(c), for those portions of the bifurcation curves lying to the right of the corresponding fold-Hopf (FH) bifurcations.)

5.4 Discussion

Macrophages are highly plastic cells with the propensity to polarise into a diverse spectrum of phenotypes. Our model, presented here, has sought to address the fact that many previous mathematical models of inflammation-related systems take one of two approaches to describing diverse macrophage populations: either by incorporating a single homogenised population that averages phenotype-specific interactions; or, by incorporating two distinct and opposing phenotypes, typically representing *e.g.* the M1/M2 categorisation nomenclature. Instead, our model allows for intermediate phenotypes, by placing all possible macrophage phenotypes on a continuous spectrum according to their levels of pro/anti-inflammatory activity. Our model incorporates phenotype switching via nonlinear flux terms that are enhanced by environmental cues, with high concentrations of pro-inflammatory mediators driving macrophages to polarise toward pro-inflammatory phenotypes (synonymous with the M1 classification), and high concentrations of anti-inflammatory mediators driving the converse (resulting in phenotypes associated with tissue-resident macrophages and the M2 classification). Through numerical simulation (in Matlab) and bifurcation analysis (in XPPAUT), we have examined the manner in which the rates of macrophage population growth, phenotype switching, and mediator interactions affect switches between healthy and chronic outcomes.

We note that macrophage numbers in tissues can increase due to both proliferation and recruitment, or a combination of both of these (Rückerl & Allen, 2014). In our model, we do not distinguish between these mechanisms explicitly; however, we assume that the net effect of these mechanisms can be modelled via a corresponding logistic growth term (in (5.3)) up to a tissue-specific carrying capacity m_{max}^* . Importantly, our model incorporates, via the function $R(p)$, the potential for us to specify the phenotype-coordinates of macrophages that are newly added to the tissue of interest. For simplicity and mathematical tractability, we began our analysis by focusing on the case $R(p) = 1$ representing the idea that all phenotypes are recruited uniformly. While this is unlikely to be biologically realistic in many settings, this provided a useful starting point for our analysis, and allowed us to separately examine the manner in which

variations in $R(p)$ affect the resulting dynamics.

For $R(p) = 1$, we observed that the model exhibits three fundamental types of solution, as follows. Firstly, the model may attain a steady state in which all components of the model reach zero. We regard this as a ‘healthy’ state, since it encompasses no inflammatory stimuli. This zero state is stable provided that the rate of macrophage loss (γ_m^*) sufficiently outweighs the basal rate of macrophage proliferation/recruitment in the absence of pro-inflammatory mediators (c_T^*), as per (5.39). Secondly, the model may attain a chronic steady state with positive macrophage numbers and (in particular) pro-inflammatory mediators. Often, these chronic steady states are supported by a macrophage population that is mostly polarised toward pro-inflammatory phenotypes. Thirdly, the model may converge toward stable oscillatory solutions that are reminiscent of conditions that exhibit relapsing-remitting characteristics. Throughout our analysis, oscillatory solutions have always been supported by macrophage populations that are mostly polarised toward anti-inflammatory phenotypes. In many areas of parameter space, two or more of the above solutions co-exist, and the model is bistable or multistable, with resulting inflammatory outcomes dependent upon our choice of initial conditions. In Figures 5.3 and 5.4, we exposed the extent to which the existence/stability of the above solutions depends upon our model parameters. In particular, we observed that rapid rates of macrophage loss (γ_m^*) can eliminate chronic outcomes entirely (since macrophages are the only pro-inflammatory source in this model), while rapid macrophage proliferation/recruitment (c_T^*) promotes chronic outcomes, and that strong rates of macrophage phenotype switching toward pro-inflammatory phenotypes (α_1^*) promotes chronic steady-state outcomes, while phenotype switching toward anti-inflammatory phenotypes (α_2^*) can promote both resolution and low level chronic oscillations (in a manner that is dependent upon the model’s remaining parameters).

In Section 5.3.3, we examined the extent to which the observations above are sensitive to our prescription of the phenotype of newly recruited macrophages. To do so, we set the corresponding recruitment function $R(p)$ to have a Gaussian-like shape, and examined the effects of variation of the mean (μ) and standard deviation (σ) of this Gaussian. In the limit $\sigma \rightarrow \infty$, our analysis recovers the case $R(p) = 1$ exactly. For $\sigma \sim \mathcal{O}(1)$, while the fundamental solutions discussed for $R(p) = 1$ above still persist, the locations of corresponding bifurcation points shift somewhat as a function of the recruited macrophage phenotype. Our analysis revealed the stability of the healthy (zero) state exhibits very weak sensitivity to the phenotype of recruited macrophages, and instead depends more broadly on overall macrophage numbers. This is partially an artefact

of the fact that our prescription of the pro-inflammatory mediator production function $f_2(p)$ in (5.7) equips all macrophages with $p \neq 1$ with at least some pro-inflammatory influence. Chronic solutions, however, exhibit more sensitivity to recruited phenotypes, with recruitment weighted toward pro-inflammatory phenotypes ($\mu \rightarrow 1$) resulting in the expansion of regions of parameter space that permit chronic outcomes and (in some cases) the creation of new chronic steady state configurations. Meanwhile, biasing macrophage recruitment toward anti-inflammatory phenotypes ($\mu \rightarrow -1$) largely promotes resolution of inflammation. We highlight, once again, that the function $R(p)$ here incorporates both proliferation of existing macrophages and recruitment of new macrophages from the vasculature. This provides a potentially complex landscape of newly added macrophage phenotypes, with proliferation of existing tissue-resident macrophages more likely to provide macrophages polarised toward anti-inflammatory activity, and recruitment of macrophages from the blood stream more likely to provide macrophages that are pro-inflammatory in nature. In most biologically relevant cases, we expect the latter of these mechanisms to dominate, with Figure 5.6 illustrating that this can result in a relatively complex spectrum of chronic outcomes.

It is helpful to draw comparisons of our PDE model against previous ODE models of similar macrophage interactions in inflammatory settings. In particular, we note that our PDE model presented here is designed as a natural extension of the model presented in Chapter 3 to account for intermediate macrophage phenotypes. Broadly, we find that many of our observations share commonality with those of the model in Chapter 3. The macro-scale roles of each parameter indicated in Figure 5.3 largely align with those of the previous ODE model: large rates of macrophage loss (γ_m) drive the model toward a healthy zero state, while γ_m small yields chronic configurations; oscillatory solutions exist for reasonably large macrophage populations (m_{max} large); and strong macrophage polarisation toward pro-inflammatory phenotypes (α_1) drives chronic outcomes with the converse (α_2) generally driving resolution. While these overarching conclusions result readily from both the ODE and PDE constructions of the model, some intermediate bifurcations do differ slightly. For example, one key difference between these models is that the ODE model exhibits a healthy steady state with positive anti-inflammatory components (macrophages and mediators), while the PDE model exhibits just a unique healthy state at zero. In the ODE model, the zero state tends to change stability through collision with the positive healthy state at a transcritical bifurcation, whereas in the PDE model the zero state bifurcates to a solution in which macrophages are slightly biased toward pro-inflammatory phenotypes (e.g. yellow configurations in Figure 5.3). This is an artefact, partly, of our choice of f_2 , which is non-zero for all $p \neq -1$, rendering all macrophage phenotypes with $p \neq -1$ slightly

pro-inflammatory. We note that it is common for models of inflammation to regard a steady state at zero to correspond to resolution (Reynolds *et al.*, 2006; Dunster *et al.*, 2014; Bayani *et al.*, 2020a; Dunster *et al.*, 2023; Nelson *et al.*, 2023) on the basis that the macrophage population being modelled represents the extent to which macrophage numbers in a given tissue are elevated above a certain baseline level of tissue-resident macrophages.

Our PDE model is in line with this perspective; however, we note that a reformulation of the model in which a baseline population of entirely anti-inflammatory macrophages sits at or below $p = -1$, for example, would be a simple task to allow the model to recover the potential for positive healthy steady states to exist. Furthermore, we note that our PDE model incorporates a more advanced description of macrophage proliferation/recruitment than the corresponding ODE model of Chapter 3 does, which focuses entirely on proliferation of existing macrophages and a resultant source of entirely anti-inflammatory macrophages. Through our analysis above, particularly that of Section 5.3.3, we have illustrated that this more-advanced description has the potential to generate a more diverse range of solutions than is afforded by the corresponding ODE model. Additionally, a key observation from the PDE model is that oscillatory solutions are generally supported by a macrophage population that is largely polarised toward anti-inflammatory phenotypes. In the corresponding ODE model (which incorporates two explicit and opposing phenotypes) we can draw similar observations with oscillatory solutions having a high proportion of anti-inflammatory macrophages; however, our PDE model more readily exposes the extent to which intermediate phenotypes may play a supporting role.

In constructing our PDE model, we have modelled the complex range of macrophage phenotypes on a continuous spectrum of inflammatory activity. This has presented novel mathematical insight into the role of intermediate phenotypes, in particular. However, we note that the biological classification of specific macrophage phenotypes and where they may sit on our inflammatory spectrum is an extremely complex task that is hampered not only by the multi-factorial nature of macrophages' roles in inflammation, but also by a significant lack of experimental data against which to validate mathematical models of inflammation in general. In order to construct the model, we have deployed reasonably speculative choices of fluxes representing phenotype-switching (\mathbf{q}^{+*} , \mathbf{q}^{-*}) and terms representing the extent to which differing phenotypes produce differing levels of pro/anti-inflammatory mediators ($f_1(p)$ and $f_2(p)$, which we assume are linear in p here). Throughout, our approach has been to make the simplest possible choices of such terms, while retaining essential biological realism.

However, we note that our choices of f_1 and f_2 , in particular, are likely to somewhat over-simplify a more complex dependence upon phenotype. Our model elucidates the role that intermediate phenotypes can play in a complex inflammatory environment, but (as with any other mathematical model of inflammation) requires greater availability of experimental data in order to fully justify some inherent modelling assumptions. This remains an area for consideration in the future, should further experimental data become available.

Conclusions

The growing interest in inflammation is due to its association with a wide array of chronic diseases. Macrophages play a crucial role in resolving inflammation and its progression, changing their role according to their environment, and this plasticity and diversity of macrophage phenotypes is a potential therapeutic target in inflammatory diseases. In this work, we have presented a series of mathematical models to elucidate the manner in which macrophage phenotype selection impacts inflammatory dynamics. Below, we briefly summarise the key conclusions of this thesis, and outline potential targets for future investigation.

6.1 Thesis summary

In this work, we have presented and analysed a series of related models of inflammatory dynamics that include increasing levels of complexity regarding descriptions of macrophage phenotypes and other aspects of the inflammatory response. Our proposed models seek to further elucidate the potential impact that distinct modelling choices regarding macrophage phenotype descriptions have upon resulting model dynamics, by systematically building the complexity of the corresponding models and carefully analysing the resultant changes in our models' predictions.

In Chapter 2, we presented and analysed a simple model of inflammatory dynamics that omits a detailed description of the range of macrophage phenotypes that a typical inflammatory environment involves, focusing instead on the interactions of a single macrophage population with groups of generic pro- and anti-inflammatory mediators. Through numerical simulation (in Matlab) and bifurcation analysis (in XPPAUT), our model exhibits a simple switch between resolved (healthy) and chronic steady state solutions. Furthermore, the model offers various possible outcomes depending on our

choice of parameters or the model's initial conditions. These outcomes include monostability with either resolution guaranteed or chronic outcomes guaranteed, or bistability with both healthy and chronic outcomes permissible and the resulting outcome is determined by initial conditions. The main feature of chronic conditions is the accumulation of monocyte-derived macrophages in the inflamed tissue, leaving the body in a persistent state of alert due to the elevated concentration levels of pro-inflammatory mediators produced by macrophages. Since the macrophage population is the inducing source of inflammation in this model, a guaranteed strategy for resolving inflammation revolves around reducing the size of macrophage populations. This means that manipulating parameter choices that negatively affect the size of the macrophage population, thereby reducing the number of macrophages, promotes a healthy response in general. In view of this, to ensure resolution, we may either increase the rate of macrophage loss (γ_m) or decrease the rate of macrophage recruitment in the absence of mediators (by reducing c_T). Likewise, reducing the rates of anti-inflammatory mediators' decay (γ_g) or pro-inflammatory mediators' production (κ_c) shifts the model toward a healthy outcome. Since all macrophages exhibit a pro-inflammatory effect in this model, complete elimination of the macrophage population is essential for attaining resolution of inflammation. However, we note that even in healthy tissues, macrophages must be present at low baseline levels to maintain general health, making this assumption biologically unrealistic. It is noteworthy that many existing models of inflammatory dynamics assume that the entire removal of macrophages is a healthy response, which considers the macrophage variable as describing an elevation of macrophage numbers above the healthy baseline, rather than absolute population size.

In Chapter 3, we separated macrophages into two populations with pro- and anti-inflammatory functions. We note that this in itself is still an oversimplification of the actual inflammatory environment that occurs *in vivo*, as macrophage populations are numerous and not yet universally classified. In addition to the trivial healthy steady state observed in the model presented in Chapter 2, the model in Chapter 3 admits a non-trivial healthy configuration where macrophage numbers are positive. Specifically, this configuration suggests a scenario devoid of pro-inflammatory macrophages and mediators while retaining the existence of anti-inflammatory macrophages and mediators, which are essential for maintaining the tissue's healthy state. A positive healthy state is considered more biologically realistic and acceptable than a zero healthy state. However, the existence of this positive healthy state depends on the parameters that control the size of the macrophage population; if $\gamma_m < c_T$, the zero-state is unstable, and the positive healthy state exists, with stability governed by (3.28).

The model of Chapter 3 also exhibits oscillatory solutions (chronic states) that were not observed in the simple model of Chapter 2. The existence of these oscillations depends entirely on the choices of the macrophage phenotype switching rates (α_1 and α_2). These oscillations are most evident when the total macrophage population (m_{max}) is large enough to allow the emergence of multiple inflammatory dynamics and significant differences between the sizes of pro- and anti-inflammatory macrophage populations. Conversely, these oscillations are eliminated entirely when m_{max} is sufficiently small. The rates of macrophage phenotype switching reflect the difference in sizes between the pro- and anti-inflammatory macrophage populations in an intuitive manner. The parameter choices that promote the model's pro-inflammatory feedbacks and increase the size of the pro-inflammatory macrophage populations (α_1 large or α_2 small), can expand regions of bistability or chronicity and have a significant influence over the potential for oscillatory outcomes. It is noteworthy that very small values of α_1 can eliminate oscillations entirely, which suggests that bidirectional phenotype switching specifically underpins the existence of these oscillations. On the other hand, parameter choices that promote the model's anti-inflammatory feedbacks and increase the likelihood of larger populations of anti-inflammatory macrophages, such as α_1 small or α_2 large, can eliminate chronic outcomes entirely.

In Chapter 4, we incorporated populations of active and apoptotic neutrophils into our analysis and examined the resulting dynamics – neutrophils are the most pivotal cell type in causing inflammatory damage. Upon analysis of our model, it became evident that introducing an additional feedback loop of neutrophil populations into the model resulted in the emergence of various potential stable steady states. These outcomes included two distinct healthy states similar to those presented in Chapter 3 (zero and positive healthy states). The model also still exhibits oscillatory solutions similar to those in the model of Chapter 3. In addition, chronic outcomes are observed, similar to the model of Chapter 3, where inflammation persists but at a relatively low level. Notably, a new chronic state emerged, characterized by severe and sustained inflammation driven by very high numbers of both neutrophils and pro-inflammatory macrophages, signifying a crucial interaction between these cell types that might promote and perpetuate inflammation. Briefly, the model presented in Chapter 4 shares the same dynamics as the model in Chapter 3, but with the existence of a new, severely inflamed chronic state. In the limit $\beta_a \rightarrow \infty$, the pro-inflammatory feedback from apoptotic neutrophils is suppressed. As a result, the effect of neutrophils becomes very small compared to that of macrophages, the dynamics of macrophages and mediators become independent of neutrophils, and our model qualitatively returns to the model presented in Chapter 3. If we consider the rate of macrophage phenotype switching,

we note the potential existence of an additional severely inflamed chronic state, particularly when β_a is small. In cases where α_1 is large or α_2 is small, we have strong polarisation toward pro-inflammatory macrophage phenotypes, which upscales neutrophil-driven dynamics since the removal of apoptotic neutrophils is primarily driven by anti-inflammatory macrophage phenotypes. As a result, the model exhibits the scope to be multistable, with the potential for healthy outcomes, low-level inflammation, or severe inflammation (driven by neutrophils) for the same parameters, and the resulting inflammatory condition is determined by initial conditions. In the opposing limit, the model recovers the one presented in Chapter 3. Our analysis revealed that the model is less sensitive to the rates of neutrophil apoptosis (ν) and phagocytosis of apoptotic neutrophils (ϕ) when compared to the influence of phenotype switching via α_1 and α_2 . This finding contrasts with previous models (Herald, 2010; Penner *et al.*, 2012; Dunster *et al.*, 2014; Bayani *et al.*, 2020a,b) that have only included a single homogenised macrophage population and focused on these parameters (ϕ and ν) as potential therapeutic targets. This highlights the importance of including distinct macrophage phenotypes in inflammation models and suggests that manipulation of macrophage polarisation states could be a promising therapeutic target.

In Chapter 5, we presented a partial differential equation (PDE) model that considers macrophage phenotypes to lie on a continuous spectrum of inflammatory activity, with a range of intermediate phenotypes lying between the fully pro-inflammatory and fully anti-inflammatory activities. Our model incorporates phenotype switching via nonlinear flux terms that are enhanced by environmental cues, with high concentrations of pro-inflammatory mediators driving macrophages to polarise toward pro-inflammatory phenotypes (synonymous with the M1 classification), and high concentrations of anti-inflammatory mediators driving the converse (resulting in phenotypes associated with tissue-resident macrophages and the M2 classification). We began our analysis by focusing on the case $R(p) = 1$, representing the idea that all phenotypes are recruited uniformly. Our model exhibits three fundamental types of solution for $R(p) = 1$, as follows. Firstly, the model may attain a steady state in which all components of the model reach zero. We consider this state as "healthy", since it involves no inflammatory stimuli. This zero steady state is stable provided that the rate of macrophage loss (γ_m^*) sufficiently exceeds the rate of macrophage proliferation/recruitment in the absence of pro-inflammatory mediators (c_T^*), as per (5.39). Secondly, the model may attain a chronic steady state with pro-inflammatory mediators and positive macrophage numbers. These chronic states are often supported primarily by pro-inflammatory macrophage populations. Thirdly, the model may converge toward stable oscillatory solutions, supported mostly by anti-inflammatory macrophage

populations. In many regions of parameter space, two or more of the above solutions co-exist, and the model displays bistable or multistable behaviour, with the resulting inflammatory outcomes depending upon our choice of initial conditions. In addition, the stability/existence of the above solutions depends on our model parameters, such that rapid rates of macrophage loss (γ_m^*) can eliminate chronic outcomes entirely, while rapid macrophage proliferation/recruitment (c_T^*) promotes chronic outcomes, and high rates of macrophage phenotype switching toward pro-inflammatory phenotypes (α_1^*) promotes chronic steady state outcomes.

We then examined the extent to which the observations above are sensitive to our prescription of the phenotype of newly recruited macrophages by setting $R(p)$ to have a Gaussian-like shape and investigating the effects of variation of the mean (μ) and standard deviation (σ) of this Gaussian. Our analysis recovered the case $R(p) = 1$ exactly in the limit as $\sigma \rightarrow \infty$. For small σ , while the fundamental solutions for the case $R(p) = 1$ above still persist, the locations of corresponding bifurcation points shift somewhat as a function of the recruited macrophage phenotype. Our analysis revealed that the stability of the healthy (zero) state exhibits very weak sensitivity to the phenotype of recruited macrophages, and instead depends more on overall macrophage numbers. However, chronic solutions exhibit more sensitivity to recruited phenotypes, with recruitment weighted toward pro-inflammatory phenotypes ($\mu \rightarrow 1$) expanding regions of parameter space that permit chronic outcomes. Meanwhile, biasing macrophage recruitment toward anti-inflammatory phenotypes ($\mu \rightarrow -1$) largely promotes resolution of inflammation.

Our PDE model is an extension of the ODE model presented in Chapter 3 to account for intermediate macrophage phenotypes. Broadly, we found that many of our observations largely align with those of the model in Chapter 3. For instance, large rates of macrophage loss (γ_m) drive the model toward a healthy zero state, while γ_m small yields chronic configurations, and strong macrophage polarisation toward pro-inflammatory phenotypes (α_1) drives chronic outcomes with the converse (α_2) generally driving resolution. While these overall conclusions result easily from both the ODE and PDE constructions of the model, some intermediate bifurcations do differ slightly. For instance, one major difference between these models is that the ODE model emits a healthy steady state with positive anti-inflammatory components (macrophages and mediators), while the PDE model exhibits only a unique healthy state at zero. In the ODE model, the zero state changes its stability by colliding with the positive healthy state at a transcritical bifurcation, whereas in the PDE model the zero state bifurcates by colliding with a solution in which macrophages are slightly biased toward pro-

inflammatory phenotypes. This is partly due to our choice of f_2 , which is non-zero for all $p \neq -1$, rendering all macrophage phenotypes with $p \neq -1$ slightly pro-inflammatory. In addition, a key observation from the PDE model is that oscillatory solutions are generally supported by a macrophage population that is largely polarised toward anti-inflammatory phenotypes. This observation was also the case in Chapter 3. From what we have seen, most of the oscillations in Chapter 3 generally have $m_a \gg m_p$. We note that the PDE model includes a more advanced description of macrophage proliferation/recruitment than the corresponding ODE model of Chapter 3, resulting in a more diverse range of solutions than is afforded by the corresponding ODE model.

In summary, in this work, we developed a series of mathematical models of inflammation. We further highlighted the fact that explicitly incorporating distinct macrophage phenotypes in models of inflammation is key in fully describing resultant dynamics, and also indicates that manipulation of macrophage polarisation states could itself be a viable therapeutic target. We initially chose to focus on two opposing polarisation states, the first anti-inflammatory (which could be equated with resident macrophages that exist in a wide range of tissues, or the traditionally labelled M2 phenotype), and the second pro-inflammatory (which could be equated with the M1 phenotype). This is doubtlessly an over-simplification in itself; however, this approach enabled us to expose how model outcomes (such as the existence of a second healthy steady state in which inflammation is suppressed by a continual presence of anti-inflammatory macrophages) and dynamics (including oscillations) depend upon our models' inclusion of distinct macrophage phenotypes. We believe that models that exhibit this additional healthy outcome, which is dependent on a resident macrophage population, are physiologically more realistic than those with only a trivial healthy state. We also developed an alternative approach to modelling macrophage phenotypes, which is to consider these as lying on a continuous spectrum of pro/anti-inflammatory activity. This would allow the capture of more subtle macrophage phenotypes that no doubt play a role in multiple disease states (Tabas & Bornfeldt, 2016; Chauhan *et al.*, 2016; Hesketh *et al.*, 2017; Atri *et al.*, 2018). These models have emerged as potent tools in exploring novel therapeutic interventions, offering insights into manipulating macrophage phenotypes as potential targets for therapeutic strategies.

6.2 Targets for future work

The association of inflammation with a wide range of chronic diseases has prompted scientists from diverse scientific domains to conduct extensive research in order to com-

prehend the complexities inherent in the inflammatory response and provide deeper insights into the mechanisms that perpetuate chronic inflammatory conditions. Mathematical inflammation models have significantly contributed to understanding the complex nature of the inflammatory response and identifying the pathways that drive inflammation to develop into chronic conditions. These models highlight vital factors and pathways that govern the inflammatory response and focus on interactions between immune cells, cytokines, and other mediators. Mathematical models play a significant role in developing and refining therapeutic interventions for inflammation, such as targeting specific pro-inflammatory cytokines (Masters *et al.*, 2013; Cohen & Mosser, 2013), removing apoptotic neutrophils (Liang *et al.*, 2007; Kraakman *et al.*, 2014; Dunster *et al.*, 2014) and regulating the levels of pro-inflammatory mediators (Waugh & Sherratt, 2007). Moving forward, we can delve deeper into understanding the inflammatory response through exploration of various suggested aspects.

6.2.1 Context-specific models

Our research focused on examining how macrophage phenotypes and generic pro- and anti-inflammatory mediators influence the outcome of the inflammatory response in a general context. The results of our work are interesting and can be further expanded and investigated in future studies. However, our models are deliberately generic in context, with relevance to various inflammatory conditions or affected tissues. One target for future work, is to consider the design of models that examine specific cytokines, disease scenarios or distinct tissues. Specifically, we suggest that future studies could focus on examining specific cytokines that stimulate pro- and anti-inflammatory macrophages (including Interleukins IL-1, IL-6, IL-10, tumour necrosis, and tumour growth factor) rather than assuming the existence of generic mediators. This approach would provide a more precise understanding of the dynamics of the inflammatory response.

The behaviour of macrophages varies depending on the type of tissue in which they are located and the pathological conditions to which they are exposed. The search for a more accurate characterization of macrophages, identifying their diverse phenotypes and responses to environmental cues, remains an ongoing challenge. Therefore, the classification of macrophages into specific phenotypes is very complex and still unresolved, especially given that the diversity and complexity of documented macrophage polarisation states are expanding Murray *et al.* (2014). Future efforts could include developing models that incorporate more than two specific macrophage phenotypes with two neutrophil populations (activated neutrophils and apoptotic neutrophils),

which may reveal new therapeutic interventions and provide insights into manipulating macrophage phenotypes as potential targets for therapeutic strategies. In addition, enhancing these models with detailed descriptions of individual mediators may provide a more comprehensive understanding of macrophage plasticity and their diverse responses to stimuli. However, at this stage, we don't have enough information (or data) to build such a model accurately. This remains a challenge.

A key point of interest that prompts further studies is the introduction of inflammatory stimuli (or pathogens) and the inclusion of additional immune cells, such as T and B lymphocyte cells, in our models. This approach will offer a better understanding of the complex interactions underlying the inflammatory response, leading to more targeted investigations of potential therapeutic interventions.

This work could also be expanded and modified to more precisely describe and explore specific inflammatory mechanisms and diseases that arise from persistent inflammatory responses such as atherosclerosis (Thon *et al.*, 2019), heart disease (Wirtz & von Känel, 2017), and psoriasis (Ringham *et al.*, 2019). This approach will provide valuable insights into the progression of diseases and assist in developing tailored therapeutic strategies.

While the modelling presented in this thesis relates to a wide range of medical conditions, one specific group of chronic diseases that are a priority for ongoing work are those related to tumour development. The pursuit of potential therapeutic targets remains crucial in the treatment of tumour-associated diseases. Macrophages exhibit a dual role; they can induce both pro-tumour and anti-tumour effects in response to the type, concentration and longevity of exposure to stimulating agents. Targeting specific macrophage phenotypes associated with tumour growth or suppression could lead to innovative therapeutic strategies (Tamura *et al.*, 2018; Shu *et al.*, 2020). With careful parameterisation and validation against experimental data, mathematical models of inflammation offer great potential to supplement laboratory and clinical studies to guide the identification of therapeutic interventions related to a broad range of medical conditions.

6.2.2 Addressing the lack of corresponding experimental data

The significant lack of experimental data is a major obstacle in the mathematical modelling of inflammation, against which we can validate and calibrate our models. The lack of empirical data hampers the development of proposed therapeutic interventions, the accuracy and reliability of our mathematical representations of inflammatory pro-

cesses, and the clinical applicability of inflammation models. This insufficiency undermines our ability to evaluate these models' efficacy and predictive power. On the other hand, the availability of experimental data helps expand the horizons of mathematical models of inflammation, increase the effectiveness of inflammatory models, and enhance their predictive power and clinical relevance. Consequently, future efforts in this field should focus on obtaining extensive experimental data that can be used to validate and improve mathematical models of inflammation, thus enhancing our understanding of chronic inflammatory diseases and enabling more accurate predictions of inflammatory dynamics. This challenge needs the cooperation of the scientific community to bridge the gap between theoretical and experimental studies, allowing the effectiveness of inflammation models to be enhanced and their applicability in clinical and therapeutic contexts.

In our constant endeavour to improve our models, parametrisation remains a significant challenge in our work. Mathematical models have been developed to understand how macrophages change their function in diabetic conditions (Marée *et al.*, 2008; Masters *et al.*, 2013; Richards & Endres, 2014). These models specifically focus on the role of macrophages in removing apoptotic cells. Comparison of the models against *in vitro* experimental data led to improving the accuracy of the models and directed further experiments, helping to understand the mechanisms that contribute to the reduced rate of removal of apoptotic cells observed in macrophages from diabetic-prone mice. While generic models of the inflammatory response have shown some success in particular disease contexts (Reynolds *et al.*, 2006; Kumar *et al.*, 2008; Torres *et al.*, 2019), their effectiveness is limited by the lack of available data and the difficulty in inferring many parameters included in such models. To tackle this, we need to develop an appropriate experimental design that accurately captures the parameters of interest to which the model is sensitive, including those responsible for immune cell recruitment, regulation of pro-inflammatory mediators, and chemotaxis.

6.2.3 Alternative modelling approaches

We used ordinary and partial differential equations in our models to understand the underlying dynamics of inflammation. However, considering the various techniques that can be used in mathematical modelling, an interesting approach for future studies would be to replicate our analysis within the context of an agent-based model. Agent-based models offer the capability to simulate and study individual cells' precise interactions and behaviours, providing a more accurate reflection of biological systems. Compared to mathematical representations such as bifurcation diagrams, these models

are inherently more accessible and understandable for biologists, facilitating clearer interpretation of results. While agent-based models of inflammation have been proposed previously (Vodovotz *et al.*, 2008; Vodovotz & An, 2019; Bayani *et al.*, 2020b), these do not fully account for the diverse range of macrophage phenotypes. An agent-based model that carefully accounts for macrophage polarisation may offer more clinical relevance and provide new perspectives to enhance our understanding of inflammatory dynamics and potentially lead to new therapeutic interventions.

Macrophages play a critical role in promoting the inflammatory response and tissue repair process. They are characterized by their ability to move and migrate towards inflammatory stimuli. However, our current models lack spatial descriptions encompassing the leukocyte's chemotaxis, cells' motion, mediator spreading, and the positions (such as vasculature) from which macrophages are recruited. Addressing this gap in our work, we recommend future studies to develop spatial models of the inflammatory response and investigate the biological interactions occurring at the tissue level between macrophage (M1 and M2) phenotypes, neutrophils and pro-and anti-inflammatory mediators. These models can be tailored to fit individual tissue configurations, accounting for factors such as proximity to blood vessels.

List of bifurcations

Bifurcation analysis is a powerful tool for understanding the behaviour of dynamical systems. The system's qualitative behaviour can undergo significant changes as parameters vary. These qualitative changes are called bifurcations, and the parameter values at which they occur are called bifurcation points. Bifurcation points usually involve changes in the system's behaviour, such as changes in the stability of fixed points, the emergence of new fixed points, the onset of oscillations, or the disappearance of fixed points. This appendix briefly overviews the various local bifurcations discussed in our chapters, see Table A.1.

Type of bifurcation	Brief description	Reference
Saddle node	Two fixed points move toward each other, collide and mutually annihilate.	Strogatz (2018), (p. 46)
Transcritical	Two fixed points move toward each other, collide, exchange stabilities and move apart.	Strogatz (2018), p. 52
Hopf	One fixed point changes stability at the same time that a periodic orbit is created or destroyed.	Strogatz (2018), p. 249
Homoclinic	A periodic orbit collides with a saddle point resulting in the orbit being destroyed.	Strogatz (2018), p. 263
Fold-Hopf	Tangential intersection of curves of saddle node (fold) and Hopf bifurcations.	Kuznetsov <i>et al.</i> (1998), p. 299
Bogdanov-Takens	Non-tangential intersection of curves of saddle node (fold) and Hopf bifurcations.	Kuznetsov <i>et al.</i> (1998), p. 298

Table A.1: Summary of the bifurcation points appearing in Chapters 2–5.

References

- K. Abbas and M. Rydh. Satellite image classification and segmentation by using jseg segmentation algorithm. *International Journal of Image, Graphics and Signal Processing*, 4(10):48, 2012.
- L. A. Abdulkhaleq, M. A. Assi, R. Abdullah, M. Zamri-Saad, Y. H. Taufiq-Yap and M. N. M. Hezmee. The crucial roles of inflammatory mediators in inflammation: A review. *Veterinary World*, 11(5):627, 2018.
- N. R. Aggarwal, L. S. King and F. R. D'Alessio. Diverse macrophage populations mediate acute lung inflammation and resolution. *American Journal of Physiology-Lung Cellular and Molecular Physiology*, 306(8):L709–L725, 2014.
- M. M. Ahamada, Y. Jia and X. Wu. Macrophage polarization and plasticity in systemic lupus erythematosus. *Frontiers in Immunology*, 12:734008, 2021.
- S. M Aitcheson, F. D. Frentiu, S. E. Hurn, K. Edwards and R. Z. Murray. Skin wound healing: normal macrophage function and macrophage dysfunction in diabetic wounds. *Molecules*, 26(16):4917, 2021.
- C. Akgul, D. A. Moulding and S. W. Edwards. Molecular control of neutrophil apoptosis. *FEBS Letters*, 487(3):318–322, 2001.
- K. A. K. Al-Dulaimi, J. Banks, V. Chandran, I. Tomeo-Reyes and K. Nguyen Thanh. Classification of white blood cell types from microscope images: Techniques and challenges. *Microscopy Science: Last Approaches on Educational Programs and Applied Research (Microscopy Book Series, 8)*, pages 17–25, 2018.
- S. Amor, L. A. Peferoen, D. Y. Vogel, M. Breur, P. van der Valk, D. Baker and J. M. van Noort. Inflammation in neurodegenerative diseases—an update. *Immunology*, 142(2): 151–166, 2014.
- K. I. Andreasson, A. D. Bachstetter, M. Colonna, F. Ginhoux, C. Holmes, B. Lamb, G. Landreth, D. C. Lee, D. Low, M. A. Lynch *et al.* Targeting innate immunity for

- neurodegenerative disorders of the central nervous system. *Journal of Neurochemistry*, 138(5):653–693, 2016.
- S. D. Anker and S. von Haehling. Inflammatory mediators in chronic heart failure: an overview. *Heart*, 90(4):464–470, 2004.
- W. Ansar, S. Ghosh, W. Ansar and S. Ghosh. Inflammation and inflammatory diseases, markers, and mediators: Role of CRP in some inflammatory diseases. *Biology of C Reactive Protein in Health and Disease*, pages 67–107, 2016.
- C. Atri, F. Z. Guerfali and D. Laouini. Role of human macrophage polarization in inflammation during infectious diseases. *International Journal of Molecular Sciences*, 19(6):1801, 2018.
- N. Baghel, U. Verma and K. K. Nagwanshi. WBCs-Net: Type identification of white blood cells using convolutional neural network. *Multimedia Tools and Applications*, 81(29):42131–42147, 2022.
- M. Baker, S. Denman-Johnson, B. S. Brook, I. Gaywood and M. R. Owen. Mathematical modelling of cytokine-mediated inflammation in rheumatoid arthritis. *Mathematical Medicine and Biology: a Journal of the IMA*, 30(4):311–337, 2013.
- E. O. Bangsgaard, P. G. Hjorth, M. S. Olufsen, J. Mehlsen and J. T. Ottesen. Integrated inflammatory stress (itis) model. *Bulletin of Mathematical Biology*, 79:1487–1509, 2017.
- A. Bayani, J. L. Dunster, J. J. Crofts and M. R. Nelson. Mechanisms and points of control in the spread of inflammation: a mathematical investigation. *Bulletin of Mathematical Biology*, 82:1–22, 2020a.
- A. Bayani, J. L. Dunster, J. J. Crofts and M. R. Nelson. Spatial considerations in the resolution of inflammation: elucidating leukocyte interactions via an experimentally-calibrated agent-based model. *PLoS Computational Biology*, 16(11):e1008413, 2020b.
- C. Bianca, L. Guerrini and J. Riposo. A delayed mathematical model for the acute inflammatory response to infection. *Applied Mathematics & Information Sciences*, 9(6): 2775, 2015.
- J. Bie, B. Zhao, J. Song and S. Ghosh. Improved insulin sensitivity in high fat-and high cholesterol-fed Ldlr^{-/-} mice with macrophage-specific transgenic expression of cholesteryl ester hydrolase: role of macrophage inflammation and infiltration into adipose tissue. *Journal of Biological Chemistry*, 285(18):13630–13637, 2010.

- S. K. Biswas and A. Mantovani. Macrophage plasticity and interaction with lymphocyte subsets: cancer as a paradigm. *Nature Immunology*, 11(10):889–896, 2010.
- Z. T. Bloomgarden. Inflammation and insulin resistance. *Diabetes Care*, 26(6):1922–1926, 2003.
- M. Blüher and D. Müller-Wieland. Adipose tissue dysfunction. *Frontiers in Endocrinology*, 13:999188, 2022.
- R. Brady, D. O. Frank-Ito, H. T. Tran, S. Janum, K. Møller, S. Brix, J. T. Ottesen, J. Mehlsen and M. S. Olufsen. Personalized mathematical model predicting endotoxin-induced inflammatory responses in young men. *ArXiv Preprint ArXiv:1609.01570*, 2016.
- R. Brady, D. O. Frank-Ito, H. T. Tran, S. Janum, K. Møller, S. Brix, J. T. Ottesen, J. Mehlsen and M. S. Olufsen. Personalized mathematical model of endotoxin-induced inflammatory responses in young men and associated changes in heart rate variability. *Mathematical Modelling of Natural Phenomena*, 13(5):42, 2018.
- D. R. Brenner, D. Scherer, K. Muir, J. Schildkraut, P. Boffetta, M. R. Spitz, L. Le Marchand, A. T. Chan, E. L. Goode, C. M. Ulrich *et al.* A review of the application of inflammatory biomarkers in epidemiologic cancer research. *Cancer Epidemiology, Biomarkers & Prevention*, 23(9):1729–1751, 2014.
- T. A. Butterfield, T. M. Best and M. A. Merrick. The dual roles of neutrophils and macrophages in inflammation: a critical balance between tissue damage and repair. *Journal of Athletic Training*, 41(4):457, 2006.
- J. Candido and T. Hagemann. Cancer-related inflammation. *Journal of Clinical Immunology*, 33:79–84, 2013.
- Q. Cao, D. C. H. Harris and Y. Wang. Macrophages in kidney injury, inflammation, and fibrosis. *Physiology*, 30(3):183–194, 2015.
- E. Z. P. Chai, K. S. Siveen, M. K. Shanmugam, F. Arfuso and G. Sethi. Analysis of the intricate relationship between chronic inflammation and cancer. *Biochemical Journal*, 468(1):1–15, 2015.
- P. Chandrasoma and C. R. Taylor. *Concise Pathology*, 3e. The McGraw-Hill Companies, New York, NY, 1998.
- A. Chaudhury, C. Duvoor, V. S. Reddy Dendi, S. Kraleti, A. Chada, R. Ravilla, A. Marco, N. S. Shekhawat, M. T. Montales, K. Kuriakose *et al.* Clinical review of antidiabetic drugs: implications for type 2 diabetes mellitus management. *Frontiers in Endocrinology*, 8:6, 2017.

- A. Chauhan, D. H. Adams, S. P. Watson and P. F. Lalor. Platelets: No longer bystanders in liver disease. *Hepatology*, 64(5):1774–1784, 2016.
- L. Chen, H. Deng, H. Cui, J. Fang, Z. Zuo, J. Deng, Y. Li, X. Wang and L. Zhao. Inflammatory responses and inflammation-associated diseases in organs. *Oncotarget*, 9(6):7204, 2018.
- Y. Chen and X. Zhang. Pivotal regulators of tissue homeostasis and cancer: macrophages. *Experimental Hematology & Oncology*, 6(1):1–8, 2017.
- O. Chertov, D. Yang, O.M. Howard and J. J. Oppenheim. Leukocyte granule proteins mobilize innate host defenses and adaptive immune responses. *Immunological Reviews*, 177:68–78, 2000.
- A. Classen, J. Lloberas and A. Celada. Macrophage activation: classical vs. alternative. In *Macrophages and Dendritic Cells*, pages 29–43. Springer, 2009.
- H. B. Cohen and D. M. Mosser. Extrinsic and intrinsic control of macrophage inflammatory responses. *Journal of Leukocyte Biology*, 94(5):913–919, 2013.
- F. Colotta, P. Allavena, A. Sica, C. Garlanda and A. Mantovani. Cancer-related inflammation, the seventh hallmark of cancer: links to genetic instability. *Carcinogenesis*, 30(7):1073–1081, 2009.
- R. L. Cooper, R. A. Segal, R. F. Diegelmann and A. M. Reynolds. Modeling the effects of systemic mediators on the inflammatory phase of wound healing. *Journal of Theoretical Biology*, 367:86–99, 2015.
- N. G. Cruz, L. P. Sousa, M. O. Sousa, N. T. Pietrani, A. P. Fernandes and K. B. Gomes. The linkage between inflammation and type 2 diabetes mellitus. *Diabetes Research and Clinical Practice*, 99(2):85–92, 2013.
- P. Dandona, A. Aljada and A. Bandyopadhyay. Inflammation: the link between insulin resistance, obesity and diabetes. *Trends in Immunology*, 25(1):4–7, 2004.
- L. C. Davies, S. J. Jenkins, J. E. Allen and P. R. Taylor. Tissue-resident macrophages. *Nature Immunology*, 14(10):986–995, 2013.
- K. A. Deans and N. Sattar. "anti-inflammatory" drugs and their effects on type 2 diabetes. *Diabetes Technology & Therapeutics*, 8(1):18–27, 2006.
- P. Deepak, J. E. Axelrad and A. N. Ananthakrishnan. The role of the radiologist in determining disease severity in inflammatory bowel diseases. *Gastrointestinal Endoscopy Clinics*, 29(3):447–470, 2019.

- B. M. Delavary, W. M. van der Veer, M. van Egmond, F. B. Niessen and R. H. J. Beelen. Macrophages in skin injury and repair. *Immunobiology*, 216(7):753–762, 2011.
- C. Deppermann and P. Kubes. Start a fire, kill the bug: The role of platelets in inflammation and infection. *Innate Immunity*, 24(6):335–348, 2018.
- A. Dobрева, R. Brady-Nicholls, K. Larripa, C. Puelz, J. Mehlsen and M. S. Olufsen. A physiological model of the inflammatory-thermal-pain-cardiovascular interactions during an endotoxin challenge. *The Journal of Physiology*, 599(5):1459–1485, 2021.
- M. Y. Donath and S. E. Shoelson. Type 2 diabetes as an inflammatory disease. *Nature Reviews Immunology*, 11(2):98–107, 2011.
- T. W. Du Clos. Function of c-reactive protein. *Annals of Medicine*, 32(4):274–278, 2000.
- J. L. Dunster. The macrophage and its role in inflammation and tissue repair: mathematical and systems biology approaches. *Wiley Interdisciplinary Reviews: Systems Biology and Medicine*, 8(1):87–99, 2016.
- J. L. Dunster, H. M. Byrne and J. R. King. The resolution of inflammation: a mathematical model of neutrophil and macrophage interactions. *Bulletin of Mathematical Biology*, 76(8):1953–1980, 2014.
- J. L. Dunster, J. M. Gibbins and M. R. Nelson. Exploring the constituent mechanisms of hepatitis: a dynamical systems approach. *Mathematical Medicine and Biology: a Journal of the IMA*, 40(1):24–48, 2023.
- S. A. Eming, T. Krieg and J. M. Davidson. Inflammation in wound repair: molecular and cellular mechanisms. *Journal of Investigative Dermatology*, 127(3):514–525, 2007.
- A. Engin. The pathogenesis of obesity-associated adipose tissue inflammation. *Obesity and Lipotoxicity*, pages 221–245, 2017.
- B. Ermentrout. *Simulating, analyzing, and animating dynamical systems: a guide to XPPAUT for researchers and students*. SIAM, Philadelphia, 2002.
- N. Esser, N. Paquot and A. J. Scheen. Anti-inflammatory agents to treat or prevent type 2 diabetes, metabolic syndrome and cardiovascular disease. *Expert Opinion on Investigational Drugs*, 24(3):283–307, 2015.
- L. Ferrero-Miliani, O.H. Nielsen, P.S. Andersen and S. Girardin. Chronic inflammation: importance of NOD2 and NALP3 in interleukin-1 β generation. *Clinical & Experimental Immunology*, 147(2):227–235, 2007.

- L. Ferrucci and E. Fabbri. Inflammageing: chronic inflammation in ageing, cardiovascular disease, and frailty. *Nature Reviews Cardiology*, 15(9):505–522, 2018.
- N. G. Frangogiannis. The inflammatory response in myocardial injury, repair, and remodelling. *Nature Reviews Cardiology*, 11(5):255–265, 2014.
- S. C. Funes, M. Rios, J. Escobar-Vera and A. M. Kalergis. Implications of macrophage polarization in autoimmunity. *Immunology*, 154(2):186–195, 2018.
- D. Furman, J. Campisi, E. Verdin, P. Carrera-Bastos, S. Targ, C. Franceschi, L. Ferrucci, D. W. Gilroy, A. Fasano, G. W. Miller *et al.* Chronic inflammation in the etiology of disease across the life span. *Nature Medicine*, 25(12):1822–1832, 2019.
- R. V. Furth. *Mononuclear phagocytes: characteristics, physiology and function*. Springer Science & Business Media, 2012.
- C. Gabay. Interleukin-6 and chronic inflammation. *Arthritis Research & Therapy*, 8(2):1–6, 2006.
- S. Gajbhiye and J. Aate. Blood report analysis-a review. *Tropical Journal of Pharmaceutical and Life Sciences*, 10(5):63–79, 2023.
- D. L. Gandy and M. R. Nelson. Analyzing Pattern Formation in the Gray–Scott Model: An XPPAUT Tutorial. *SIAM Review*, 64(3):728–747, 2022.
- H. Ghoti, J. Amer, A. Winder, E. Rachmilewitz and E. Fibach. Oxidative stress in red blood cells, platelets and polymorphonuclear leukocytes from patients with myelodysplastic syndrome. *European Journal of Haematology*, 79(6):463–467, 2007.
- F. Ginhoux and M. Guilliams. Tissue-resident macrophage ontogeny and homeostasis. *Immunity*, 44(3):439–449, 2016.
- V. Gkretsi, L. C. Zacharia and T. Stylianopoulos. Targeting inflammation to improve tumor drug delivery. *Trends in Cancer*, 3(9):621–630, 2017.
- S. Gordon. Phagocytosis: an immunobiologic process. *Immunity*, 44(3):463–475, 2016.
- S. Gordon and F. O. Martinez. Alternative activation of macrophages: mechanism and functions. *Immunity*, 32(5):593–604, 2010.
- S. Gordon, A. Plüddemann and F. Martinez Estrada. Macrophage heterogeneity in tissues: phenotypic diversity and functions. *Immunological Reviews*, 262(1):36–55, 2014.

- C. Grabher, A. Cliffe, K. Miura, J. Hayflick, R. Pepperkok, P. Rørth and J. Wittbrodt. Birth and life of tissue macrophages and their migration in embryogenesis and inflammation in medaka. *Journal of Leukocyte Biology*, 81(1):263–271, 2007.
- D.N. Granger and E. Senchenkova. *Inflammation and the Microcirculation*. Colloquium Series on Integrated Systems Physiology: From Molecule to Function. Biota Publishing, 2010. ISBN 9781615041664.
- W. S. T. Griffin. Inflammation and neurodegenerative diseases. *The American Journal of Clinical Nutrition*, 83(2):470S–474S, 2006.
- E. Gwyer Findlay and T. Hussell. Macrophage-mediated inflammation and disease: a focus on the lung. *Mediators of Inflammation*, 2012, 2012.
- T. S. Han and M. E. Lean. A clinical perspective of obesity, metabolic syndrome and cardiovascular disease. *JRSM Cardiovascular Disease*, 5:2048004016633371, 2016.
- C. Haslett. Granulocyte apoptosis and its role in the resolution and control of lung inflammation. *American Journal of Respiratory and Critical Care Medicine*, 160 (supplement_1):S5–S11, 1999.
- M. C. Herald. General model of inflammation. *Bulletin of Mathematical Biology*, 72(4): 765, 2010.
- M. Hesketh, K. B. Sahin, Z. E. West and R. Z. Murray. Macrophage phenotypes regulate scar formation and chronic wound healing. *International Journal of Molecular Sciences*, 18(7):1545, 2017.
- D. Hirayama, T. Iida and H. Nakase. The phagocytic function of macrophage-enforcing innate immunity and tissue homeostasis. *International Journal of Molecular Sciences*, 19(1):92, 2018.
- X. Hu, R. K. Leak, Y. Shi, J. Suenaga, Y. Gao, P. Zheng and J. Chen. Microglial and macrophage polarization—new prospects for brain repair. *Nature Reviews Neurology*, 11(1):56–64, 2015.
- X. Huang, Y. Li, M. Fu and H.B. Xin. Polarizing macrophages in vitro. In *Macrophages*, pages 119–126. Springer, 2018.
- M. Hulsmans, S. Clauss, L. Xiao, A. D. Aguirre, K. R. King, A. Hanley, W. J. Hucker, E. M. Wülfers, G. Seemann, G. Courties *et al.* Macrophages facilitate electrical conduction in the heart. *Cell*, 169(3):510–522, 2017.

- S. E. Inzucchi, R. M. Bergenstal, J. B. Buse, M. Diamant, E. Ferrannini, M. Nauck, A. L. Peters, A. Tsapas, R. Wender and D. R. Matthews. Management of hyperglycemia in type 2 diabetes: a patient-centered approach: position statement of the American Diabetes Association (ADA) and the European Association for the Study of Diabetes (EASD). *Diabetes Spectrum*, 25(3):154–171, 2012.
- P. Italiani and D. Boraschi. From monocytes to M1/M2 macrophages: phenotypical vs. functional differentiation. *Frontiers in Immunology*, 5:514, 2014.
- J. Jackson. Immunology: host responses to biomaterials. In *In Situ Tissue Regeneration*, pages 35–47. Elsevier, 2016.
- U. Jaggi, M. Yang, H. H. Matundan, S. Hirose, P. K. Shah, B. G. Sharifi and H. Ghiasi. Increased phagocytosis in the presence of enhanced M2-like macrophage responses correlates with increased primary and latent HSV-1 infection. *PloS Pathogens*, 16(10): e1008971, 2020.
- S. J. Jenkins and J. E. Allen. The expanding world of tissue-resident macrophages. *European Journal of Immunology*, 51(8):1882–1896, 2021.
- L. Jiang, C. Tang and H. Zhou. White blood cell classification via a discriminative region detection assisted feature aggregation network. *Biomedical Optics Express*, 13(10):5246–5260, 2022.
- U. Juhas, M. Ryba-Stanisławowska, P. Szargiej and J. Myśliwska. Different pathways of macrophage activation and polarization. *Advances in Hygiene and Experimental Medicine*, 69:496–502, 2015.
- V. Kain and G. V. Halade. Big eater macrophages dominate inflammation resolution following myocardial infarction. *Journal of Molecular and Cellular Cardiology*, 100(87): 225–227, 2015.
- K. Kakleas, A. Soldatou, F. Karachaliou and K. Karavanaki. Associated autoimmune diseases in children and adolescents with type 1 diabetes mellitus (T1DM). *Autoimmunity Reviews*, 14(9):781–797, 2015.
- K. G. Kannan, T. R. G. Babu, R. Praveena, P. Sukumar, G. Sudha and M. Birunda. Classification of wbc cell classification using fully connected convolution neural network. In *Journal of Physics: Conference Series*, volume 2466, page 012033. IOP Publishing, 2023.
- M. Karin. Nuclear factor- κ B in cancer development and progression. *Nature*, 441(7092): 431–436, 2006.

- A. D. Khamael, J. Banks, K. Nugyen, A. Al-Sabaawi, I. Tomeo-Reyes and V. Chandran. Segmentation of white blood cell, nucleus and cytoplasm in digital haematology microscope images: A review—challenges, current and future potential techniques. *IEEE Reviews in Biomedical Engineering*, 14:290–306, 2020.
- M. H. Kim, W. Liu, D. L. Borjesson, F. R. E. Curry, L. S. Miller, A. L. Cheung, F. T. Liu, R. R. Isseroff and S. I. Simon. Dynamics of neutrophil infiltration during cutaneous wound healing and infection using fluorescence imaging. *Journal of Investigative Dermatology*, 128(7):1812–1820, 2008.
- W. Koenig. Inflammation and coronary heart disease: an overview. *Cardiology in Review*, 9(1):31–35, 2001.
- E. Kolaczowska and P. Kubes. Neutrophil recruitment and function in health and inflammation. *Nature Reviews Immunology*, 13(3):159–175, 2013.
- M. J. Kraakman, A. J. Murphy, K. Jandeleit-Dahm and H. L. Kammoun. Macrophage polarization in obesity and type 2 diabetes: weighing down our understanding of macrophage function? *Frontiers in Immunology*, 5:470, 2014.
- A. J. Krentz and C. J. Bailey. Oral antidiabetic agents: current role in type 2 diabetes mellitus. *Drugs*, 65:385–411, 2005.
- F. Krombach, S. Münzing, A.M. Allmeling, J. T. Gerlach, J. Behr and M. Dörger. Cell size of alveolar macrophages: an interspecies comparison. *Environmental Health Perspectives*, 105(suppl 5):1261–1263, 1997.
- R. Kumar, C. C. Chow, J. D. Bartels, G. Clermont and Y. Vodovotz. A mathematical simulation of the inflammatory response to anthrax infection. *Shock*, 29(1):104, 2008.
- R. Kumar, G. Clermont, Y. Vodovotz and C. C. Chow. The dynamics of acute inflammation. *Journal of Theoretical Biology*, 230(2):145–155, 2004.
- H. Kuper, H. O. Adami and D. Trichopoulos. Infections as a major preventable cause of human cancer. *Journal of Internal Medicine*, 249(S741):61–74, 2001.
- V. Küppers, D. Vestweber and D. Schulte. Locking endothelial junctions blocks leukocyte extravasation, but not in all tissues. *Tissue Barriers*, 1(1):4157–70, 2013.
- A. Kuryłowicz and K. Koźniewski. Anti-inflammatory strategies targeting metaflammation in type 2 diabetes. *Molecules*, 25(9):2224, 2020.
- Y. A. Kuznetsov. *Elements of applied bifurcation theory*, volume 112. Springer Science & Business Media, 2013.

- Y. A. Kuznetsov, I. A. Kuznetsov and Y. Kuznetsov. *Elements of applied bifurcation theory*, volume 112. Springer, 1998.
- J. L. Langowski, X. Zhang, L. Wu, J. D. Mattson, T. Chen, K. Smith, B. Basham, T. McClanahan, R. A. Kastelein and M. Oft. IL-23 promotes tumour incidence and growth. *Nature*, 442(7101):461–465, 2006.
- D. L. Laskin, V. R. Sunil, C. R. Gardner and J. D. Laskin. Macrophages and tissue injury: agents of defense or destruction? *Annual Review of Pharmacology and Toxicology*, 51: 267, 2011.
- T. Lawrence and D. W. Gilroy. Chronic inflammation: a failure of resolution? *International Journal of Experimental Pathology*, 88(2):85–94, 2007.
- J. Lee, F. R. Adler and P. S. Kim. A mathematical model for the macrophage response to respiratory viral infection in normal and asthmatic conditions. *Bulletin of Mathematical Biology*, 79(9):1979–1998, 2017.
- T. Lelekov-Boissard, G. Chapuisat, J. P. Boissel, E. Grenier and M. A. Dronne. Exploration of beneficial and deleterious effects of inflammation in stroke: dynamics of inflammation cells. *Philosophical Transactions of the Royal Society A: Mathematical, Physical and Engineering Sciences*, 367(1908):4699–4716, 2009.
- C. P. Liang, S. Han, T. Senokuchi and A. R. Tall. The macrophage at the crossroads of insulin resistance and atherosclerosis. *Circulation Research*, 100(11):1546–1555, 2007.
- P. Libby. Role of inflammation in atherosclerosis associated with rheumatoid arthritis. *The American Journal of Medicine*, 121(10):S21–S31, 2008.
- D. Lissner, M. Schumann, A. Batra, L. I. Kredel, A. A. Kühl, U. Erben, C. May, J. D. Schulzke and B. Siegmund. Monocyte and M1 macrophage-induced barrier defect contributes to chronic intestinal inflammation in IBD. *Inflammatory Bowel Diseases*, 21(6):1297–1305, 2015.
- C. Liu, D. Chu, K. Kalantar-Zadeh, J. George, H. A. Young and G. Liu. Cytokines: from clinical significance to quantification. *Advanced Science*, 8(15):2004433, 2021.
- C. Liu, X. Feng, Q. Li, Y. Wang, Q. Li and M. Hua. Adiponectin, TNF- α and inflammatory cytokines and risk of type 2 diabetes: a systematic review and meta-analysis. *Cytokine*, 86:100–109, 2016.

- C. H. Liu, N. D. Abrams, D. M. Carrick, P. Chander, J. Dwyer, M. R. Hamlet, F. Macchiarini, M. PrabhuDas, G. L. Shen, P. Tandon *et al.* Biomarkers of chronic inflammation in disease development and prevention: challenges and opportunities. *Nature Immunology*, 18(11):1175–1180, 2017.
- M. Madjid and J. T. Willerson. Inflammatory markers in coronary heart disease. *British Medical Bulletin*, 100(1), 2011.
- P. Małkowska and M. Sawczuk. Cytokines as biomarkers for evaluating physical exercise in trained and non-trained individuals: a narrative review. *International Journal of Molecular Sciences*, 24(13):11156, 2023.
- A. Mantovani, P. Allavena, A. Sica and F. Balkwill. Cancer-related inflammation. *Nature*, 454(7203):436–444, 2008.
- A. Mantovani, M. A. Cassatella, C. Costantini and S. Jaillon. Neutrophils in the activation and regulation of innate and adaptive immunity. *Nature Reviews Immunology*, 11(8):519–531, 2011.
- A. Mantovani, A. Sica and M. Locati. Macrophage polarization comes of age. *Immunity*, 23(4):344–346, 2005.
- A. Mantovani, S. Sozzani, M. Locati, P. Allavena and A. Sica. Macrophage polarization: tumor-associated macrophages as a paradigm for polarized M2 mononuclear phagocytes. *Trends in Immunology*, 23(11):549–555, 2002.
- A. F. Marée, M. Komba, C. Dyck, M. Łabecki, D. T. Finegood and L. Edelstein-Keshet. Quantifying macrophage defects in type 1 diabetes. *Journal of Theoretical Biology*, 233(4):533–551, 2005.
- A. F. M. Marée, M. Komba, D. T. Finegood and L. Edelstein-Keshet. A quantitative comparison of rates of phagocytosis and digestion of apoptotic cells by macrophages from normal (balb/c) and diabetes-prone (nod) mice. *Journal of Applied Physiology*, 104(1):157–169, 2008.
- A. F. M. Marée, R. Kublik, D. T. Finegood and L. Edelstein-Keshet. Modelling the onset of type 1 diabetes: can impaired macrophage phagocytosis make the difference between health and disease? *Philosophical Transactions of the Royal Society A: Mathematical, Physical and Engineering Sciences*, 364(1842):1267–1282, 2006.
- K. E. Martin and A. J. García. Macrophage phenotypes in tissue repair and the foreign body response: Implications for biomaterial-based regenerative medicine strategies. *Acta Biomaterialia*, 133:4–16, 2021.

- F. O. Martinez and S. Gordon. The M1 and M2 paradigm of macrophage activation: time for reassessment. *F1000prime Reports*, 6, 2014.
- F. O. Martinez, L. Helming and S. Gordon. Alternative activation of macrophages: an immunologic functional perspective. *Annual Review of Immunology*, 27:451–483, 2009.
- F. O. Martinez, A. Sica, A. Mantovani and M. Locati. Macrophage activation and polarization. *Frontiers in Bioscience-Landmark*, 13(2):453–461, 2008.
- T. A. Masters, B. Pontes, V. Viasnoff, Y. Li and N. C. Gauthier. Plasma membrane tension orchestrates membrane trafficking, cytoskeletal remodeling, and biochemical signaling during phagocytosis. *Proceedings of the National Academy of Sciences*, 110(29):11875–11880, 2013.
- R. Medzhitov. Origin and physiological roles of inflammation. *Nature*, 454(7203):428–435, 2008.
- V. M. Milenkovic, E. H. Stanton, C. Nothdurfter, R. Rupprecht and C. H. Wetzel. The role of chemokines in the pathophysiology of major depressive disorder. *International Journal of Molecular Sciences*, 20(9):2283, 2019.
- C. Mills. M1 and M2 macrophages: oracles of health and disease. *Critical Reviews in Immunology*, 32(6), 2012.
- S. Minucci, R. L. Heise, M. S. Valentine, F. J. K. Gninzeko and A. M. Reynolds. Mathematical modeling of ventilator-induced lung inflammation. *Journal of Theoretical Biology*, 526:110738, 2021.
- S. B. Minucci, R. L. Heise, M. S. Valentine, F. J. K. Gninzeko and A. M. Reynolds. Understanding the role of macrophages in lung inflammation through mathematical modeling. *BioRxiv*, 2020.
- S. Mirza, M. Hossain, C. Mathews, P. Martinez, P. Pino, J. L. Gay, A. Rentfro, J. B. McCormick and S. P. Fisher-Hoch. Type 2-diabetes is associated with elevated levels of TNF-alpha, IL-6 and adiponectin and low levels of leptin in a population of Mexican Americans: a cross-sectional study. *Cytokine*, 57(1):136–142, 2012.
- A. Mohammadi, C. N. Blesso, G. E. Barreto, M. Banach, M. Majeed and A. Sahebkar. Macrophage plasticity, polarization and function in response to curcumin, a diet-derived polyphenol, as an immunomodulatory agent. *The Journal of Nutritional Biochemistry*, 66:1–16, 2019.

- D. M. Mosser. The many faces of macrophage activation. *Journal of Leukocyte Biology*, 73(2):209–212, 2003.
- D. M. Mosser and J. P. Edwards. Exploring the full spectrum of macrophage activation. *Nature Reviews Immunology*, 8(12):958–969, 2008.
- D. M. Mosser, K. Hamidzadeh and R. Goncalves. Macrophages and the maintenance of homeostasis. *Cellular & Molecular Immunology*, 18(3):579–587, 2021.
- X. Mu, Y. Li and G. C. Fan. Tissue-resident macrophages in the control of infection and resolution of inflammation. *Shock (Augusta, Ga.)*, 55(1):14, 2021.
- W. A. Muller. Getting leukocytes to the site of inflammation. *Veterinary Pathology*, 50(1):7–22, 2013.
- P. J. Murray. Macrophage polarization. *Annual Review of Physiology*, 79:541–566, 2017.
- P. J. Murray, J. E. Allen, S. K. Biswas, E. A. Fisher, D. W. Gilroy, S. Goerdt, S. Gordon, J. A. Hamilton, L. B. Ivashkiv, T. Lawrence *et al.* Macrophage activation and polarization: nomenclature and experimental guidelines. *Immunity*, 41(1):14–20, 2014.
- M. R. Nelson, J. M. Gibbins and J. L. Dunster. Platelet-driven routes to chaos in a model of hepatitis. *Chaos, Solitons & Fractals*, 170:113338, 2023.
- Y. Niu, Q. Xue and Y. Fu. Natural glycan derived biomaterials for inflammation targeted drug delivery. *Macromolecular Bioscience*, 21(9):2100162, 2021.
- J. A. Noble. Immunogenetics of type 1 diabetes: a comprehensive review. *Journal of Autoimmunity*, 64:101–112, 2015.
- A. Ortega-Gómez, M. Perretti and O. Soehnlein. Resolution of inflammation: an integrated view. *EMBO Molecular Medicine*, 5(5):661–674, 2013.
- R. Pahwa, A. Goyal, P. Bansal and I. Jialal. *Chronic Inflammation*. StatPearls Publishing, Treasure Island (FL), 2021.
- R. Pahwa, A. Goyal and I. Jialal. *Chronic Inflammation*. StatPearls Publishing, Treasure Island (FL), 2018.
- A. Palma, A. S. Jarrah, P. Tieri, G. Cesareni and F. Castiglione. Gene regulatory network modeling of macrophage differentiation corroborates the continuum hypothesis of polarization states. *Frontiers in Physiology*, 9:1659, 2018.

- R. C. Paolicelli, G. Bolasco, F. Pagani, L. Maggi, M. Scianni, P. Panzanelli, M. Giustetto, T. A. Ferreira, E. Guiducci, L. Dumas *et al.* Synaptic pruning by microglia is necessary for normal brain development. *Science*, 333(6048):1456–1458, 2011.
- F. Paolini P., S. Simoni, L. Parnetti and L. Gaetani. The contribution of small vessel disease to neurodegeneration: focus on alzheimer’s disease, parkinson’s disease and multiple sclerosis. *International Journal of Molecular Sciences*, 22(9):4958, 2021.
- N. Parameswaran and S. Patial. Tumor necrosis factor- α signaling in macrophages. *Critical Reviews in Eukaryotic Gene Expression*, 20(2), 2010.
- A. Parihar, T. D. Eubank and A. I. Doseff. Monocytes and macrophages regulate immunity through dynamic networks of survival and cell death. *Journal of Innate Immunity*, 2(3):204–215, 2010.
- K. Penner, B. Ermentrout and D. Swigon. Pattern formation in a model of acute inflammation. *SIAM Journal on Applied Dynamical Systems*, 11(2):629–660, 2012.
- M. E. Piché, A. Tchernof and J. P. Després. Obesity phenotypes, diabetes, and cardiovascular diseases. *Circulation Research*, 126(11):1477–1500, 2020.
- G. Piedrafita, F. Montero, F. Morán, M. L. Cardenas and A. Cornish-Bowden. A simple self-maintaining metabolic system: robustness, autocatalysis, bistability. *PLoS Computational Biology*, 6(8):e1000872, 2010.
- D. Placha and J. Jampilek. Chronic inflammatory diseases, anti-inflammatory agents and their delivery nanosystems. *Pharmaceutics*, 13(1):64, 2021.
- A. Plüddemann, S. Mukhopadhyay and S. Gordon. The interaction of macrophage receptors with bacterial ligands. *Expert Reviews in Molecular Medicine*, 8(28):1–25, 2006.
- M. Ponzoni, F. Pastorino, D. Di Paolo, P. Perri and C. Brignole. Targeting macrophages as a potential therapeutic intervention: impact on inflammatory diseases and cancer. *International Journal of Molecular Sciences*, 19(7):1953, 2018.
- F. Porcheray, S. Viaud, A.C. Rimaniol, C. Leone, B. Samah, N. Dereuddre-Bosquet, D. Dormont and G. Gras. Macrophage activation switching: an asset for the resolution of inflammation. *Clinical & Experimental Immunology*, 142(3):481–489, 2005.
- R. Prasad, S. K. Sagar, S. Parveen and R. Dohare. Mathematical modeling in perspective of vector-borne viral infections: a review. *Beni-Suef University Journal of Basic and Applied Sciences*, 11(1):102, 2022.

- J. Prinyakupt and C. Pluempitiwiriyaewej. Segmentation of white blood cells and comparison of cell morphology by linear and naïve bayes classifiers. *Biomedical Engineering Online*, 14(1):1–19, 2015.
- R. M. Ransohoff and M. A. Brown. Innate immunity in the central nervous system. *The Journal of Clinical Investigation*, 122(4):1164–1171, 2012.
- S. Raza, N. McDerment, P. A. Lacaze, K. Robertson, S. Watterson, Y. Chen, M. Chisholm, G. Eleftheriadis, S. Monk, M. O’Sullivan *et al.* Construction of a large scale integrated map of macrophage pathogen recognition and effector systems. *BMC Systems Biology*, 4(1):1–18, 2010.
- P. Reddy, D. Lent-Schochet, N. Ramakrishnan, M. McLaughlin and I. Jialal. Metabolic syndrome is an inflammatory disorder: A conspiracy between adipose tissue and phagocytes. *Clinica Chimica Acta*, 496:35–44, 2019.
- A. Reynolds, J. Rubin, G. Clermont, J. Day, Y. Vodovotz and G. B. Ermentrout. A reduced mathematical model of the acute inflammatory response: I. derivation of model and analysis of anti-inflammation. *Journal of Theoretical Biology*, 242(1):220–236, 2006.
- D. M. Richards and R. G. Endres. The mechanism of phagocytosis: two stages of engulfment. *Biophysical Journal*, 107(7):1542–1553, 2014.
- E. Rigamonti, P. Zordan, C. Sciorati, P. Rovere-Querini and S. Brunelli. Macrophage plasticity in skeletal muscle repair. *BioMed Research International*, 2014, 2014.
- L. K. Riley and J. Rupert. Evaluation of patients with leukocytosis. *American Family Physician*, 92(11):1004–1011, 2015.
- L. Ringham, P. Prusinkiewicz and R. Gniadecki. Skin patterning in psoriasis by spatial interactions between pathogenic cytokines. *Isience*, 20:546–553, 2019.
- G. Rogler. Immune cells: Monocytes and macrophages. *Crohn’s Disease and Ulcerative Colitis: From Epidemiology and Immunobiology to a Rational Diagnostic and Therapeutic Approach*, pages 119–122, 2017.
- J. Rombouts and L. Gelens. Dynamic bistable switches enhance robustness and accuracy of cell cycle transitions. *PLOS Computational Biology*, 17(1):e1008231, 2021.
- C. Rosales. Neutrophil: a cell with many roles in inflammation or several cell types? *Frontiers in Physiology*, 9:113, 2018.

- E. A. Ross, A. Devitt and J. R. Johnson. Macrophages: the good, the bad, and the gluttony. *Frontiers in Immunology*, 12:708186, 2021.
- D. Rückerl and J. E. Allen. Macrophage proliferation, provenance, and plasticity in macroparasite infection. *Immunological Reviews*, 262(1):113–133, 2014.
- U. Saqib, S. Sarkar, K. Suk, O. Mohammad, M. S. Baig and R. Savai. Phytochemicals as modulators of M1-M2 macrophages in inflammation. *Oncotarget*, 9(25):17937, 2018.
- D. Schulz, Y. Severin, V. R. T. Zanotelli and B. Bodenmiller. In-depth characterization of monocyte-derived macrophages using a mass cytometry-based phagocytosis assay. *Scientific Reports*, 9(1):1925, 2019.
- C. N. Serhan, N. Chiang and T. E. Van Dyke. Resolving inflammation: dual anti-inflammatory and pro-resolution lipid mediators. *Nature Reviews Immunology*, 8(5): 349–361, 2008.
- C. N. Serhan and J. Savill. Resolution of inflammation: the beginning programs the end. *Nature Immunology*, 6(12):1191–1197, 2005.
- A. Shapouri-Moghaddam, S. Mohammadian, H. Vazini, M. Taghadosi, S.A. Esmaeili, F. Mardani, B. Seifi, A. Mohammadi, J. T. Afshari and A. Sahebkar. Macrophage plasticity, polarization, and function in health and disease. *Journal of Cellular Physiology*, 233(9):6425–6440, 2018.
- J. A. Sherratt and J. C. Dallon. Theoretical models of wound healing: past successes and future challenges. *Comptes Rendus Biologies*, 325(5):557–564, 2002.
- E. R. Sherwood and T. Toliver-Kinsky. Mechanisms of the inflammatory response. *Best Practice & Research Clinical Anaesthesiology*, 18(3):385–405, 2004.
- Y. Shu, J. Huang, Y. Dong and Y. Takeuchi. Mathematical modeling and bifurcation analysis of pro-and anti-tumor macrophages. *Applied Mathematical Modelling*, 88:758–773, 2020.
- A. Sica, P. Invernizzi and A. Mantovani. Macrophage plasticity and polarization in liver homeostasis and pathology. *Hepatology*, 59(5):2034–2042, 2014.
- A. Sica, A. Mantovani *et al.* Macrophage plasticity and polarization: in vivo veritas. *The Journal of Clinical Investigation*, 122(3):787–795, 2012.
- M. H. Sieweke and J. E. Allen. Beyond stem cells: self-renewal of differentiated macrophages. *Science*, 342(6161):1242974, 2013.

- Å. Sjöholm and T. Nyström. Inflammation and the etiology of type 2 diabetes. *Diabetes/metabolism research and Reviews*, 22(1):4–10, 2006.
- A. M. Smith, J. A. McCullers and F. R. Adler. Mathematical model of a three-stage innate immune response to a pneumococcal lung infection. *Journal of Theoretical Biology*, 276(1):106–116, 2011.
- A. M. Smith, F. Z. Rahman, B.H. Hayee, S. J. Graham, D. J. Marks, G. W. Sewell, C. D. Palmer, J. Wilde, B. M. Foxwell, I. S. Gloger *et al.* Disordered macrophage cytokine secretion underlies impaired acute inflammation and bacterial clearance in Crohn’s disease. *Journal of Experimental Medicine*, 206(9):1883–1897, 2009.
- O. Soehnlein and L. Lindbom. Phagocyte partnership during the onset and resolution of inflammation. *Nature Reviews Immunology*, 10(6):427–439, 2010.
- F. J. Solis and D. Azofeifa. Mathematical modeling of the immune system response to pathogens. *Mathematical Methods in the Applied Sciences*, 43(14):8273–8289, 2020.
- R. D. Stout, C. Jiang, B. Matta, I. Tietzel, S. K. Watkins and J. Suttles. Macrophages sequentially change their functional phenotype in response to changes in microenvironmental influences. *The Journal of Immunology*, 175(1):342–349, 2005.
- S. H. Strogatz. *Nonlinear dynamics and chaos with student solutions manual: With applications to physics, biology, chemistry, and engineering*. CRC Press, 2018.
- C. Summers, S. M. Rankin, A. M. Condliffe, N. Singh, A. M. Peters and E. R. Chilvers. Neutrophil kinetics in health and disease. *Trends in Immunology*, 31(8):318–324, 2010.
- E. Suryani, W. Wiharto and N. Polvonov. Identification and counting white blood cells and red blood cells using image processing case study of leukemia. *ArXiv Preprint ArXiv:1511.04934*, 2015.
- I. Tabas and K. E. Bornfeldt. Macrophage phenotype and function in different stages of atherosclerosis. *Circulation Research*, 118(4):653–667, 2016.
- O. Takeuchi and S. Akira. Pattern recognition receptors and inflammation. *Cell*, 140(6):805–820, 2010.
- S. Tamoutounour, M. Guilliams, F. M. Sanchis, H. Liu, D. Terhorst, C. Malosse, E. Pollet, L. Ardouin, H. Luche, C. Sanchez *et al.* Origins and functional specialization of macrophages and of conventional and monocyte-derived dendritic cells in mouse skin. *Immunity*, 39(5):925–938, 2013.

- R. Tamura, T. Tanaka, Y. Yamamoto, Y. Akasaki and H. Sasaki. Dual role of macrophage in tumor immunity. *Immunotherapy*, 10(10):899–909, 2018.
- P. R. Taylor, L. Martinez-Pomares, M. Stacey, H.H. Lin, G. D. Brown and S. Gordon. Macrophage receptors and immune recognition. *Annual Review of Immunology*, 23(1): 901–944, 2005.
- R. Taylor. Insulin resistance and type 2 diabetes. *Diabetes*, 61(4):778, 2012.
- C. Tecchio, A. Micheletti and M. A. Cassatella. Neutrophil-derived cytokines: facts beyond expression. *Frontiers in Immunology*, 5:508, 2014.
- M. P. Thon, M. R. Myerscough and M. W. Gee. A spatially resolved and quantitative model of early atherosclerosis. *Bulletin of Mathematical Biology*, 81(10):4022–4068, 2019.
- W. T’Jonck, M. Guilliams and J. Bonnardel. Niche signals and transcription factors involved in tissue-resident macrophage development. *Cellular Immunology*, 330:43–53, 2018.
- C. J. Tomlin and J. D. Axelrod. Biology by numbers: mathematical modelling in developmental biology. *Nature Reviews Genetics*, 8(5):331–340, 2007.
- M. Torres, J. Wang, P. J. Yannie, S. Ghosh, R. A. Segal and A. M. Reynolds. Identifying important parameters in the inflammatory process with a mathematical model of immune cell influx and macrophage polarization. *PLoS Computational Biology*, 15(7): e1007172, 2019.
- B. C. Trapnell, J. A. Whitsett and K. Nakata. Pulmonary alveolar proteinosis. *New England Journal of Medicine*, 349(26):2527–2539, 2003.
- O. Vasieva, M. Rasolonjanahary and B. Vasiev. Mathematical modelling in developmental biology. *Reproduction (Cambridge, England)*, 145(6):R175–84, 2013.
- Y. Vodovotz and G. An. Agent-based models of inflammation in translational systems biology: A decade later. *Wiley Interdisciplinary Reviews: Systems Biology and Medicine*, 11(6):e1460, 2019.
- Y. Vodovotz, G. An *et al.* *Complex systems and computational biology approaches to acute inflammation*. Springer, 2013.
- Y. Vodovotz, G. Clermont, C. Chow and G. An. Mathematical models of the acute inflammatory response. *Current Opinion in Critical Care*, 10(5):383–390, 2004.

- Y. Vodovotz, M. Csete, J. Bartels, S. Chang and G. An. Translational systems biology of inflammation. *PLoS Computational Biology*, 4(4):e1000014, 2008.
- E. Voronov, D. S. Shouval, Y. Krelin, E. Cagnano, D. Benharroch, Y. Iwakura, C. A. Dinarello and R. N. Apte. Il-1 is required for tumor invasiveness and angiogenesis. *Proceedings of the National Academy of Sciences*, 100(5):2645–2650, 2003.
- X. Wang, Y. Zhao, D. Zhou, Y. Tian, G. Feng and Z. Lu. Gab2 deficiency suppresses high-fat diet-induced obesity by reducing adipose tissue inflammation and increasing brown adipose function in mice. *Cell Death & Disease*, 12(2):212, 2021.
- Y. Wang, T. Yang, Y. Ma, G. V. Halade, J. Zhang, M. L. Lindsey and Y. F. Jin. Mathematical modeling and stability analysis of macrophage activation in left ventricular remodeling post-myocardial infarction. *BMC Genomics*, 13(6):1–8, 2012.
- H. V. Waugh and J. A. Sherratt. Macrophage dynamics in diabetic wound healing. *Bulletin of Mathematical Biology*, 68(1):197, 2006.
- H. V. Waugh and J. A. Sherratt. Modeling the effects of treating diabetic wounds with engineered skin substitutes. *Wound Repair and Regeneration*, 15(4):556–565, 2007.
- A. Weigert, C. Olesch and B. Brüne. Sphingosine-1-phosphate and macrophage biology—how the sphinx tames the big eater. *Frontiers in Immunology*, 10:1706, 2019.
- K. E. Wellen, G. S. Hotamisligil *et al.* Inflammation, stress, and diabetes. *The Journal of Clinical Investigation*, 115(5):1111–1119, 2005.
- L. Wen and A. Duffy. Factors influencing the gut microbiota, inflammation, and type 2 diabetes. *The Journal of Nutrition*, 147(7):1468S–1475S, 2017.
- P. H. Wirtz and R. von Känel. Psychological stress, inflammation, and coronary heart disease. *Current Cardiology Reports*, 19:1–10, 2017.
- Y. T. Wondmkun. Obesity, insulin resistance, and type 2 diabetes: associations and therapeutic implications. *Diabetes, Metabolic Syndrome and Obesity*, pages 3611–3616, 2020.
- T. A. Wynn, A. Chawla and J. W. Pollard. Macrophage biology in development, homeostasis and disease. *Nature*, 496(7446):445–455, 2013.
- J. Yao, X. Huang, M. Wei, W. Han, X. Xu, R. Wang, J. Chen and L. Sun. High-efficiency classification of white blood cells based on object detection. *Journal of Healthcare Engineering*, 2021:1–11, 2021.

- S. Yona, K. W. Kim, Y. Wolf, A. Mildner, D. Varol, M. Breker, D. Strauss-Ayali, S. Viukov, M. Williams, A. Misharin *et al.* Fate mapping reveals origins and dynamics of monocytes and tissue macrophages under homeostasis. *Immunity*, 38(1):79–91, 2013.
- A. Yousuf, W. Ibrahim, N. J. Greening and C. E. Brightling. T2 biologics for chronic obstructive pulmonary disease. *The Journal of Allergy and Clinical Immunology: In Practice*, 7(5):1405–1416, 2019.
- F. Zatterale, M. Longo, J. Naderi, G. A. Raciti, A. Desiderio, C. Miele and F. Beguinot. Chronic adipose tissue inflammation linking obesity to insulin resistance and type 2 diabetes. *Frontiers in Physiology*, 10:1607, 2020.
- C. Zhang, M. Yang and A. C. Ericsson. Function of macrophages in disease: current understanding on molecular mechanisms. *Frontiers in Immunology*, 12:620510, 2021.
- Y. Zhou, Y. Hong and H. Huang. Triptolide attenuates inflammatory response in membranous glomerulo-nephritis rat via downregulation of NF- κ B signaling pathway. *Kidney and Blood Pressure Research*, 41(6):901–910, 2016.
- W. Zhu, J. Yu, Y. Nie, X. Shi, Y. Liu, F. Li and X. Zhang. Disequilibrium of M1 and M2 macrophages correlates with the development of experimental inflammatory bowel diseases. *Immunological Investigations*, 43(7):638–652, 2014.
- P. Zimmet, K. Alberti and J. Shaw. Global and societal implications of the diabetes epidemic. *Nature*, 414(6865):782–787, 2001.